

**BEHAVIOR OF REINFORCED CONCRETE FRAME WITH MASONRY INFILL  
WALLS HAVING OPENING SUBJECTED TO LATERAL LOADING**

by

**ABU SAYED MOHAMMAD AKID**

A thesis submitted in partial fulfillment of the requirements for the degree of  
Master of Science in Civil Engineering



Department of Civil Engineering  
Khulna University of Engineering & Technology  
Khulna 9203, Bangladesh

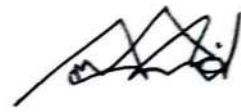
November, 2018

## DECLARATION

This is to certify that the thesis work entitled "Behavior of Reinforced Concrete Frame with Masonry Infill Walls having Opening Subjected to Lateral Loading" has been carried out by Abu Sayed Mohammad Akid in the Department of Civil Engineering, Khulna University of Engineering & Technology, Khulna, Bangladesh. The above thesis work or any part of this work has not been submitted anywhere for the award of any degree or diploma.



Dr. Muhammad Harunur Rashid  
Professor


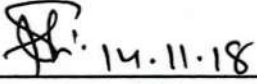


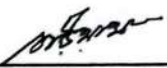


Abu Sayed Mohammad Akid  
Roll No. 1501556

## APPROVAL

This is to certify that the thesis work submitted by Abu Sayed Mohammad Akid entitled "Behavior of Reinforced Concrete Frame with Masonry Infill Walls having Opening Subjected to Lateral Loading" has been approved by the board of examiners for the partial fulfillment of the requirements for the degree of Master of Science in the Department of Civil Engineering, Khulna University of Engineering & Technology, Khulna, Bangladesh in November 2018.

### BOARD OF EXAMINERS

1.   
14.11.18  
\_\_\_\_\_  
Dr. Muhammad Harunur Rashid  
Professor  
Department of Civil Engineering  
Khulna University of Engineering & Technology, Khulna. Chairman  
(Supervisor)
2.   
14.11.18  
\_\_\_\_\_  
Dr. Md. Shahjahan Ali  
Professor & Head  
Department of Civil Engineering  
Khulna University of Engineering & Technology, Khulna. Member
3.   
\_\_\_\_\_  
Dr. Abu Zakir Morshed  
Professor  
Department of Civil Engineering  
Khulna University of Engineering & Technology, Khulna. Member
4.   
\_\_\_\_\_  
Dr. Ismail Saifullah  
Assistant Professor  
Department of Civil Engineering  
Khulna University of Engineering & Technology, Khulna. Member
5.   
\_\_\_\_\_  
Dr. Tarif Uddin Ahmed  
Professor  
Department of Civil Engineering  
Rajshahi University of Engineering & Technology, Rajshahi. Member  
(External)

**DEDICATED  
TO  
MY  
PARENTS  
AND  
BELOVED  
SISTERS**

## ACKNOWLEDGEMENT

At first, I would like to express intense gratitude to almighty ALLAH that the project was completed within perfect time.

I offer my deepest deference and sincerest gratitude to my honorable supervisor Prof. Dr. Muhammad Harunur Rashid, Department of Civil Engineering, Khulna University of Engineering & Technology (KUET), Khulna, Bangladesh who has supported me throughout my thesis with his knowledge and experience. I would never have been able to complete my dissertation without his continuous guidance, supervision, valuable instructions and affectionate encouragement at every stage of this research.

I would like to thank the members of my dissertation committee, Prof. Dr. Md. Shahjahan Ali, Prof. Dr. Abu Zakir Morshed, Assist. Prof. Dr. Ismail Saifullah and Prof. Dr. Tarif Uddin Ahmed for providing useful suggestions for my dissertation.

I am also grateful to all Civil Engineering laboratory technicians for their cooperation during laboratory experiment of this study.

Last but not least, I would like to express my deepest gratitude to my parents and beloved sisters who have always believed in me and sacrificed so much throughout my life.

Abu Sayed Mohammad Akid

## **ABSTRACT**

Reinforced Concrete frames having masonry infill have been widely used in building system. The ground floor is generally open for car parking or other facilities in this type of building. It is a common practice in conventional structural design of buildings often to ignore the interaction of masonry infill with the frame. But observations of past research have revealed that the actual behavior of infill frame with open ground floor due to lateral loading is significantly different to that of bare frame. Therefore, an extensive experimental analysis in the laboratory and computational analysis in software have been performed to study the behavior of masonry infill Reinforced Concrete frames having opening keeping open ground floor subjected to lateral loading.

In the experimental work, three different types of specimen such as two storied single bay RC bare frame, infill frames having door and window opening have been constructed and tested under in-plane lateral loading. A total of 36 numbers of building frames without infill and with infill having opening of door and window have been analyzed in STAAD.Pro software for parametric study considering variation in number of floor and beam-column aspect ratios by Equivalent Static Analysis (ESA) and Response Spectrum Analysis (RSA). The masonry infill has been modeled as equivalent diagonal strut and the size, shape and other properties have been calculated using different published equations of literature. Bangladesh National Building Code has been followed for earthquake load in the analysis and base shear, sway, inter story drift, bending moment, and shear in ESA and RSA of these frames are evaluated and compared.

It has been observed from experimental analysis that the strength and stiffness have been increased and displacement is reduced for RC infill frame having opening than bare frame. First crack is observed as flexure crack at ground floor beam for bare frame and stair crack at the infill for infill frame having opening. From parametric study it is noticed that the presence of infill walls in upper stories make those floors much stiffer compared to ground floor resulting major deflection at ground floor level. The bending moment and shear force are also concentrated at ground floor level where infill walls are absent in both ESA and RSA. The maximum moment and shear in RC infill frame having opening is decreasing significantly in RSA compared to ESA due to interaction of infill to the frame. Thus Equivalent Static Analysis showed conservative results compared to Response Spectrum Analysis for conventional design of buildings as bare frame.

## CONTENTS

	<b>PAGE</b>
<b>TITLE PAGE</b>	i
<b>DECLARATION</b>	ii
<b>CERTIFICATE OF RESEARCH</b>	iii
<b>DEDICATION</b>	iv
<b>ACKNOWLEDGEMENT</b>	v
<b>ABSTRACT</b>	vi
<b>CONTENTS</b>	vii
<b>LIST OF TABLES</b>	xi
<b>LIST OF FIGURES</b>	xiii
<b>NOMENCLATURE</b>	xvii
<b>CHAPTER I      INTRODUCTION</b>	<b>1</b>
1.1    Background of the Study	1
1.2    Objectives of the Study	3
1.3    Organization of the Thesis	4
<b>CHAPTER II    LITERATURE REVIEW</b>	<b>5</b>
2.1    Introduction	5
2.2    Chronological Literature Review of Analytical and Experimental Studies	5
2.3    Literature Review for Parametric Study	9
2.3.1    Response of Masonry Infill RC Frame under Lateral Loading	9
2.3.2    Review of Definitions of Soft Story from Code	13
2.3.3    Effect of Earthquake on Buildings with Soft Story	13
2.3.4    Dynamic Response Spectrum Method	15
2.3.4.1    Modal Shape	16

2.3.4.2	Number of Modes	17
2.3.4.3	Combination of the Modes	18
2.3.4.4	Scaling of Results	18
2.3.4.5	Method of Modal Combination	18
2.4	Material Properties	19
2.4.1	Solid Clay Brick Units	20
2.4.2	Mortar	21
2.4.3	Verification of the Masonry Properties	23
2.4.3.1	Selection of $f'_m$ from Code Tables	23
2.4.3.2	Modulus of Elasticity, $E_m$	24
2.4.4	Equivalent Strut Width	27
2.4.4.1	Eccentricity of Equivalent Strut	30
2.4.4.2	Partially Infill Frames	30
2.4.4.3	Perforated Panels	31
2.4.4.4	Existing Infill Damage	32
2.4.4.5	Plastic Hinge Placement	33
<b>CHAPTER III</b>	<b>RESEARCH METHODOLOGY</b>	<b>35</b>
3.1	Introduction	35
3.2	Details of Laboratory Test Specimens	35
3.3	Test Setup	36
3.4	Data Acquisition	38
3.5	Material Test Results	41
3.5.1	Concrete Tests	41
3.5.2	Steel Reinforcements Tests	42
3.5.3	Brick and Mortar Tests	42
3.6	Modeling of the Frame	42
3.7	Types of Analysis and Loads	44
3.8	Component Properties of the Model	44
3.8.1	Determination of $E_c$ , $E_m$ and $f'_m$	44
3.8.2	Determination of Equivalent Strut Width	45



3.9	Properties of Masonry Infill	45
3.10	Comparison of the Experimental Results for Parametric Study	48
3.11	Observed Parameters	50
3.11.1	Panel Aspect Ratio	50
3.11.2	Number of Story in Vertical Direction	50
3.11.3	Nature of Infill Wall having Opening in the Panel	51
3.12	Modeling Techniques	51
<b>CHAPTER IV</b>	<b>RESULTS AND DISCUSSION</b>	<b>52</b>
4.1	Introduction	52
4.2	Experimental Investigation	52
4.3	Two Storied Single Bay Bare Frame (Specimen 1)	52
4.4	Two Storied Single Bay Infill Frame having Door Opening (Specimen 2)	57
4.5	Two Storied Single Bay Infill Frame having Window Opening (Specimen 3)	62
4.6	Comparison of Theoretical Results in STAAD.Pro with the Experimental Results	66
4.7	Theoretical Investigation	67
4.8	Results of Parametric Study	67
4.9	Effect of Infill having Opening on Story Sway	67
4.9.1	Top Deflection of Frames	67
4.9.2	Story wise Deflection of Frames	69
4.9.3	Story Wise Deflection Pattern with respect to ESA Deflection of Bare Frame	73
4.9.4	Inter Story Drift	76
4.10	Effect of Infill having Opening on Maximum Bending Moment	78

4.11	Effect of Infill having Opening on Maximum Shear Force	82
4.12	Effect of Infill having Opening on Base Shear	87
4.13	Mode Shapes of Frames	88
<b>CHAPTER V</b>	<b>CONCLUSIONS AND RECOMMENDATIONS</b>	89
5.1	General	89
5.2	Conclusions	89
5.3	Recommendations	90
<b>REFERENCES</b>		91
<b>APPENDIX A1</b>		97
<b>APPENDIX A2</b>		104
<b>APPENDIX B1</b>		111
<b>APPENDIX B2</b>		113
<b>APPENDIX B3</b>		115
<b>APPENDIX B4</b>		121

## LIST OF TABLES

<b>Table No.</b>	<b>Description</b>	<b>Page No.</b>
2.1	Physical requirements of solid bricks (ASTM C 62)	20
2.2	Mortar types for classes of construction (ASTM C 270)	21
2.3	Property specifications for mortar (ASTM C 270)	22
2.4	Compressive strength of mortar (psi) (ASTM C 270)	23
2.5	Compressive strength of masonry based on the compressive strength of the clay masonry units and type of mortar used in construction (ACI / ASCE / TMS Table 1.6. 2.1)	23
2.6	Specified compressive strength of masonry, $f'_m$ (psi), based on specifying the compressive strength of masonry units (ACI 530.1-92/ASCE 6-92/TMS 602-92)	24
2.7	Specified compressive strength of clay masonry assemblages $f'_m$ (psi) (ACI/ ASCE/TMS, 1992)	25
2.8	Clay masonry $f'_m$ , $E_m$ , n and G values based on clay masonry unit strength and the mortar type (ACI/ ASCE/TMS, 1992)	26
2.9	In-plane damage reduction factor (Al-Chaar, 2002)	33
3.1	Amount of reinforcements in the specimen	36
3.2	Properties of concrete of the specimen	42
3.3	Parameters for lateral force calculation (BNBC, 1993)	43
3.4	Properties of RC frame components	45
3.5	Properties of infill frame having door opening	46
3.6	Properties of infill frame having window opening	47
4.1	Top deflection of 4 storied building	68
4.2	Top deflection of 7 storied building	68
4.3	Top deflection of 10 storied building	69
4.4	Inter story drift at ground floor level of 4 storied building	77
4.5	Inter story drift at ground floor level of 7 storied building	77
4.6	Inter-story drift at ground floor level of 10 storied building	78

4.7	Maximum moment and their governing location for 4 storied building for fixed support	79
4.8	Maximum moment and their governing location for 7 storied building for fixed support	79
4.9	Maximum moment and their governing location for 10 storied building for fixed support	80
4.10	Maximum moment and their governing location for 4 storied building for hinged support	81
4.11	Maximum moment and their governing location for 7 storied building for hinged support	81
4.12	Maximum moment and their governing location for 10 storied building for hinged support	82
4.13	Maximum shear and their governing location for 4 storied building	83
4.14	Maximum shear and their governing location for 7 storied building	83
4.15	Maximum shear and their governing location for 10 storied building	84
4.16	Base shear of all types of frames	87
A1.1	Instrumentation plan for Specimen 1, RC bare frame	97
A1.2	Instrumentation plan for Specimen 2, infill RC frame having door opening	99
A1.3	Instrumentation plan for Specimen 3, infill RC frame having window opening	101

## LIST OF FIGURES

<b>Figure No.</b>	<b>Description</b>	<b>Page No.</b>
2.1	(a) The diagonal compression strut of masonry infill (b) Material modeling of masonry infill as diagonal strut (Holmes, 1961)	6
2.2	Change in lateral load transfer mechanism due to masonry infill (Murty and Jain, 2000)	10
2.3	Interactive behavior of frame and infill (Smith and Coull, 1991)	11
2.4	Analogous braced frame (Smith and Coull, 1991)	11
2.5	Modes of infill failure (Smith and Coull, 1991)	12
2.6	Modes of frame failure (Smith and Coull, 1991)	12
2.7	Open ground story building (a) actual building (b) building being assumed in current design practice (Haque, 2007)	13
2.8	Effects of masonry infill on the first mode shape of a typical frame of a ten story RC building (a) displacement profile (b) fully infill frame (c) open ground floor frame (EERI, 2001)	14
2.9	Soft story building acting as an inverted pendulum (Haque, 2007)	15
2.10	Normalized Response Spectra for 5% Damping Ratio (BNBC, 1993)	17
2.11	Specimen deformation shape (Al-Chaar, 2002)	27
2.12	Equivalent diagonal strut (Al-Chaar, 2002)	28
2.13	Strut geometry (Al-Chaar, 2002)	28
2.14	Placement of strut (Al-Chaar, 2002)	30
2.15	Partially infill frame (Al-Chaar, 2002)	31
2.16	Perforated panel (Al-Chaar, 2002)	31
2.17	Possible strut placement for perforated panel (Al-Chaar, 2002)	32
2.18	Visual damage classification (Al-Chaar, 2002)	33
2.19	Distance to beam hinge (Al-Chaar, 2002)	34
2.20	Plastic hinge placement (Al-Chaar, 2002)	34
3.1	Bricks used for infill in the specimen	36

3.2	Base fixation of the specimen and test setup of reaction frame	37
3.3	Strain gauge, adhesive used on the surface of specimen	38
3.4	LVDTs, data logger and computer set used for testing of specimens	39
3.5	Reinforcement details for two storied single bay RC frame	39
3.6	Instrumentation plan for (a) Specimen 1 (b) Specimen 2 (c) Specimen 3	41
3.7	Model of two storied single bay RC (a) bare frame (b) infill frame having door opening and (c) infill frame having window opening	48
3.8	Model of 4 bay 4 storied building frame	48
3.9	Model of 4 bay 7 storied building frame	49
3.10	Model of 4 bay 10 storied building frame	49
4.1	Specimen 1, Instrumentation of two storied single bay bare frame	54
4.2	Specimen 1, Formation of cracks in two storied single bay bare frame	55
4.3	Specimen 1, Failure of two storied single bay bare frame	55
4.4	Specimen 1, Experimental load deflection curve for LVDT-3	56
4.5	Specimen 1, Load vs strain curve for strain gauge S1	56
4.6	Specimen 2, Instrumentation and first crack formation of two storied single bay infill frame having door opening	58
4.7	Specimen 2, Formation of cracks in two storied single bay infill frame having door opening	59
4.8	Specimen 2, Failure of two storied single bay infill frame having door opening	60
4.9	Specimen 2, Experimental load deflection curve for LVDT-3	61
4.10	Specimen 2, Load vs strain curve for strain gauge S13	61
4.11	Specimen 3, Instrumentation and first crack formation of two storied single bay infill frame having window opening	63
4.12	Specimen 3, Formation of cracks of two storied single bay infill frame having window opening	65
4.13	Specimen 3, Experimental load deflection curve for LVDT-3	65

4.14	Specimen 3, Load vs strain curve for strain gauge S2	66
4.15	Story wise deflection of (a) 4 storied (b) 7 storied and (c) 10 storied building frames for fixed support with aspect ratio of 1:1	71
4.16	Story wise deflection of (a) 4 storied (b) 7 storied and (c) 10 storied building frames for hinged support with aspect ratio of 1:1	72
4.17	Story wise deflection pattern of (a) 4 storied (b) 7 storied and (c) 10 storied building frames for fixed support with respect to ESA deflection of bare frame with aspect ratio of 1:1	74
4.18	Story wise deflection pattern of (a) 4 storied (b) 7 storied and (c) 10 storied building frames for hinged support with respect to ESA deflection of bare frame with aspect ratio of 1:1	76
4.19	Governing location of (a) maximum moment and (b) maximum shear for 4 storied building	85
4.20	Governing location of (a) maximum moment and (b) maximum shear for 7 storied building	85
4.21	Governing location of (a) maximum moment and (b) maximum shear for 10 storied building	86
4.22	Mode shapes of 4 bay 7 storied building	88
A2.1	Specimen 1, Experimental load deflection curve for (a) LVDT-1, (b) LVDT-5 and (c) LVDT-4	105
A2.2	Specimen 2, Experimental load deflection curve for (a) LVDT-1, (b) LVDT-5 and (c) LVDT-4	106
A2.3	Specimen 3, Experimental load deflection curve for (a) LVDT-1, and (b) LVDT-5	107
A2.4	Specimen 1, Load vs strain for strain gauge (a) S1 and (b) S8	108
A2.5	Specimen 2, Load vs strain for strain gauge (a) S9 and (b) S10	109
A2.6	Specimen 3, Load vs strain for strain gauge (a) S8 and (b) S9	110
B4.1	Story wise deflection of (a) 4 storied (b) 7 storied and (c) 10 storied building frames for fixed support with aspect ratio of 1:1.5	122
B4.2	Story wise deflection of (a) 4 storied (b) 7 storied and (c) 10 storied building frames for fixed support with aspect ratio of 1:2	123

B4.3	Story wise deflection of (a) 4 storied (b) 7 storied and (c) 10 storied building frames for fixed support with aspect ratio of 1:2.5	125
B4.4	Story wise deflection of (a) 4 storied (b) 7 storied and (c) 10 storied building frames for hinged support with aspect ratio of 1:1.5	126
B4.5	Story wise deflection of (a) 4 storied (b) 7 storied and (c) 10 storied building frames for hinged support with aspect ratio of 1:2	128
B4.6	Story wise deflection of (a) 4 storied (b) 7 storied and (c) 10 storied building frames for hinged support with aspect ratio of 1:2.5	129
B4.7	Story wise deflection pattern of (a) 4 storied (b) 7 storied and (c) 10 storied building for fixed support with respect to ESA deflection of bare frame with aspect ratio of 1:1.5	131
B4.8	Story wise deflection pattern of (a) 4 storied (b) 7 storied and (c) 10 storied building for fixed support with respect to ESA deflection of bare frame with aspect ratio of 1:2	132
B4.9	Story wise deflection pattern of (a) 4 storied (b) 7 storied and (c) 10 storied building for fixed support with respect to ESA deflection of bare frame with aspect ratio of 1:2.5	134
B4.10	Story wise deflection pattern of (a) 4 storied (b) 7 storied and (c) 10 storied building for hinged support with respect to ESA deflection of bare frame with aspect ratio of 1:1.5	135
B4.11	Story wise deflection pattern of (a) 4 storied (b) 7 storied and (c) 10 storied building for hinged support with respect to ESA deflection of bare frame with aspect ratio of 1:2	137
B4.12	Story wise deflection pattern of (a) 4 storied (b) 7 storied and (c) 10 storied building for hinged support with respect to ESA deflection of bare frame with aspect ratio of 1:2.5	138



## NOMENCLATURE

<b>Nomenclature</b>	<b>Name</b>
RC	: Reinforced Concrete
BNBC	: Bangladesh National Building Code
ESA	: Equivalent Static Analysis
RSA	: Response Spectrum Analysis
UBC	: Uniform Building Code
IBC	: International Building Code
ASTM	: American Society for Testing and Materials
MPa	: Mega Pascal
psi	: Pound per Square Inch
%	: Percentage
$f'_m$	: Compressive Strength of the Entire Masonry Assemblage
ACI	: American Concrete Institute
ASCE	: American Society of Civil Engineers
TMS	: The Masonry Society
$E_m$	: Modulus of Elasticity of Masonry Unit
$f'_c$	: Concrete Compressive Strength of Cylindrical Specimen at 28 Days
w	: Weight
n	: Modular Ratio
G	: Modulus of Rigidity
$E_s$	: Modulus of Elasticity of Steel
$E_c$	: Modulus of Elasticity of Concrete
a	: Equivalent Width of Infill Strut
t	: Thickness of the Masonry Infill Panel
$\lambda_1 H$	: Relative Infill to Frame Stiffness
H	: Height of the Confining Frame
$\theta$	: Angle of the Concentric Equivalent Strut
$I_{col}$	: Moment of Inertia of Column
h	: Height of the Infill Panel
D	: Diagonal Length of Infill
$(R_1)_i$	: Reduction Factor for in-plane Evaluation due to Presence of Openings

$(R_2)_i$	:	Reduction Factor for in-plane Evaluation due to Existing Infill Damage
$a_{red}$	:	Reduced Equivalent Strut Width
$l_{column}$	:	Distance of Strut Pin-connected to Column from the Face of Beam
$\theta_{column}$	:	Angle between Strut and Beam
$l$	:	Length of the Infill Panel
$A_{open}$	:	Area of the Opening
$A_{panel}$	:	Area of the Infill Panel
$L_{beam}$	:	Hinged Placed at a Minimum Distance from the Face of the Column
$\theta_{beam}$	:	Distance of Strut Pin-connected to the Column from the Face of the Column
SRSS	:	Square Root of Sum of Squares
CQC	:	Complete Quadratic Combination
mm	:	Millimeter
kN	:	Kilo Newton
MS	:	Mild Steel
$\sigma$	:	Steel Ratio
c/c	:	Centre to Centre Distance
$^{\circ}\text{C}$	:	Degree Celsius
LVDTs	:	Linear Variable Displacement Transducers
GPa	:	Giga Pascal
z	:	Seismic Zone Coefficient
I	:	Structural Importance Coefficient
R	:	Response Modification Coefficient
S	:	Site Coefficient
T	:	Time Period
d	:	Depth
S	:	Strain Gauge
ID	:	Inter Story Drift
$C_t$	:	Time Period Coefficient
V	:	Design Base Shear
$h_n$	:	Height of Structure

# CHAPTER I

## INTRODUCTION

### 1.1 Background of the Study

Masonry is one of the oldest construction materials currently used around the world. This material has been widely used for hundreds of years by various cultures in typical construction to satisfy the demands of accessibility, aesthetics, functionality, cost etc. It has been commonly used in Reinforced Concrete (RC) frame building structures as infill where it is intended to act as an environmental divider rather than a structural element. The primary function of masonry infill wall is either to protect the inside of the structure from the environment (rain, snow, wind etc.) or to divide inside spaces. In either case, common practice has always been to ignore the consideration of infill during the design and analysis of reinforced or steel concrete frame structures (Al-Chaar, 2002).

Infill-frame refers to a structural system in which a traditional masonry wall is combined with a relatively modern structural Reinforced Concrete or steel frame (Mohyeddin-Kermani, 2011). This combination is such that the exterior masonry walls and/or interior partitions are built as an infill panel between the frame members, namely beams and columns.

Over the last few decades, tremendous efforts have been directed toward understanding the effect of masonry infill walls on Reinforced Concrete frame subjected to lateral loading. Since the 1950s, Reinforced Concrete frames with masonry infill panels have become popular in high seismic zones because they are economical. As masonry infill walls are used for insulation and partition purposes rather than structural purposes and generally considered as nonstructural elements in structural design, the combined behavior of masonry infill and RC frame cannot be calculated according to building code specifications (Al-Chaar, 1998). The inherent uncertainties of the infill walls introduce

difficulty to regard them as structural members. These uncertainties are associated to both the infill wall and the surrounding frame (Sonmez, 2013).

The variability in the material properties of the constituent elements and high nonlinearity of the masonry panels make it difficult to predict the actual behavior of the infill walls. Moreover, the properties of the infill wall highly depend on the quality of the bricks, mortar and the workmanship. Typically, quality control of these factors is poor in most applications. In addition, the properties of the frames such as reinforcement detailing, member capacities, number of bays and stories are the factors that influence the behavior of the infill frames (Sonmez, 2013).

Performance of buildings in the recent earthquakes clearly illustrates that the presence of infill walls has significant structural implications (Mondal and Jain, 2008). Various experimental investigations conducted in the past have shown that the masonry infill walls in a Reinforced Concrete frame not only add significant strength and stiffness but also influence the dynamic behavior of the entire building (Al-Chaar, 1998). When masonry infill walls are considered to interact with their surrounding frames, the lateral stiffness and lateral load capacity of the structure largely increase compared to those of the bare frames while decreasing the average drifts. Therefore, the structural contribution of infill walls cannot simply be neglected particularly in regions of moderate and high seismicity. Also the frame-infill interaction may cause substantial increase in both stiffness and strength of the frame in spite of the presence of openings such as door and window (Mondal and Jain, 2008). This interaction can be advantageous, if the infill walls are located appropriately throughout the structure and taken into account in the analysis process, if possible. However, these effects may or may not be advantageous depending on the case. If separation joints between infill and bounding frame are not provided, interaction of the frame and infill wall reveals a different behavior than what is expected. Infill walls are stiff but brittle elements. If the surrounding frame is not strong enough, infill walls can cause unforeseen damages such as premature failures in columns such as shear, compression or tension failures (Sonmez, 2013).

Thus infill walls have been identified as a contributing factor to catastrophic structural failures in earthquakes. Frame or partial infill interaction can cause brittle shear failures of

Reinforced Concrete columns and short column effect. Furthermore, infill wall can over-strengthen the upper stories of a structure and result in a soft first story, which is highly undesirable from the perspective of seismic safety (Al-Chaar and Mehrabi, 2008). This mechanism of soft story development is more likely to occur in the structures without infill walls at bottom story. However, it is not uncommon to have formation of soft stories after losing the lower story infill walls due to the high drift concentration in lower stories (Sonmez, 2013).

The review of the literature showed that a number of both experimental and numerical studies have focused to find out the effect of masonry infill walls on RC frames in the last 50 years. Infill frame exhibit a complex composite behavior which is affected by numerous factors such as material properties, relative dimensions, type of loading, opening size and location etc. Despite all research efforts, research into the behavior of Reinforced Concrete frame with masonry infill walls having opening due to lateral loading still needs to be investigated in the laboratory and its parametric study from static and dynamic points of view. This research work aimed to investigate the behavior of Reinforced Concrete frame with masonry infill walls having opening subjected to lateral loading by experimental investigation and parametric study in terms of static and dynamic analysis.

## **1.2 Objectives of the Study**

The main objectives of this research include:

- i. To study the behavior of reinforced concrete frame with masonry infill wall having opening subjected to in-plane lateral loading.
- ii. To compare the results of Equivalent Static Analysis with Response Spectrum Analysis for RC frame with masonry infill walls having opening, varying number of story and aspect ratios.
- iii. To investigate the effect in the deflection, inter story drift, base shear, moment and shear of RC frame due to lateral loading in presence of infill having opening.

### **1.3 Organization of the Thesis**

The thesis is organized as per detail given below:

Chapter I presents an introduction to the RC frame with masonry infill structural system and explains the aim of this research.

Chapter II presents a literature review in chronological order of the most relevant experimental works pertaining to RC frames with masonry infill walls subjected to lateral loading. This chapter includes the literature related to the dynamic response of masonry infill RC frame due to lateral loading, material properties and equivalent strut concept.

Chapter III presents the experimental program including testing, instrumentation, test setup, mechanical properties of materials. This chapter also represents the determination of various parameters from code and analytical calculations to carry out the parametric study in Equivalent Static Analysis and Response Spectrum Analysis.

Chapter IV describes the experimental test results including descriptions of the strength, displacement and crack formation for each specimen. The results from parametric study such as base shear, deflection, inter story drift, shear, moment and mode shapes are compared and analyzed to find out the effects of infill walls having opening on RC frame in Equivalent Static Analysis and Response Spectrum Analysis.

Finally in Chapter V, salient conclusions and recommendations of this study are given in this chapter followed by the references.

Appendix A shows the instrumentation plan for specimens, load-deflection and load-strain figures of experimental analysis. Appendix B shows the verification of base shear, calculation of equivalent strut width, input file for Equivalent Static Analysis and Response Spectrum Analysis and also figures of parametric study.

## **CHAPTER II**

### **LITERATURE REVIEW**

#### **2.1 Introduction**

This chapter covers literature review of infill frames which is categorized in three groups of articles. First section presents a review of research on in-plane behavior of infill frames in chronological order; hence it provides information on both experimental and theoretical studies. Although, the emphasis of this thesis is on Reinforced Concrete infill frames, some of the important studies on infill steel frames are also reviewed due to similarities between them, specifically in the behavior of infill panels. The second section represents the articles related to response of masonry infill RC frame due to lateral loading, definition of soft story and dynamic Response Spectrum Method. In the third section, material properties such as brick, mortar, selection of masonry properties, equivalent strut width concept depending on various codes and published literature are described.

#### **2.2 Chronological Literature Review of Analytical and Experimental Studies**

The concept of the equivalent strut from in-plane loading testing on a three story three bay steel frame with infill was first proposed by Polyakov in 1956. From this study, it was found that stresses from the frame to the infill were only transmitted in compression zone of infill-to-frame interface and deformations were concentrated at the ends of compression diagonals whereas deformations diminished towards the ends of tension diagonals.

Three types of one story one bay specimens were tested under in-plane lateral loading and some approximate relationships were generated to predict the behavior of walls (Benjamin and Williams, 1958). In this study it was found that the aspect ratio has an important influence on ultimate strength and rigidity and the greater the aspect ratio, is the greater the strength. Plain brick masonry wall panels showed significant strengths when properly confined by a frame.

The first research on modeling of infill panel as an equivalent diagonal strut was published by Holmes in 1961. A method had been proposed for predicting the deformations and strength of infill frames based on the equivalent diagonal strut concept. It was assumed that infill wall acts as a diagonal compression strut, as shown in Figure 2.1, of the same thickness and elastic modulus as the infill with a width equal to one-third the diagonal length. It was also concluded that at the infill failure, the lateral deflection of the infill frame was small compared to the deflection of the corresponding bare frame.

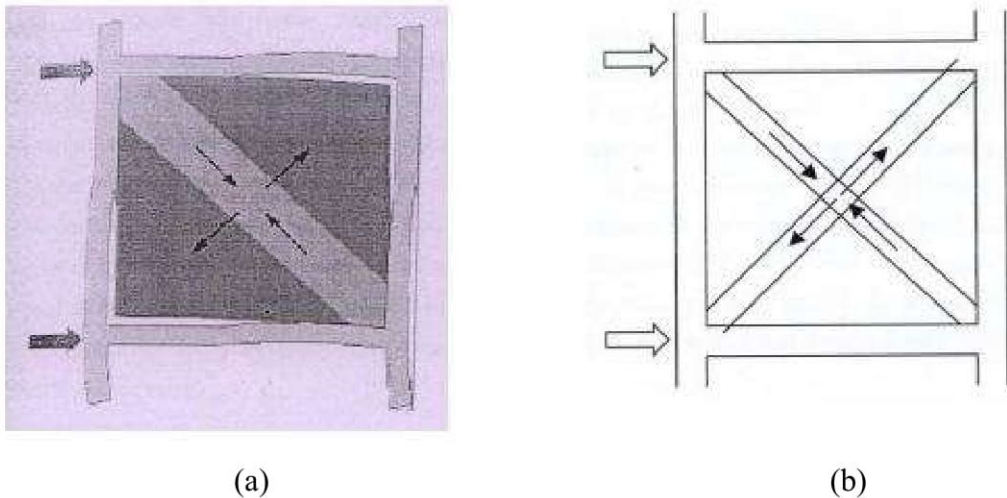


Figure 2.1: (a) The diagonal compression strut of masonry infill (b) Material modeling of masonry infill as diagonal strut (Holmes, 1961)

Laboratory tests were conducted in 1962 by Smith on infill panels constructed of mortar only considering a small scale of about 1:20. It was found that for an infill surrounded by a frame, the stiffer the frame, the longer was the length of contact between the panel and frame and the longer the contact length, the wider the effective width of the equivalent diagonal strut. Smith then expanded upon his earlier investigation and further studied the length of contact between the infill and the surrounding frame in 1966. A parameter,  $\lambda$  was developed to determine this contact length. The parameter,  $\lambda$  was used to determine the width of the equivalent strut and the relative stiffness between the frame and infill.

A method of analysis was developed for infill frames based on the equivalent strut concept by Smith and Carter, later in 1969. Infill and frame were not assumed to be constructed integrally, nor were they deliberately bonded together. The lateral stiffness of the infill



frames was calculated based on an effective width of the equivalent strut deduced from strains in stress analysis. Possible failure modes identified were tensile failure of windward columns and shear failure of the columns and beams and their connections.

The interaction of Reinforced Concrete frames with masonry filler walls was studied considering the effects of openings on wall, frame reinforcement and vertical loads due to static lateral loads (Fiorato et al., 1970). A total of 27 tests were carried out using one-eighth scale models of Reinforced Concrete frames. Eight one story one bay infill frames, twelve five story one bay infill frames and six two story three bay infill frames were tested. It was concluded that Reinforced Concrete frames with filler walls subjected to lateral load do not behave as frames at any other loading stage. The critical stage in the response of the frame-wall system was the development of a shearing crack, which ideally forms along a single joint separating the wall into two parts. The frame did contribute significantly to the capacity of the structures after cracking of the wall.

The effects of openings in the infill and shear connectors between the frame and infill were investigated considering the effects of the location of openings in the infill on lateral stiffness and ultimate load by Mallick and Garg in 1971. Openings at either end of a loaded corner without shear connectors reduce the stiffness by 75% and they reduce the stiffness by 85 to 90% compared to infill frames without openings. The stiffness is reduced by 60 to 70% for infill frames with shear connectors and openings, versus one without openings. A central opening within the infill panel reduced stiffness by 25 to 50% as compared to the frames without openings. Doors are best placed in the center of the lower half and windows are best placed at mid-height of the left or right side, toward the vertical edge as possible.

The influence of initial gaps on infill frame behavior is studied to determine how the behavior of infill frames is affected by the presence of initial gaps between the infill and frame (Riddington, 1984). The testing specimen included steel frames of different stiffness such as with no infill, an infill with no initial gaps and an infill with initial gaps. The panels had square dimensions and were approximately full-scale. It was found that the presence of gaps is undesirable because of the reductions in stiffness. This problem is likely to occur when masonry infill is used with concrete beams and columns. Gaps are

often left in the masonry to allow for creep in the concrete members. If no gaps are provided, the creep of a concrete column could cause a crushing failure in the compression corner of the mortar of the infill.

The behavior of RC frames with masonry infill was investigated by Al-Chaar et al. in 1996. Two half-scale specimens were tested with brick masonry infill, but one had a strong frame and the other had a weak frame. A third specimen, identified as the large frame, contained low modulus concrete masonry units and was full-scale. The failure mechanism, load versus drift behavior, diagonal deformation and joint rotation were all examined for each of the three different specimens. The strong frame failed due to diagonal tension cracking and showed ductile behavior. The weak frame failed from diagonal cracking and hinged in the windward column and although at lower load resistance, it also showed ductile behavior. The large frame failed from poor bonding between blocks and exhibited joint slippage between all courses. Overall, it was concluded that more research is needed in the area of infill frames. However, it was considered safe to conclude that, if structurally designed, infill frames give significant strength, ductility and energy dissipation increases with respect to plane frames. These increases are very desirable in seismic regions.

Bennett suggested in 1996 that the equivalent strut of Smith and Carter (1969) can be considered for seismic analysis of existing structures. They added two important additional restrictions on the equivalent strut. First, for very stiff columns, the strut formation predicts significantly high contact lengths. It was suggested that the contact length be limited to 20% of the infill height, to avoid unreasonably high stiffness of the infill. Second, it is suggested that the cracked moment of inertia for beams and columns be taken as one-half of the gross moment of inertia.

Five, one story half-scale, non-ductile RC frames were tested by Al-Chaar (1998). Four of these specimens are infill with either a concrete masonry unit (CMU) wall or a clay brick wall. One of the infill frames was a single bay with CMU infill, one was a single bay with brick infill, one was a two bay with CMU infill, and one was a three bay with brick infill. The single bay infill frame with a CMU wall failed mainly by shear. A shear crack observed at the top of the windward column and a shear crack formed at the bottom of the

leeward column. In the single bay frame infill with a brick wall, it was observed a hinge in the middle of the windward column, a hinge in the beam at the windward joint, and a separation between the leeward column and the base because of the inability of the reinforcement to develop resistance. The failure mechanism of the two bay specimen was by the formation of two hinges on the windward and center columns, shear cracking in the infill wall and shear cracking at the base of the leeward column. The failure of the specimen with three bays was dominated by shear cracks in all four columns.

Thirteen half-scale infill RC frames were tested by Colangelo in 2005. Pseudo-dynamic tests were performed on single bay single story specimens designed to represent the first story in a four story building. Inclined cracks were observed at top of the columns in the frames not designed for lateral loads and had an aspect ratio of 0.57. Increases in stiffness, peak strength and ductility demand were found compared to these of a bare frame.

Two phase large scale experimental study was conducted by Stavridis in 2009. The first phase consisted of four 2/3-scale infill RC frames with different opening configurations tested quasi-statically. It was stated that the presence of openings in the infill wall affected the behavior of the system in terms of stiffness, strength and mode of failure. It was found that shear failure could take place when the developed struts in the solid masonry wall acted against the RC frames. It was also suggested that these brittle failures could be avoided if openings were located such that the behavior was controlled by flexure.

## **2.3 Literature Review for Parametric Study**

The literature review for parametric study is given below:

### **2.3.1 Response of Masonry Infill RC Frame under Lateral Loading**

The masonry infill walls are used as partitioning, providing building envelop, avoiding fire hazard, temperature and sound barrier etc. in RC frame. When lateral force acts on the structure, stiffness is developed on the upper floors due to interaction between masonry infill walls and the surrounding frame. This stiffening action is usually not considered in the design of structure (Alam, 2014). The presence of masonry infill wall in RC frames

changes the lateral load transfer mechanism of the structure from predominant frame action to predominant truss action (Murty and Jain, 2000), as shown in Figure 2.2, which is responsible for reduction in bending moments and increase in axial forces in the frame members.

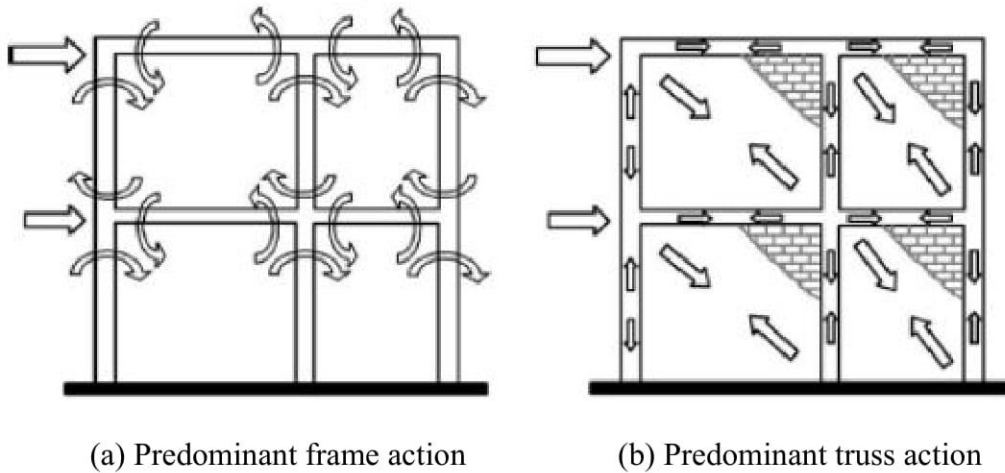


Figure 2.2: Change in lateral load transfer mechanism due to masonry infill (Murty and Jain, 2000)

Masonry infill walls confined by Reinforced Concrete (RC) frames on all four sides play an important role in resisting the lateral seismic loads on building frame. The behavior of masonry infill frames has been extensively studied (Murty and Jain, 2000; Smith and Coull, 1991) in attempts to develop a rational approach for design of such frames. Experimentally masonry infill walls were found to have a very high initial lateral stiffness and low deformability (Moghaddam and Dowling, 1987).

Researchers have concluded that proper use of infill in frames could result in significant increases in the strength and stiffness of structures subjected to seismic excitations (Mehrabi et al., 1996; Klingner and Bertero, 1978; Bertero and Brokken, 1983). However, the locations of infill in a building must be carefully selected to avoid or minimize torsional effects as well as soft story effect. Architectural restrictions have to be considered when assigning these locations. The high in-plane rigidity of the masonry wall significantly stiffens the relatively flexible frame. Therefore, a relatively stiff and tough bracing system is resulted. The wall braces the frame partly by its in-plane shear resistance and partly by its behavior as a diagonal bracing strut as shown in Figure 2.3.

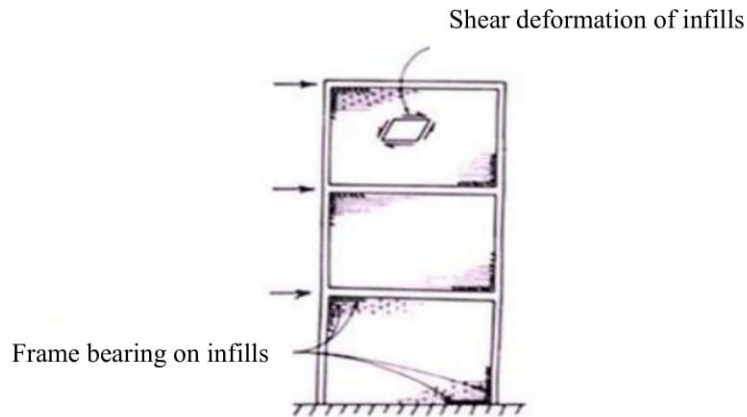


Figure 2.3: Interactive behavior of frame and infill (Smith and Coull, 1991)

When the frame is subjected to horizontal loading, it deforms with double curvature bending of the columns and beams. The translation of the upper part of the column in each story and the shortening of the leading diagonal of the frame cause the column to lean against the wall as well as to compress the wall along its diagonal. It is roughly analogous to a diagonally braced frame, shown in Figure 2.4. The nature of the forces in the frame can be understood by referring to the analogous braced frame shown in Figure 2.4. The windward column or the column facing the seismic load first is in tension and the leeward column or the other side of the building facing seismic load last is in compression. Since the infill bears on the frame not as exactly a concentrated force at the corners, but over the short lengths of the beam and column adjacent to each compression corner, the frame members are subjected also to transverse shear and a small amount of bending. Consequently the frame members or their connections are liable to fail by axial force or shear and especially by tension at the base of the windward column (Smith and Coull, 1991).

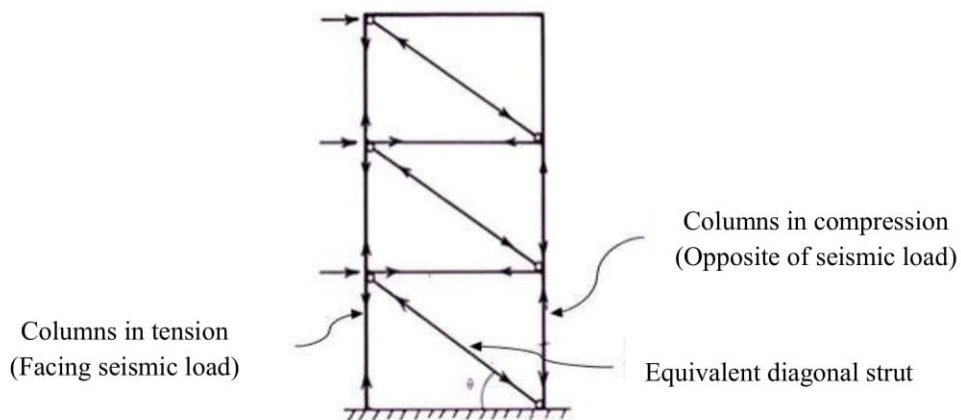


Figure 2.4: Analogous braced frame (Smith and Coull, 1991)

The potential modes of failure of masonry infill frame structure are occurred due to the interaction of infill walls with frame. The failure criteria are: tension failure of tensioning column due to overturning moments, flexure or shear failure of columns, compression failure of the diagonal strut, diagonal tension cracking of the panel and sliding shear failure of the masonry along horizontal mortar beds. Failure modes are described by the Figures 2.5 and 2.6. The perpendicular tensile stresses are caused by the divergence of compressive stress trajectories on the opposite sides of loading diagonal as they approach the mid region of infill. The shear failure of wall steps down through the joints of masonry and participated by horizontal shear stresses in bed joints. The diagonal cracking is initiated at and spreads from the middle of infill, where tensile stresses are a maximum, tending to stop near compression corners, where tension is suppressed the diagonal cracking of the wall is through the masonry along a line or line parallel to loading diagonal and caused by tensile stresses perpendicular to loading diagonal (Alam, 2014).

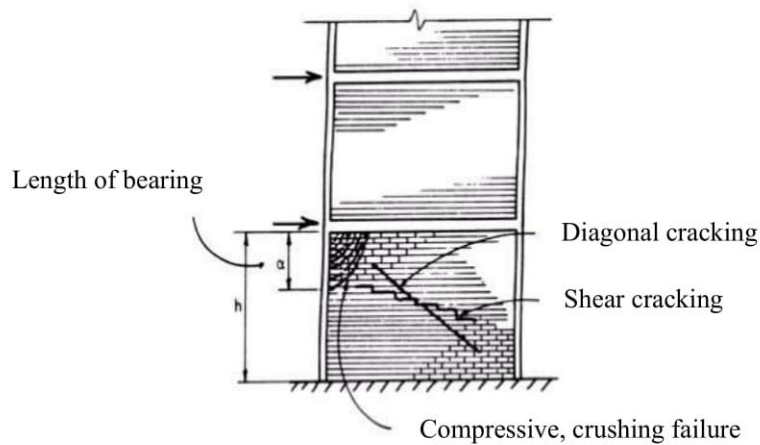


Figure 2.5: Modes of infill failure (Smith and Coull, 1991)

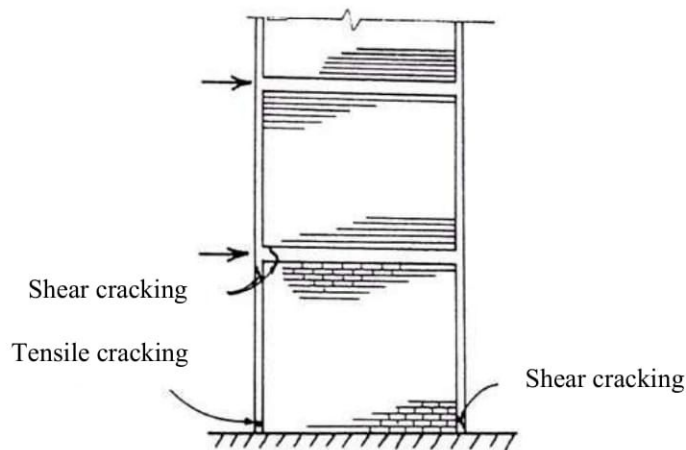


Figure 2.6: Modes of frame failure (Smith and Coull, 1991)

### 2.3.2 Review of Definitions of Soft Story from Code

According to BNBC (1993) and UBC (2000) a soft story is the one in which the lateral stiffness is less than 70% of that in the story above or less than 80% of the average stiffness of the three storeys above and in IBC (2000) an extreme soft story is one in which the lateral stiffness is less than 60 percent of that in the story above or less than 70 percent of the average stiffness of the three stories above. The vertical geometric irregularity shall be considered to exist where the horizontal dimensions of the lateral-force-resisting system in any story is more than 130 percent of that in an adjacent story. The most common form of vertical discontinuity arises due to the unintended effect of infill component. Usually in analysis only the bare frame effect is considered ignoring the effect of infill walls and code has no clear suggestion about the infill walls on frames. The problem is most severe in structures having relatively flexible lateral load resisting system because the infill can compose a significant portion of the total stiffness (Rashid, 2005).

### 2.3.3 Effect of Earthquake on Buildings with Soft Story

Open ground story buildings are inherently poor systems with sudden drop in stiffness and strength in the ground story. In the current practice, stiff masonry walls Figure 2.7 (a) are neglected and only bare frames are considered in design calculations Figure 2.7 (b).

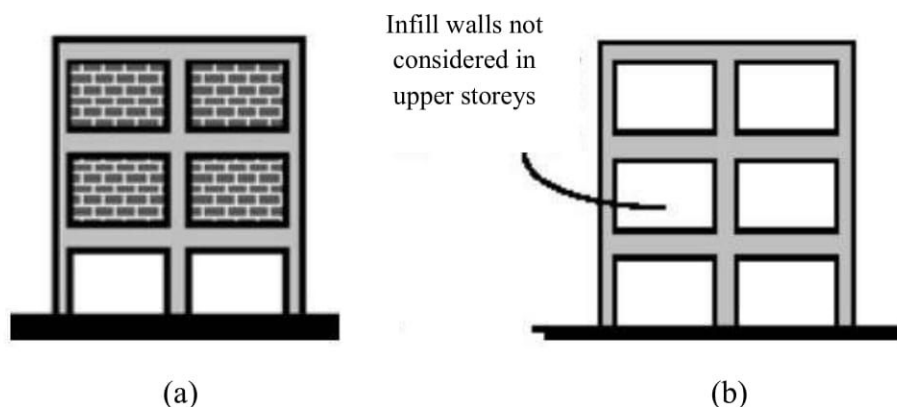


Figure 2.7: Open ground story building (a) actual building (b) building being assumed in current design practice (Haque, 2007)

In case of a fully infill frame, lateral displacements are uniformly distributed throughout the height as shown in Figure 2.8 (a) and (b). On the other hand, in the case of open ground floor buildings, most of the lateral displacement is accumulated at the ground level itself because this floor is the most flexible due to absence of infill shown in Figure 2.8 (c). Similarly, the seismic story shear forces and subsequently the bending moments concentrate in the open ground story, instead of gradually varying as in fully infill frame shown in Figure 2.8 (c) and (b) (Haque, 2007).

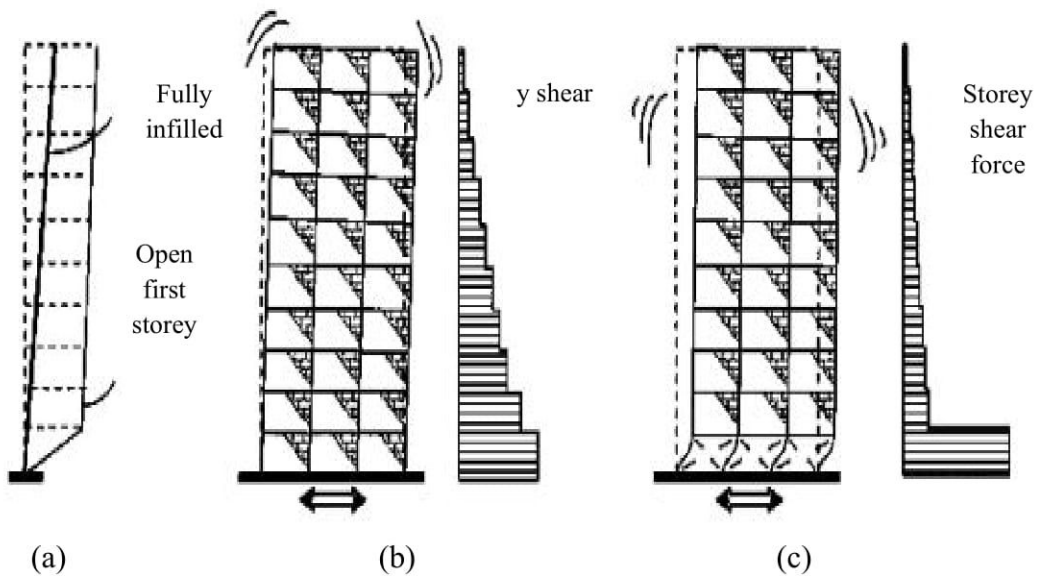


Figure 2.8: Effects of masonry infill on the first mode shape of a typical frame of a ten story RC building (a) displacement profile (b) fully infill frame (c) open ground floor frame (EERI, 2001)

Due to the presence of walls in upper stories makes them much stiffer than the open ground story. Thus, the upper story moves almost together as a single block and most of the horizontal displacement of the building occurs in the soft ground story itself. In common language, this type of buildings can be explained as a building on chopsticks. Thus, such buildings swing back-and-forth like inverted pendulums during earthquake shaking (Figure 2.9) and the columns in the open ground story are severely stressed. If the columns are weak (do not have the required strength to resist these high stresses) so that they do not have adequate ductility, they may be severely damaged which may even lead to collapse of the building (Haque, 2007).



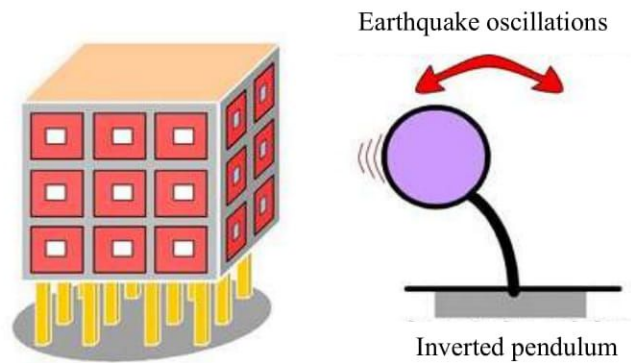


Figure 2.9: Soft story building acting as an inverted pendulum (Haque, 2007)

### 2.3.4 Dynamic Response Spectrum Method

The dynamic response method conforms to the criteria established in BNBC (1993). The mass and mass moment of inertia of various components of a structure required for dynamic analysis should be calculated based on the seismic dead load. The ground motion representation should be one having 20% probability of being exceeded in 50 years. Response Spectrum Method is used to analyze the dynamic responses of a structure subjected to lateral loading. In this method, multiple modes of response of a structure are taken into account. A response spectrum is simply a plot of the peak or steady-state response (displacement, velocity or acceleration) of a series of oscillators of varying natural frequency that are forced into motion by the same vibration. From the resulting plot one can assess the pick of the natural frequency for a particular mass of the linear structure. To get the dynamic impact all significant modes should be considered. The consideration of number of mode should be at least the number of floors. One such use is in assessing the peak response of buildings to earthquakes. The science of strong ground motion may use some values from the ground response spectrum (calculated from recordings of surface ground motion from seismographs) for correlation with seismic damage. If the input used in calculating a response spectrum is steady-state periodic, then the steady-state result is recorded. Damping must be present, or else the response will be infinite. For transient input (such as seismic ground motion), the peak response is reported. Some level of damping is generally assumed but a value will be obtained even with no damping. For single degree freedom system the peak response can be determined directly from the response spectrum for the ground motion without carrying out a response history analysis. But for multiple degrees freedom system the peak response determined directly

from the response spectrum for the ground motion is not identical to the response history analysis result. For this reason, response spectrum analysis procedure is for structures excited by a single component of ground motion; thus simultaneous action of the other two components is excluded and multiple support excitations is not considered (Alam, 2014). According to BNBC 1993, the response spectrum to be used in the dynamic analysis shall be any one of the following:

Site specific design spectra: A site specific response spectra shall be developed based on the geologic, tectonic, seismologic and characteristics associated with the specific site. The spectra shall be developed for a damping ratio of 0.05 unless a different value is found to be consistent with the expected structural behavior at the intensity of vibration established for the site.

Normalized response spectra: In absence of a site-specific response spectrum, the normalized response spectra shall be used in the dynamic analysis procedure as shown in Figure 2.10. The analysis should include peak dynamic response of all modes having a significant contribution to total structural response. Peak modal response should be calculated using the ordinates of the appropriate response spectrum curve which corresponds to the modal periods. Maximum modal contributions should be combined in a statistical manner to obtain an approximate total structural response. This is used in the present analysis. Response Spectrum Method is universally accepted method (Wilson, 2002) for design of structure based on dynamic analysis. A few important aspects of Response Spectrum Method are described below.

#### **2.3.4.1 Modal Shape**

The mode shape changes significantly when infill is present in the building. Vibration frequency gets almost double when infill is present in the model. There will be significant changes in the dynamic characteristics of a building when infill is present. The mode shapes and the corresponding contribution of different modes depend upon the amount and location of infill in the frame because of their high initial stiffness. For performing dynamic analysis, it is a prerequisite to determine natural frequencies and mode shape of a structure (Haque, 2007). Modal analysis is one which determines these two properties.

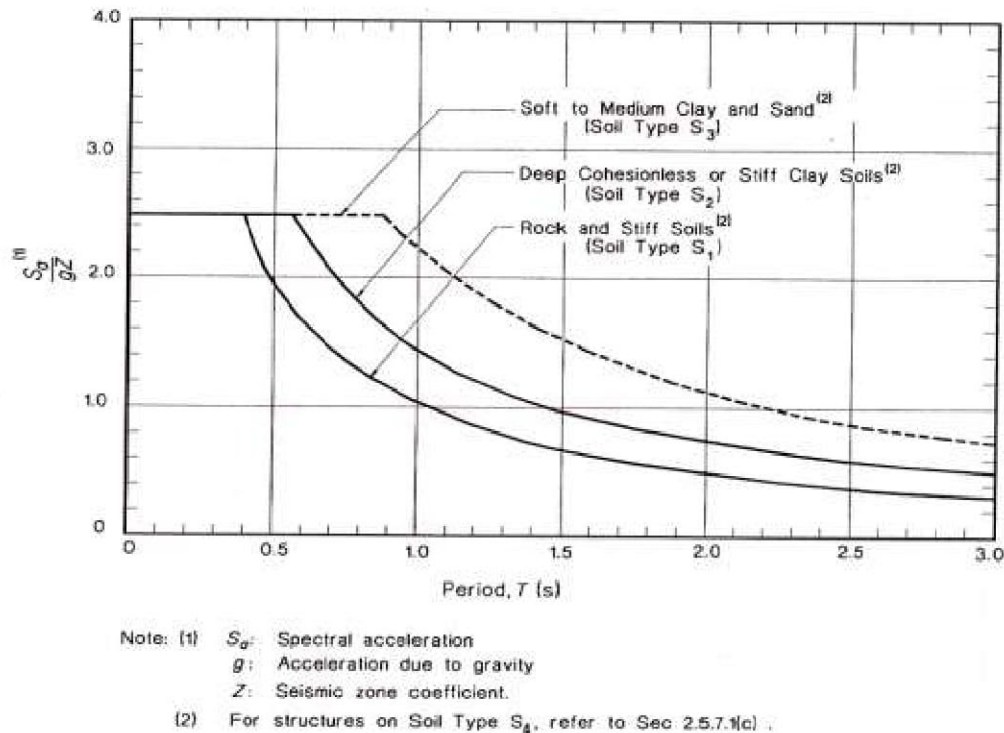


Figure 2.10: Normalized Response Spectra for 5% Damping Ratio (BNBC, 1993)

Each structure has its different mode shapes at different frequencies. Modal analysis shows how a structure vibrates through its different frequencies and produce different mode shape. The goal of modal analysis in structural mechanics is to determine the natural mode shapes and frequencies of an object or structure during free vibration. Modal Analysis is related with structural frequency. It is pseudo dynamic analysis depending on elastic property. So, modal analysis is not suitable for Non-linear analysis (Alam, 2014).

### 2.3.4.2 Number of Modes

Different mode shapes have different frequencies of vibration. Some of the modes are closely spaced showing similar pattern of vibration. All significant modes must be included in the analysis of response spectrum. The modes that are considered, at least 90 percent of the participating mass of the structure is included in the calculation of response for each principal horizontal direction. To review mode shapes in the postprocessor the modes must be expanded. In the single point response spectrum the modal expansion can be performed after the spectrum analysis based on the significance factor (BNBC, 1993).

#### **2.3.4.3 Combination of the Modes**

The peak member forces, displacements, story forces, shears and base reactions for each mode shall be combined using established procedures in order to estimate resultant maximum values of these response parameters. When two dimensional models are used for analysis, modal interaction effects shall be considered when combining modal maximum (BNBC, 1993). Among all methods CQC method is found suitable for the analysis. Different mode combination methods for single point response spectrum analysis such as: Square Root of Sum of Squares (SRSS), Complete Quadratic Combination (CQC), Double Sum (DSUM), Grouping (GRP), Naval Research Laboratory Sum (NRLSUM).

#### **2.3.4.4 Scaling of Results**

Base shear determined by response spectrum for a given direction is different from the base shear obtained by equivalent static force method. It should be adjusted which is termed as scaling of results. Scaling of base shear is done according to Bangladesh National Building Code (BNBC, 1993). Base shear of response spectrum is scaled so that this is equal with base shear found from static analysis. All corresponding parameters including deflections, member forces and moments change in proportion to the adjusted base shear and scaling.

#### **2.3.4.5 Method of Modal Combination**

The most conservative method that is used to estimate a peak value of displacement or force within a structure is to use the sum of the absolute of the modal response values. This approach assumes that the maximum modal values, for all modes, occur at the same point in time. Another very common approach is to use the Square Root of the Sum of the Squares, SRSS, on the maximum modal values in order to estimate the values of displacement or forces. The SRSS rule for modal combination developed in E. Rosenblueth's Ph.D. thesis (1951) is the peak response in each mode is squared, the squared modal peaks are summed, and the square root of the sum provides an estimate of the peak total response.

$$r_0 \approx (\sum_{n=1}^N r_{n0}^2)^{1/2} \dots \dots \dots \text{Equation 2.1}$$

This modal combination rule provides excellent response estimates for structures with well separated natural frequencies. This limitation has not always been recognized in applying this rule to practical problems and at times it has been misapplied to systems with closely spaced natural frequencies such as piping systems in nuclear power plants and multistory buildings with unsymmetrical plan. For three dimensional structures, in which a large number of frequencies are almost identical, this assumption is not justified. The relatively new method of modal combination is the Complete Quadratic Combination (CQC) method (Wilson et al., 1981) that was first published is applicable to a wider class of structures as it overcomes the limitations of the SRSS rule. It is based on random vibration theories and has found wide acceptance by most engineers and has been incorporated as an option in most modern computer programs for seismic analysis. The peak value of a typical force can now be estimated, from the maximum modal values, by the CQC method with the application of the following double summation Equation:

$$r_0 = (\sum_{i=1}^N \sum_{n=1}^N \rho_{in} r_{i0} r_{n0})^{1/2} \dots \dots \dots \text{Equation 2.2}$$

Each of the  $N^2$  terms on the right side of this Equation is the product of the peak responses in the  $i^{\text{th}}$  and the  $n^{\text{th}}$  modes and the correlation coefficient  $\rho_{in}$  for these two modes;  $\rho_{in}$  varies between 0 and 1 and  $\rho_{in} = 1$  for  $i = n$ . Thus Equation 2.2 can be rewritten as to show that the first summation on the right side is identical to the SRSS combination rule of Equation 2.1.

$$r_0 = (\sum_{n=1}^N r_{n0}^2 + \sum_{i=1}^N \sum_{n=1}^N \rho_{in} r_{i0} r_{n0})^{1/2}, i \neq n \dots \dots \dots \text{Equation 2.3}$$

## 2.4 Material Properties

The load carrying capacity of masonry infill wall depends upon the dimensions and support conditions of the frame, the compressive strength and the tensile strength of the masonry wall. Also the presence of door and window as openings has a strong influence on the behavior. In this section, the properties of infill have been discussed.

### 2.4.1 Solid Clay Brick Units

Masonry bricks have been used for structures since the earliest days of mankind due to its availability and economic aspect. In this research, solid clay brick was considered as infill material due to its availability and economic aspect. Standard specification for building brick is specified in ASTM C 62 which states that Brick are manufactured from clay, shale, or similar naturally occurring earthy substances and subjected to a heat treatment at elevated temperatures (firing). The heat treatment must develop sufficient fired bond between the particulate constituents to provide the strength and durability requirements of this specification. According to ASTM C 62 (1994), the bricks grade is given below:

Grade SW (Severe Weathering): Brick are used where high and uniform resistance to damage caused by cyclic freezing is desired and where the brick may be frozen when saturated with water.

Grade MW (Moderate Weathering): Bricks are used where moderate resistance to cyclic freezing damage is permissible or where the brick may be damp but not saturated with water when freezing occurs.

Grade NW (Negligible Weathering): Applies to Brick with little resistance to cyclic freezing damage but which are acceptable for applications protected from water absorption and freezing.

The brick shall conform to the physical requirements such as compressive strength, water absorption and the saturation coefficient for the grade specified as prescribed in Table 2.1.

Table 2.1: Physical requirements of solid bricks (ASTM C 62)

Designation	Minimum Compressive Strength Gross Area, psi (MPa)		Maximum Water Absorption by 5 hours Boiling, %		Maximum Saturation Co-efficient	
	Average of 5 bricks	Individual	Average of 5 bricks	Individual	Average of 5 bricks	Individual
Grade SW	3000 (20.7)	2500 (17.2)	17.0	20.0	0.78	0.80
Grade MW	2500 (17.2)	2200 (15.2)	22.0	25.0	0.88	0.90
Grade NW	1500 (10.3)	1250 (8.6)	No limit	No limit	No limit	No limit

## 2.4.2 Mortar

Mortar is a workable paste used to bind building blocks such as stones, bricks, and concrete masonry units together, fill and seal the irregular gaps between them, and sometimes add decorative colors or patterns in masonry walls. Mortar is a vital ingredient in masonry construction because its characteristics have a strong influence on both the strength and durability of the masonry assemblage. There were originally five types of mortar which were designated as M, S, N, O and K. The types are identified by every other letter of the word mason work. Type K is no longer referred to in the Uniform Building Code or in ASTM C 270 (1994). The requirements for mortar are provided in ASTM C 270 (1994), "Mortar for Unit Masonry". The performance of masonry is influenced by various mortar properties such as workability, bond strength, durability, extensibility and compressive strength. Since these properties vary with mortar type, it is important to select the proper mortar type for each particular application. Table 2.2 gives general guides for the selection of mortar type. Selection of mortar type should also consider all applicable building codes and engineering practice standards.

Table 2.2: Mortar types for classes of construction (ASTM C 270)

ASTM Mortar Type Designation	Construction Suitability
M	Masonry subjected to high compressive loads, severe frost action or high lateral loads from earth pressures, hurricane winds or earthquakes. Structures below or against grade such as retaining walls etc.
S	Structures requiring high flexural bond strength and subject to compressive and lateral loads.
N	General use in above grade masonry. Residential basement construction, interior walls and partitions. Masonry veneer and non-structural masonry partitions.
O	Non-load-bearing walls and partitions. Solid load bearing masonry with an actual compressive strength not exceeding 100 psi and not subject to weathering.

Property specifications are used for research so that the physical characteristics of a mortar can be determined and reproduced in subsequent tests. The property requirements for mortar are given in Table 2.3. Two methods are used to determine the compressive strength of mortar. The first method tests 2" cubes of mortar in compression after having cured for 28 days. The second method based on UBC (1994) uses mortar specimens 50 mm in diameter by 100 mm high for field test. These cylinders must have a minimum compressive strength of 10.35 MPa. Although no qualification is made for the age of the compression test cylinders, it may be assumed as 28 days. Table 2.4 is a comparison of the equivalent strength between cylinders and cube specimens for three types of mortar.

Table 2.3: Property specifications for mortar (ASTM C 270)

Mortar	Type	Average Compressive Strength at 28 days, Minimum, psi (MPa)	Water Retention, Minimum, %	Air Content Maximum, %	Aggregate Ratio (Measured in Damp, Loose Conditions)
Cement-Lime	M	2500 (17.2)	75	12	
	S	1800 (12.4)	75	12	
	N	750 (5.2)	75	14 <sup>2</sup>	
	O	350 (2.4)	75	14 <sup>2</sup>	
Mortar Cement	M	2500 (17.2)	75	12	Not less than 2 <sup>1/4</sup> and not more than 3 <sup>1/2</sup> times the sum of the separate volume of cementitious materials.
	S	1800 (12.4)	75	12	
	N	750 (5.2)	75	14 <sup>2</sup>	
	O	350 (2.4)	75	14 <sup>2</sup>	
Masonry Cement	M	2500 (17.2)	75	18	
	S	1800 (12.4)	75	18	
	N	750 (5.2)	75	20 <sup>3</sup>	
	O	350 (2.4)	75	20 <sup>3</sup>	

NOTE: 1. Laboratory-prepared mortar only.

2. When structural reinforcement is incorporated in cement lime mortar, the maximum air content shall be 12%.

3. When structural reinforcement is incorporated in masonry cement mortar, the maximum air content shall be 18%.



Table 2.4: Compressive strength of mortar (psi) (ASTM C 270)

Mortar type	2" diameter x 4" height Cylinder specimen	2" cube specimen
M	2100 (14.5 MPa)	2500 (17.2 MPa)
S	1500 (10.3 MPa)	1800 (12.4 MPa)
N	625 (4.3 MPa)	750 (5.2 MPa)

### 2.4.3 Verification of the Masonry Properties

The required or specified value,  $f'_m$  must be obtained or verified in accordance with prescribed code requirements for any structural engineering design. The Uniform Building Code (1994) has provided the following three methods to verify the specified strength of the masonry assembly,  $f'_m$ . (a) Masonry Prism Testing - UBC Section 2105.3.2, (b) Masonry Prism Test Records - UBC Section 2105.3.3 and (c) Unit Strength Method - UBC Section 2105.3.4.

#### 2.4.3.1 Selection of $f'_m$ from Code Tables

The specified compressive strength of masonry,  $f'_m$  may be selected from Tables 2.5 and 2.6 that are based on the strength of the masonry unit and mortar used. These Tables are conservative and higher values may be obtained by conducting prism tests.

Table 2.5: Compressive strength of masonry based on the compressive strength of the clay masonry units and type of mortar used in construction (ACI / ASCE / TMS Table 1.6. 2.1)

Net area compressive strength of clay masonry units in psi		Net area compressive strength of masonry in psi, $f'_m$
Type M or S mortar	Type N mortar	
2400	3000	1000
4400	5500	1500
6400	8000	2000
8400	10500	2500
10400	13000	3000
12400	---	3500
14400	---	4000

Table 2.6: Specified compressive strength of masonry,  $f'_m$  (psi), based on specifying the compressive strength of masonry units (ACI 530.1-92/ASCE 6-92/TMS 602-92)

Compressive Strength of Clay Masonry Units (psi)	Specified Compressive Strength of Masonry, $f'_m$	
	Type M or S Mortar ( psi)	Type N mortar ( psi)
14000 or more	5300	4400
12000	4700	3800
10000	4000	3300
8000	3350	2700
6000	2700	2200
4000	2000	1600
Compressive Strength of Concrete Masonry Units (psi)	Specified Compressive Strength of Masonry, $f'_m$	
	Type M or S Mortar ( psi)	Type N mortar ( psi)
4800 or more	3000	2800
3750	2500	2350
2800	1500	1850
1900	1000	1350

- NOTE: 1. Compressive strength of solid clay masonry units is based on gross area. Compressive strength of hollow clay masonry units is based on minimum net area. Values may be interpolated.
2. The specified compressive strength of masonry  $f'_m$ , is based on gross area strength when using solid units or solid grouted masonry and net area strength when using ungrouted hollow units. .
3. Mortar for unit masonry, proportion specification. These values apply to Portland cement- lime mortars without added air-entraining materials.
4. Values may be interpolated. In grouted concrete masonry the compressive strength of grout shall be equal to or greater than the compressive strength of the concrete masonry units.

#### 2.4.3.2 Modulus of Elasticity, $E_m$

Modulus of elasticity is a number that measures an object or substance's resistance to being deformed elastically (i.e., non-permanently) when a stress is applied to it. Originally,  $E_m$  for masonry was the same as for concrete, namely  $1000 f'_c$  for masonry  $1000 f'_m$ , this value changed for concrete in the UBC (1967),  $33 w^{1.5} (f'_c)^{0.5}$  to reflect the influence of the unit weight of concrete and the curvature of the stress strain curve. The value for masonry assemblies was maintained as  $E_m = 1000 f'_m$  until 1998 when it was

changed to  $750 f'_m$ . This change recognized that the masonry is not as stiff as concrete and has a lower modulus. However, no accommodation was made to further define the  $E_m$  based on weight, strength or volume of component materials. Holm, T.A. (1978), of the Solite Corporation, has suggested the Equation,  $E_m = 22 w^{1.5} (f'_m)^{0.5}$ , to reflect the influence of light weight masonry and the strength of the assembly. Similarly, the Colorado Building Code has recognized that clay masonry has a lower  $E_m$  and thus uses  $500 f'_m$ , as the modulus of elasticity of clay masonry (Amerhein, 2000). When using the ACI/ASCE/TMS Masonry Code, the modulus of elasticity is given in the Tables 2.7 and 2.8 (ACI/ASCE/TMS Specification Tables 1.6.2.1 and 1.6.2.2.).

Table 2.7: Specified compressive strength of clay masonry assemblages  $f'_m$  (psi)  
(ACI/ ASCE/TMS, 1992)

Compressive Strength of Clay Masonry Units (psi)	Specified Compressive Strength of Masonry, $f'_m$	
	Type M or S Mortar ( psi)	Type N mortar ( psi)
14000 or more	5300 (36.6 MPa)	4400 (30.3 MPa)
12000	4700 (32.4 MPa)	3800 (26.2 MPa)
10000	4000 (27.6 MPa)	3300 (22.8 MPa)
8000	3350 (23.1 MPa)	2700 (18.6 MPa)
6000	2700 (18.6 MPa)	2200 (15.2 MPa)
4000	2000 (13.8 MPa)	1600 (11.1 MPa)

NOTE:

1. Compressive strength of solid masonry units is based on the gross area. Compressive strength of hollow clay masonry units is based on minimum net area. Values may be interpolated.
2. Assumed assemblage. The specified compressive strength masonry,  $f'_m$  is based on gross area strength when using solid units or solid grouted masonry and net area strength when using ungrouted hollow units.
3. Mortar for unit masonry, proportion specification. These values apply to Portland cement-lime mortars without added air-entraining materials.

Table 2.8: Clay masonry  $f'_m$ ,  $E_m$ , n and G values based on clay masonry unit strength and the mortar type (ACI/ ASCE/TMS, 1992)

Type N Mortar				
Compressive Strength of Clay Masonry (psi)	Specified Compressive Strength of Clay Masonry Assemblage, $f'_m$ (psi)	Modulus of Elasticity $E_m = 750 f'_m$ (psi) $E_m$ maximum = 3000000 psi	Modular Ratio, $n = E_s / E_m$ where $E_s = 29000000$ (psi)	Modulus of Rigidity ( $\sigma = 0.40 E_m = 300 f'_m$ (psi) G (max) = 1200000 (psi)
14000 or more	4400	3000000	9.7	1200000
12000	3800	2850000	10.2	1140000
10000	3300	2475000	11.7	990000
8000	2700	2025000	14.3	810000
6000	2200	1650000	17.6	660000
4000	1600	1200000	24.2	480000
Type M or S Mortar				
Compressive Strength of Clay Masonry (psi)	Specified Compressive Strength of Clay Masonry Assemblage, $f'_m$ (psi)	Modulus of Elasticity $E_m = 750 f'_m$ (psi) $E_m$ maximum = 3000000 psi	Modular Ratio, $n = E_s / E_m$ where $E_s = 29000000$ (psi)	Modulus of Rigidity ( $\sigma = 0.40 E_m = 300 f'_m$ (psi) G (max) = 1200000 (psi)
14000 or more	5300	3000000	9.7	1200000
12000	4700	3000000	9.7	1200000
10000	4000	3000000	9.7	1200000
8000	3350	2512500	11.5	1005000
6000	2700	2025000	14.3	810000
4000	2000	1500000	19.3	600000

The detailed properties of the infill components have been discussed in the following section.

#### 2.4.4 Equivalent Strut Width

In-plane strength predictions of infill frames are a complex, statically indeterminate problem. The strength of a composite-infill frame system is not simply the summation of the infill properties plus those of the frame. Great efforts have been invested, both analytically and experimentally, to better understand and estimate the composite behavior of masonry-infill frames. Polyakov (1956), Smith (1962, 1966, 1969), Mainstone (1971), Klingner and Bertero (1978), to mention just a few, formed the basis for understanding and predicting infill frame in-plane behavior. Their experimental testing of infill frames under lateral loads resulted in specimen deformation shapes similar to the one illustrated in Figure 2.11.

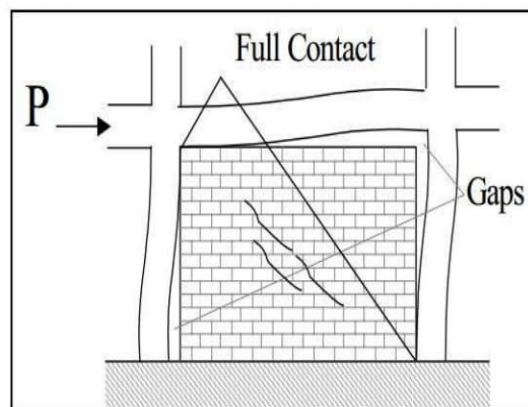


Figure 2.11: Specimen deformation shape (Al-Chaar, 2002)

During testing of the specimens, diagonal cracks developed in the center of the panel and gaps formed between the frame and the infill in the non-loaded diagonal corners of the specimens, while full contact was observed in the two loaded diagonal corners. This behavior, initially observed by Polyakov (1956), led to a simplification in infill frame analysis by replacing the masonry infill with an equivalent compressive masonry strut as shown in Figure 2.12. The equivalent masonry strut of width,  $a$ , with same net thickness and mechanical properties (such as the modulus of elasticity,  $E_m$ ) as the infill itself, is assumed to be pinned at both ends to the confining frame.

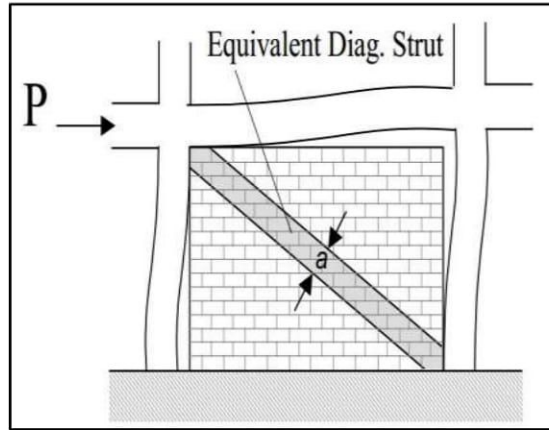


Figure 2.12: Equivalent diagonal strut (Al-Chaar, 2002)

The evaluation of the equivalent width,  $a$ , varies from one reference to the other. The most simplistic approaches presented by Paulay and Priestley (1992) and Angel et al. (1994) have assumed constant values for the strut width,  $a$ , between 12.5 to 25 percent of the diagonal dimension of the infill, with no regard for any infill or frame properties. Smith and Carter (1969), Mainstone (1971), and others, derived complex expressions to estimate the equivalent strut width,  $a$ , that consider parameters like the length of contact between the column/beam and the infill, as well as the relative stiffness of the infill to the frame. The masonry infill panel will be represented by an equivalent diagonal strut of width,  $a$  and net thickness  $t_{eff}$  as shown in Figure 2.13.

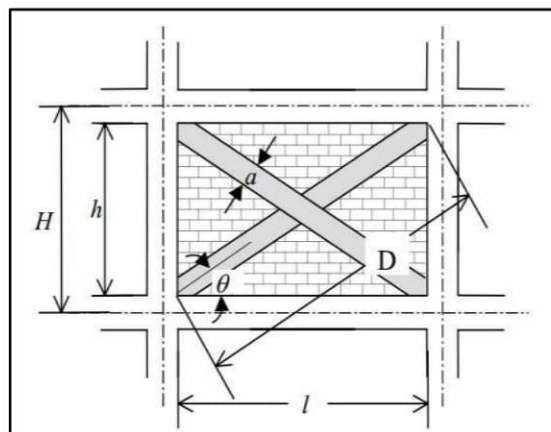


Figure 2.13: Strut geometry (Al-Chaar, 2002)

The equivalent strut width,  $a$ , depends on the relative flexural stiffness of the infill to that of the columns of the confining frame. The relative infill to frame stiffness shall be evaluated using Equation 2.4 (Smith and Carter, 1969):

$$\lambda_1 H = H [(E_m t \sin 2\theta) / (4E_c I_{col} h)]^{1/4} \dots\dots\dots \text{Equation 2.4}$$

Using this expression, Mainstone (1971) considers the relative infill to frame flexibility in the evaluation of the equivalent strut width of the panel as shown in Equation 2.5.

$$a = 0.175D (\lambda_1 H)^{-0.4} \dots\dots\dots \text{Equation 2.5}$$

Where,

- $a$  = Equivalent width of infill strut
- $t$  = Thickness of the masonry infill panel
- $E_m$  = Modulus of elasticity of the masonry unit
- $E_c$  = Modulus of elasticity of concrete
- $H$  = Height of the confining frame
- $I_{col}$  = Moment of inertia of the column
- $\theta$  = Angle of the concentric equivalent strut

However, if there is openings present and/or existing infill damage, the equivalent strut width must be reduced using Equation 2.6.

$$a_{red} = a (R_1)_i (R_2)_i \dots\dots\dots \text{Equation 2.6}$$

Where,  $(R_1)_i$  = Reduction factor for in-plane evaluation due to presence of opening defined in the section on perforated panels.

$(R_2)_i$  = Reduction factor for in-plane evaluation due to existing infill damage.

Although the expression for equivalent strut width given by Equation 2.6 was derived to represent the elastic stiffness of an infill panel, this will extend its use to determine the ultimate capacity of infill structures. The strut will be assigned strength parameters consistent with the properties of the infill it represents.

### 2.4.4.1 Eccentricity of Equivalent Strut

The equivalent masonry strut is to be connected to the frame members as depicted in Figure 2.14. The infill forces are assumed to be mainly resisted by the columns, and the struts are placed accordingly. The strut should be pin-connected to the column at a distance  $l_{column}$  from the face of the beam. This distance is defined in Equations 2.7 and 2.8 and is calculated using the strut width,  $a$ , without any reduction factors.

$$l_{column} = a / \cos \theta_{column} \dots \dots \dots \text{Equation 2.7}$$

$$\tan \theta_{column} = \{ h - ( a / \cos \theta_{column} ) \} / l \dots \dots \dots \text{Equation 2.8}$$

Using this convention, the strut force is applied directly to the column at the edge of its equivalent strut width,  $a$ .

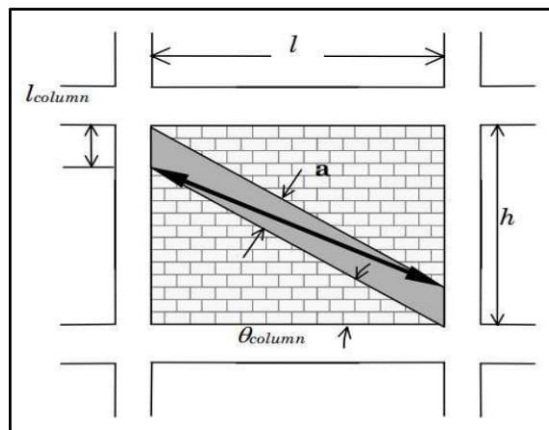


Figure 2.14: Placement of strut (Al-Chaar, 2002)

### 2.4.4.2 Partially Infill Frames

In the case of a partially infill frame, the reduced column length,  $l_{column}$ , shall be equal to the unbraced opening length for the windward column, while  $l_{column}$  for the leeward column is defined as usual shown in Figure 2.15. The strut width should be calculated from Equation 2.5, using the reduced infill height for  $h$ . Furthermore, the only reduction factor that should be taken into account is  $(R_2)_i$ , which accounts for existing infill damage.



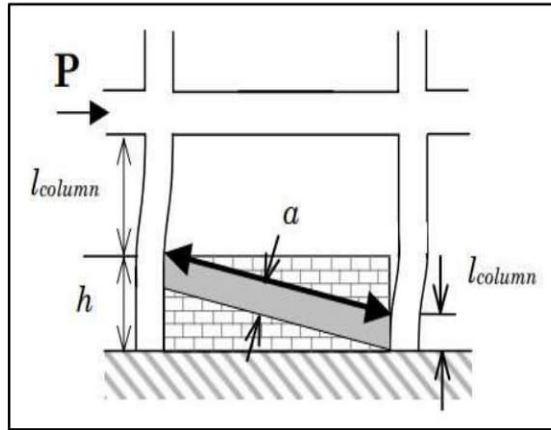


Figure 2.15: Partially infill frame (Al-Chaar, 2002)

### 2.4.4.3 Perforated Panels

In the case of a perforated masonry panel, the equivalent strut is assumed to act in the same manner as for the fully infill frame. Therefore, the eccentric strut should be placed at a distance  $l_{column}$  from the face of the beam as shown in Figure 2.16. The equivalent strut width,  $a$ , shall be multiplied, however, by a reduction factor to account for the loss in strength due to the opening. The reduction factor,  $(R_I)_i$ , is calculated using Equation 2.6.

$$(R_I)_i = 0.6 (A_{open} / A_{panel})^2 - 1.6 (A_{open} / A_{panel}) + 1 \dots \dots \dots \text{Equation 2.9}$$

Where:

$A_{open}$  = Area of the opening ( $\text{mm}^2$ )

$A_{panel}$  = Area of the infill panel ( $\text{mm}^2$ ) =  $l \times h$

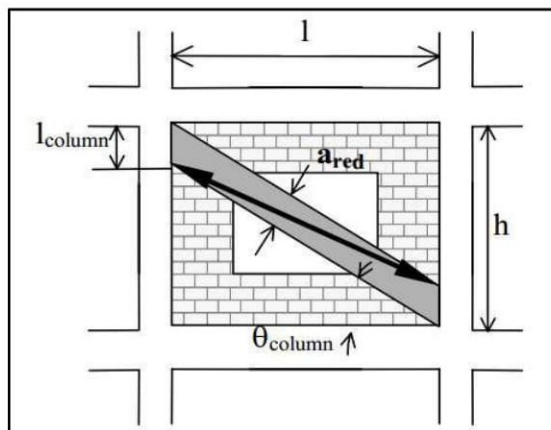


Figure 2.16: Perforated panel (Al-Chaar, 2002)

Note: If the area of the opening ( $A_{open}$ ) is greater than or equal to 60 percent of the area of the infill panel ( $A_{panel}$ ), then the effect of the infill should be neglected, i.e.  $(R_1)_i = 0$ .

Note that reducing the strut width to account for an opening does not necessarily represent the stress distributions likely to occur. This method is a simplification in order to compute the global structural capacity. Local effects due to an opening should be considered by either modeling the perforated panel with finite elements or using struts to accurately represent possible stress fields as shown in Figure 2.17.

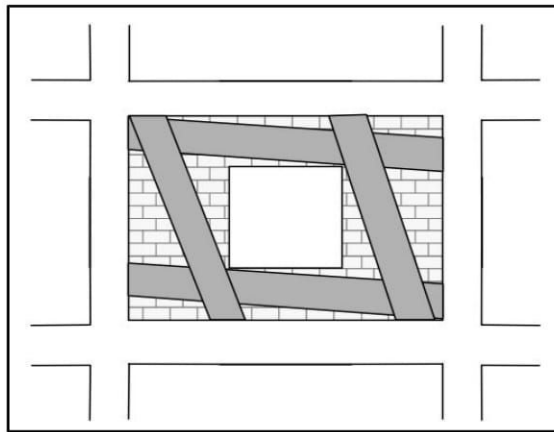


Figure 2.17: Possible strut placement for perforated panel (Al-Chaar, 2002)

#### 2.4.4.4 Existing Infill Damage

Masonry infill panel behavior deteriorates as the elastic limit is exceeded. For this reason, it is important to determine whether the masonry in the panel has exceeded the elastic limit and, if so, by how much. The extent of existing infill damage can be determined by visual inspection of the infill. Existing panel damage (or cracking) must be classified as either: no damage, moderate damage, or severe damage as presented in Figure 2.18. If in doubt as to the magnitude of existing panel damage, assume severe damage for a safer (conservative) estimate. A reduction factor for existing panel damage  $(R_2)_i$  must be obtained from Table 2.9. Notice that, if the slenderness ratio ( $h/t$ ) of the panel is greater than 21,  $(R_2)_i$  is not defined and repair is required. For panels with no existing panel damage, the reduction factor  $(R_2)_i$  must be taken as 1.0.

Table 2.9: In-plane damage reduction factor (Al-Chaar, 2002)

$h/t$	$(R_2)_i$ for Type of Damage	
	Moderate	Severe
$\leq 21$	0.7	0.4
$> 21$	Requires Repair	

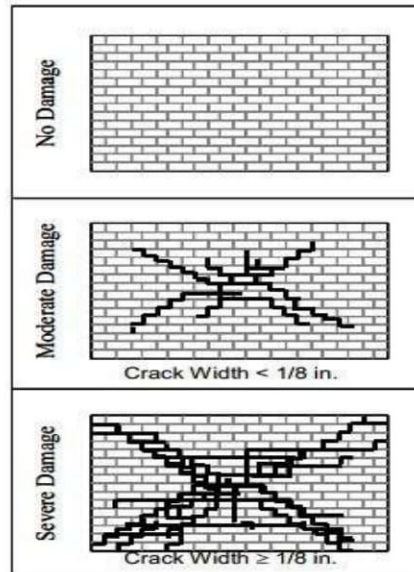


Figure 2.18: Visual damage classification (Al-Chaar, 2002)

#### 2.4.4.5 Plastic Hinge Placement

Plastic hinges in columns should capture the interaction between axial load and moment capacity. These hinges should be located at a minimum distance  $l_{column}$  from the face of the beam. Hinges in beams need only characterize the flexural behavior of the member. These hinges should be placed at a minimum distance  $l_{beam}$  from the face of the column. This distance is calculated from Equations 2.10 and 2.11 where  $\theta_{beam}$  is the angle at which the infill forces would act if the eccentricity of the equivalent strut was assumed to act on the beam as depicted in Figure 2.19.

$$l_{beam} = a / \sin \theta_{beam} \dots \dots \dots \text{Equation 2.10}$$

$$\tan \theta_{beam} = h / \{l - (a / \sin \theta_{beam})\} \dots \dots \dots \text{Equation 2.11}$$

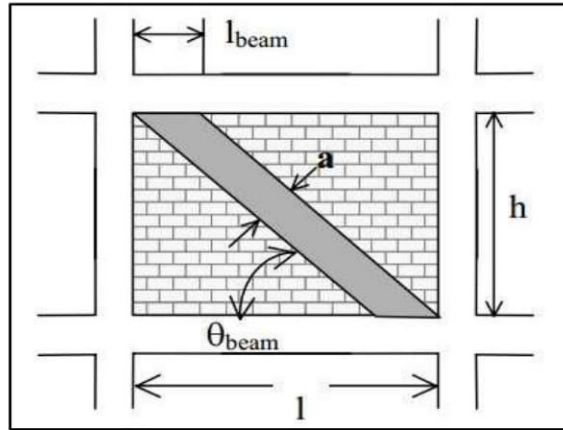


Figure 2.19: Distance to beam hinge (Al-Chaar, 2002)

Although the infill forces are assumed to act directly on the columns, hinging in the beams will still occur and  $l_{beam}$  is a reasonable estimate of the distance from the face of the column to the plastic hinge. Shear hinges must also be incorporated in both columns and beams. The equivalent strut, however, only needs hinges that represent the axial load. This hinge should be placed at the mid-span of the member. In general, the minimum number and type of plastic hinges needed to capture the inelastic actions of an infill frame are depicted in Figure 2.20.

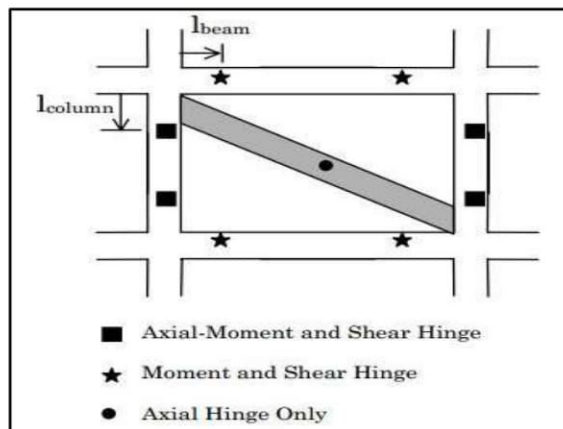


Figure 2.20: Plastic hinge placement (Al-Chaar, 2002)

Although lateral loading generally leads to hinge formation near the end of a member, inelastic deformation may occur at other locations, especially when large gravity loads are present. Therefore, the possibility of hinging near mid-span must not be overlooked. In addition, the engineer is allowed to place hinges differently if the placement is justified and good engineering judgment is used.

## CHAPTER III

### RESEARCH METHODOLOGY

#### 3.1 Introduction

This chapter describes the experimental test program and modeling of the frames for parametric study that were carried out to investigate the behavior of reinforced concrete frame with masonry infill walls having opening due to lateral loading. All experimental specimens were two storied single bay bare frame, without infill and with infill at top story having opening for door and window in the infill wall. Total three specimens of reinforced concrete (RC) frame were tested in the laboratory. Experimental tests were performed to study each specimen's load deformation behavior, ultimate strength and stiffness. Details of the test specimens, test setup, data acquisition system, instrumentation and material properties are presented in this chapter. The experimental results of the three specimens were compared then with the software results of STAAD.Pro for parametric analysis. For parametric study, total 36 numbers of building frames of 4, 7 and 10 storied and beam-column aspect ratios of 1:1, 1:1.5, 1:2, 1:2.5 were analyzed in STAAD.Pro software to investigate the behavior of RC frame with masonry infill walls due to lateral loading. They are without the effect of infill i.e. bare frame and with the effect of infill i.e. infill frame having door and window opening.

#### 3.2 Details of Laboratory Test Specimens

This section describes about the tested specimen without infill i.e. bare frame and with infill having door and window opening. Each specimen had an overall height of 2250 mm. Bay width was 1600 mm between column center lines and bay height was 975 mm. Columns were 100 mm x 150 mm in section. The beams were 150 mm deep and 100 mm wide. A base beam of 225 mm x 300 mm were also provided to lock the column. Bricks were slit to prepare its dimension of 75 mm x 50 mm x 25 mm which is shown in Figure 3.1. The amount of steel reinforcement of the specimen was also given in Table 3.1.



Figure 3.1: Bricks used for infill in the specimen

Table 3.1: Amount of reinforcements in the specimen

Parameter		Amount
Column longitudinal reinforcement		4 nos. 10 mm dia MS bar ( $\sigma = 0.021$ )
Column tie		6 mm dia tie bar @ 100 mm c/c
Beam longitudinal reinforcement	at top	2 nos. 10 mm dia MS bar ( $\rho = 0.013$ )
	at bottom	2 nos. 12 mm dia MS bar ( $\rho = 0.018$ )
Beam stirrup		6 mm dia stirrup @ 100 mm c/c

### 3.3 Test Setup

Three specimens were constructed on reinforced concrete base beams on floor. The base beam of each specimen was locked by steel channel sections at both sides and steel rods to resist uplifting. The steel reaction frame was locked by steel plates at top and steel rods at base and mid height position. A load cell of 500 kN capacity was installed horizontally for lateral loading extended from a chamber of steel reaction frame and another load cell of 1000 kN capacity was installed with a steel I beam for vertical loading. A constant vertical load of 35 kN were placed in both columns and horizontal load at top joint point was applied. This horizontal load was increased up to the failure of the frame. Greased steel plates and rollers were used between steel I beam and specimen loading point to eliminate any shear effects resulting from friction between the specimen and load cell. The base fixation of the specimen and set up of reaction frame is shown in Figure 3.2.



(a)

(b)



(c)

Figure 3.2: Base fixation of the specimen and test setup of reaction frame

Specimen 1 was a two storied single bay RC bare frame, Specimen 2 was a two storied single bay RC frame with infill having door opening at top story and Specimen 3 was similar to Specimen 2 except it had window instead of door. For Specimen 1, the temperature was  $28 \pm 2$  °C and humidity was  $64 \pm 3\%$  at the testing day. Also for Specimen 2, the temperature was  $32 \pm 2$  °C and humidity was  $69 \pm 3\%$  and for Specimen 3, the temperature was  $29 \pm 2$  °C and humidity was  $74 \pm 3\%$  at the testing day. For each specimen, static in-plane monotonic lateral load was applied keeping vertical load as constant, while parameters such as load, deflection and strain were recorded. Formation of cracks was also observed during the testing of the specimen.

### 3.4 Data Acquisition

Two types of instrumentation were employed during the testing of specimen: strain gauges and linear variable displacement transducers (LVDTs).

(a) Strain gauges: Strain gauges were installed at several locations on the surface of the concrete frame. The strain gauges were foil strain gauges utilizing a polyester resin backing having a gauge length of 30 mm. All strain gauges are connected to data logger by 0.11 mm<sup>2</sup> paralleled vinyl lead wire. At first the bonding surfaces of strain gauges were cleaned as it should be free from grease, rust, paint and dust particles. The surface should be lightly polished with abrasive paper. Then CN-E adhesive was used for installation of strain gauges. SB tape was also used as moisture and water-proofing coating. The strain gauge and adhesive which were used on the surface of specimen are shown in Figure 3.3.



Figure 3.3: Strain gauge, adhesive used on the surface of specimen

(b) Linear variable displacement transducers (LVDTs): Linear Variable Displacement Transducers (LVDTs) were used to measure the relative displacement at various locations of the specimen. Two types of LVDTs of capacity 100 mm and 50 mm were used and the level of accuracy was 0.01 mm. All LVDTs were connected to data logger by wire.

(c) Data logger: Data logger was used to record all the data during the testing of specimen. All of the transducer output signals were connected to this data logging system. The system was controlled by a personal computer through an instrument controller interface. The record channels were scanned at a predetermined sampling rate and the data were recorded as tsg files on the personal computer. RS-232C interface was equipped to enable



the optimum measurement. The LVDTs, data logger and computer set which were used for the testing of specimens are shown in Figure 3.4.



Figure 3.4: LVDTs, data logger and computer set used for testing of specimens

The reinforcement details of all three specimens are shown in Figure 3.5. Figure 3.6 (a), (b) and (c) show the instrumentation plan of Specimen 1, 2 and 3 respectively. The ordinate of placement of load cell, LVDTs and strain gauges from the base for all specimens are given in Tables A1.1, A1.2 and A1.3 of Appendix A1.

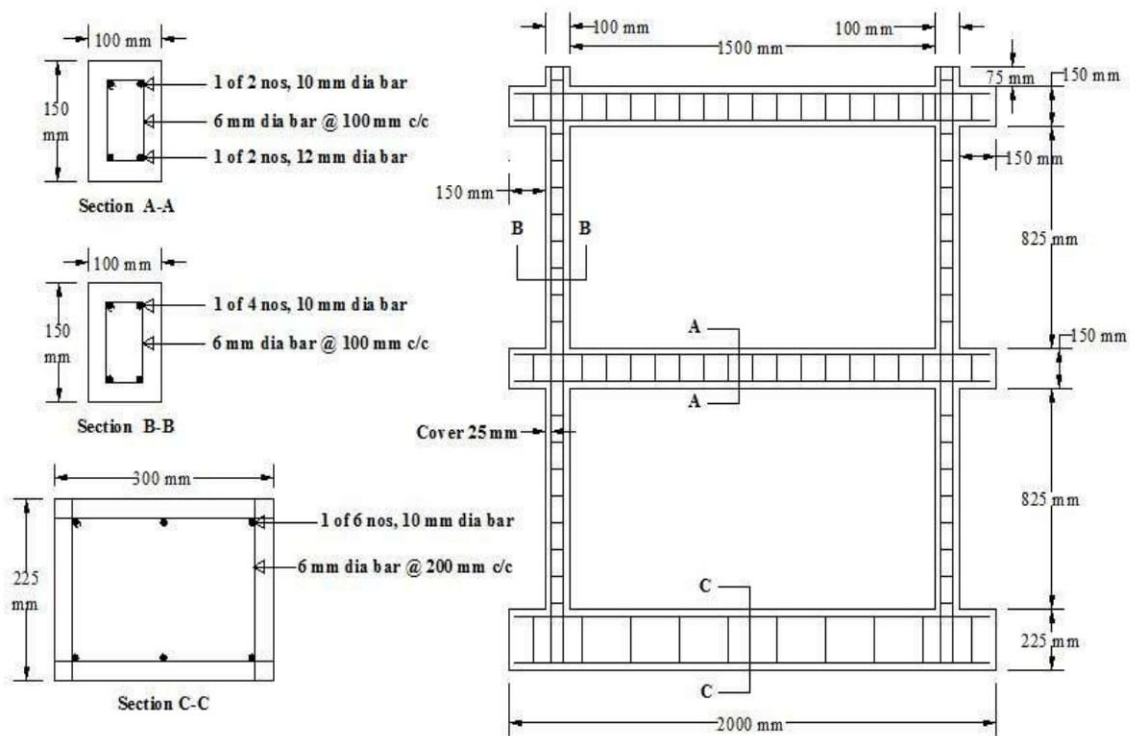
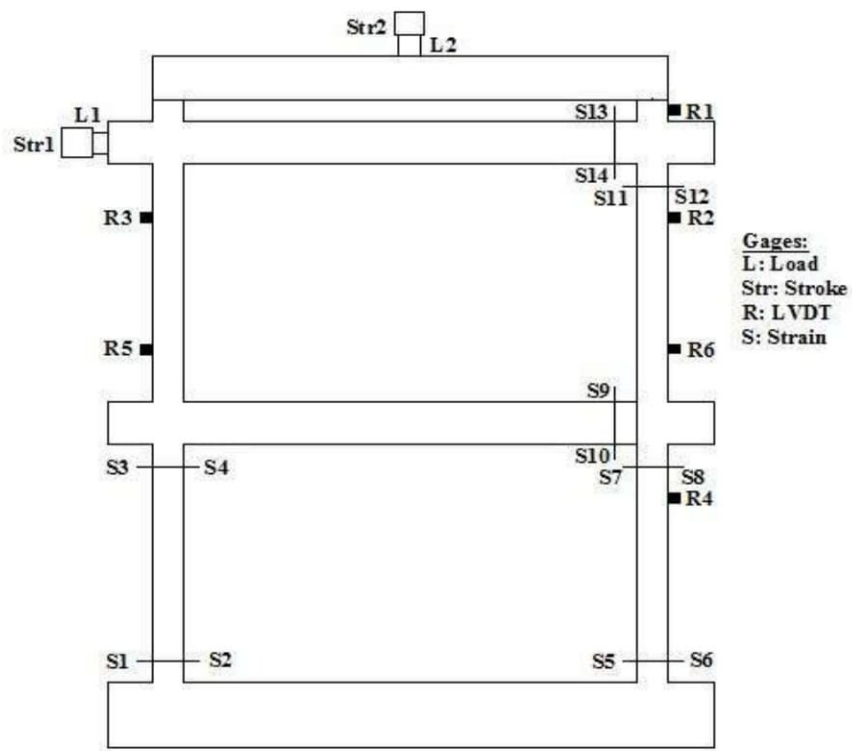
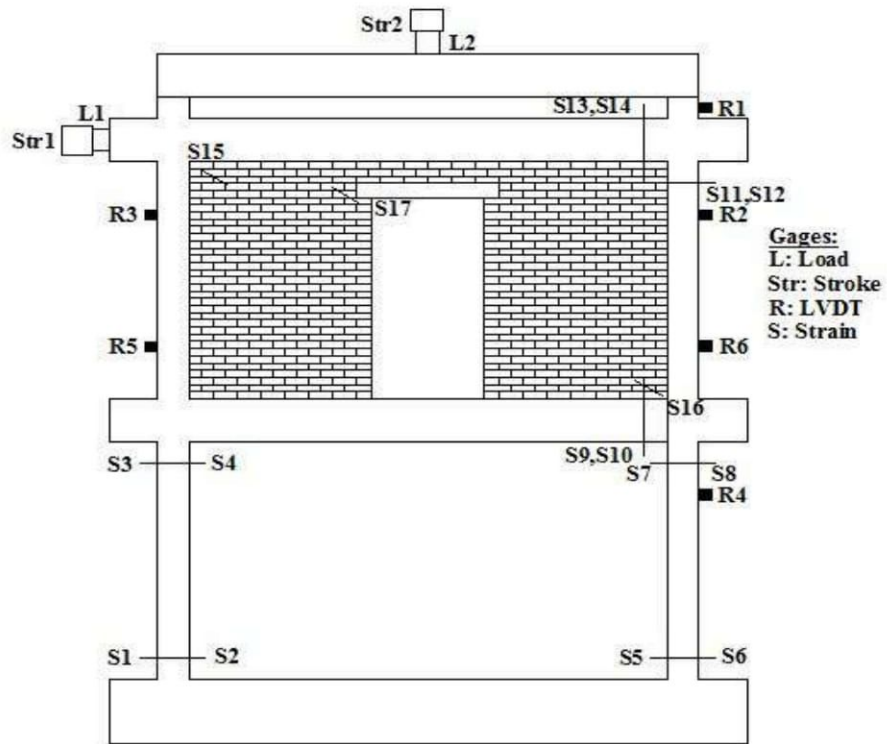


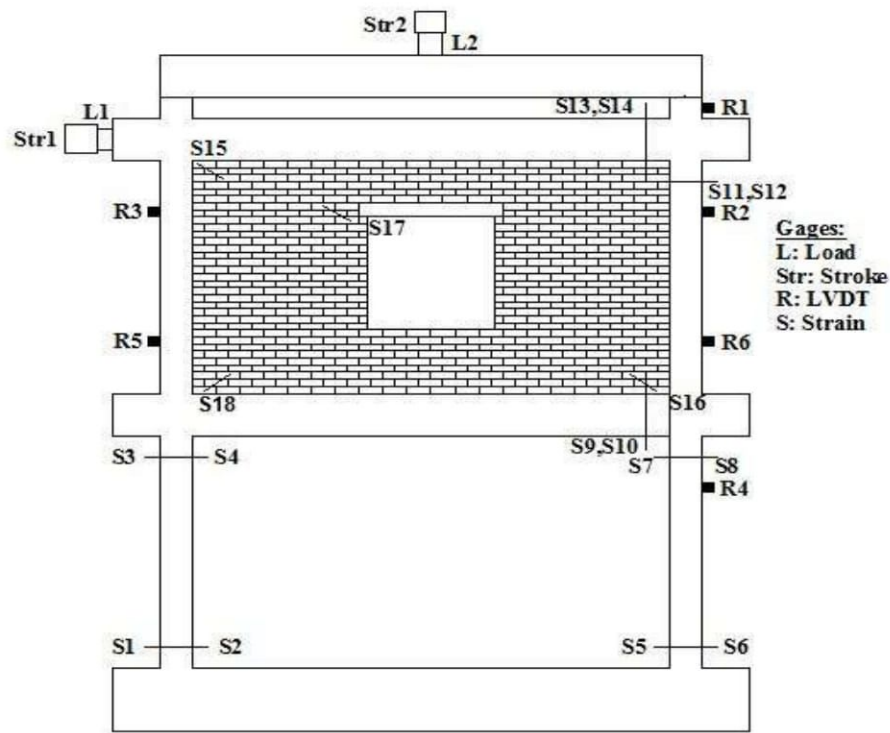
Figure 3.5: Reinforcement details for two storied single bay RC frame



(a)



(b)



(c)

Figure 3.6: Instrumentation plan for (a) Specimen 1 (b) Specimen 2 and (c) Specimen 3

### 3.5 Material Test Results

This section describes the test results of mechanical properties of materials such as compressive strength, tensile strength and modulus of elasticity.

#### 3.5.1 Concrete Tests

Concrete tests were performed for all specimens. Cylinders were made and compressive tests were performed according to ASTM C39. Strain gauges were attached to the cylinder surfaces to measure the strain. All cylinders were tested within five days of the specimen testing. According to ACI-318, the typical splitting tensile strength in psi is found from  $6.7(f'_c)^{0.5}$ , where  $f'_c$  is concrete compressive strength in psi. The cone and cone and split failure patterns were found for most of the cylinders tested. Locally available stone chips of 12.5 mm downgrade was used as coarse aggregate. Concrete was mixed in proportion of 1: 1.31: 2.36 parts by volume of cement, fine aggregate and coarse aggregate with water cement ratio 0.48. The properties of concrete of the specimen are shown in Table 3.2.

Table 3.2: Properties of concrete of the specimen

Properties	Value
Average compressive strength (MPa)	31.48
Average compressive strain (mm/mm)	0.0025
Poisson ratio	0.217
Modulus of elasticity (MPa)	26370
Average tensile strength (MPa)	3.12

### 3.5.2 Steel Reinforcements Tests

Deformed mild steel bar of diameter 10 mm and 12 mm and plain bar of diameter 6 mm were used as a tensioning device in the RC frame. The Steel reinforcements used in this work were tested according to ASTM A615 and ASTM E8. Tests were performed to confirm the information given by the steel supplier and to find the elastic modulus of the steel. The yield strength of transverse reinforcement (bar diameter = 6 mm) used in the frames was approximately 387 MPa. The stress-strain relationship for longitudinal reinforcement or main reinforcement (bar diameter = 10 mm and 12 mm) in the frames indicated a yield strength of approximately 503 MPa with a modulus of elasticity 200 GPa.

### 3.5.3 Brick and Mortar Tests

Locally available burnt clay brick was used as infill material which was Grade NW according to ASTM C 62 and N type mortar was used for masonry work according to ASTM C 270. The compressive strength tests of brick and mortar were performed according to the ASTM C 67 and C 109 respectively. The average compressive strength of brick was 9.8 MPa, whereas for mortar the average compressive strength was 4.91 MPa.

## 3.6 Modeling of the Frame

Nowadays it is possible to solve very large and complex structural models easily due to the availability of structural analysis programs and powerful computers. The major structural analysis programs offer a variety of finite elements for structural modeling. Finite element analysis tools or packages are readily available in the Civil Engineering

field. These tools or packages vary with the extent of degree of complexity, usability and versatility. Among them STAAD.Pro, ABAQUS, DIANA, ANSYS, ETABS etc. are commonly used for structural analysis.

STAAD.Pro is one of the powerful and versatile packages available for structural analysis. In this study, three types of four bay reinforced concrete frames such as bare frame (Type A), infill frame having door opening (Type B) and window opening (Type C) of three different stories (4, 7 and 10) with aspect ratios (1:1, 1:1.5, 1:2 and 1:2.5) keeping ground floor open were analyzed by STAAD.Pro. The lateral forces which were considered for the analysis in this study were calculated according to BNBC (1993). The different parameters are summarized in Table 3.3.

Table 3.3: Parameters for lateral force calculation (BNBC, 1993)

Analysis Type	Parameters	Value	
Equivalent Static Analysis	Seismic zone coefficient, z	0.15 (zone-2)	
	Structural importance coefficient, I	1	
	Response modification coefficient, RX	5	
	Response modification coefficient, RZ	5	
	Site coefficient, S	1.2	
	Time period, T	For 4 storied building	0.5204
		For 7 storied building	0.7633
For 10 storied building		0.9825	
Response Spectrum Analysis	Damping	0.05	
	Combination method	Complete Quadratic Combination (CQC)	
	Scale (normalized acceleration vs. period curve)	32.2	
	Site soil type	S <sub>2</sub>	
	Normalized acceleration vs. period data	Figure 6.2.11	

### 3.7 Types of Analysis and Loads

Two types of analysis techniques i.e. Equivalent Static Analysis and Response Spectrum Analysis had been used to find out the effects of the infill wall having opening on reinforced concrete frames. Sections 2.5.6 and 2.5.7 of BNBC (1993) had been consulted to find out Equivalent Static Analysis (ESA) and Response Spectrum Analysis (RSA) respectively. All structures were designed to resist gravitational and lateral forces. In this study, earthquake loads had been chosen for the lateral loading. The design seismic lateral forces were calculated by Equivalent Static Force Method and Dynamic Response Method of article 2.5.6 and 2.5.7 of BNBC (1993).

### 3.8 Component Properties of the Model

The infill walls were considered as strut members for the convenience of modeling (Smith and Coull, 1991). The following properties of the structural and non structural items were required to find out the property of the equivalent strut: (a) Modulus of elasticity of concrete,  $E_c$  (b) Sectional property (i.e. depth, width, moment of inertia) of the column and beam (c) Compressive strength of masonry assemble unit,  $f'_m$  (d) Modulus of elasticity of masonry unit,  $E_m$  and (e) Equivalent width of the masonry infill strut,  $a$ .

#### 3.8.1 Determination of $E_c$ , $f'_m$ , and $E_m$

Masonry bricks were considered as infill material in this work because they are widely used in Bangladesh. Solid masonry clay bricks (NW type, according to ASTM C62, 1994) were used in this work. The sectional property i.e. width and depth of beam and column were assumed according to span length and storey height of the building frame. The value of specified compressive strength of masonry,  $f'_m$  was found 13.98 MPa from Table 2.6 based on specifying the compressive strength of masonry unit of 37.37 MPa. The value of modulus of elasticity,  $E_m$  was found as 10.39 GPa from Table 2.8 (ACI/ASCE/TMS Specification Tables 1.6.2.1 and 1.6.2.2) considering the ACI/ASCE/TMS Masonry Code (1992). The concrete elastic modulus,  $E_c$  was taken as 28.58 GPa for  $f'_c$  of 37.37 MPa. All these properties of the frame components are given in Table 3.4.

Table 3.4: Properties of RC frame components

No. of Story	Aspect Ratio	Foundation Type	Concrete Compressive Strength (MPa)	Modulus of Elasticity of Concrete (GPa)	Height		Properties			
					Below Plinth Level	All Floors above Plinth Level	Columns		Beams	
							Width	Depth	Width	Depth
mm	mm	mm	mm	mm	mm	mm	mm			
4	1	Fixed /Hinged	37.37	28.58	1500	3000	300	300	250	300
	1.5						300	350	250	375
	2						300	400	250	450
	2.5						300	450	250	550
7	1	Fixed /Hinged	37.37	28.58	1500	3000	300	350	250	300
	1.5						300	400	250	375
	2						300	450	250	450
	2.5						300	500	250	550
10	1	Fixed /Hinged	37.37	28.58	1500	3000	300	400	250	300
	1.5						300	450	250	375
	2						300	500	250	450
	2.5						300	550	250	550

### 3.8.2 Determination of Equivalent Strut Width

The determination of the equivalent strut width has been adopted from Mainstone (1971) and Smith and Carter (1969) for their consistently accurate predictions of infill frame in-plane behavior when compared with experimental results (Mainstone, 1971; Smith and Carter, 1969; Klingner and Bertero, 1978; and Al-Chaar, 1998). This determination has been done by using equation 2.4, 2.5, 2.6, 2.7, 2.8 and 2.9 (Smith and Carter, 1969) from chapter two.

### 3.9 Properties of Masonry Infill

The properties of all types of frames of this study are given in Table 3.5 and 3.6. Also the model of frames is given in Figure 3.8 to 3.10. The details calculation of equivalent strut width for Model 2 of 4 storied building with aspect ratio of 1:1 is given in Appendix B2.

Table 3.5: Properties of infill frame having door opening

No. of Story	Aspect Ratio	Column size (mm x mm)	Value of						$\lambda_1 H$	$R_1$	$a$ , mm	$\theta_{column}$	$I_{Columns}$ , mm
			$f'_m$ , MPa	$E_m$ , GPa	$E_c$ , GPa	$H$ , mm	$h_{vs}$ , mm	$\theta$					
4	1	300 x 300	13.98	10.39	28.58	3000	2700	41.99	4.14	0.61	243.8	38.53	311.3
	1.5	300 x 350					2625	30.26	4.22	0.73	373.8	26.13	417.8
	2	300 x 400					2550	23.03	3.65	0.79	539.3	18.27	568.8
	2.5	300 x 450					2450	18.09	3.19	0.83	723.3	12.84	741
7	1	300 x 350	13.98	10.39	28.58	3000	2700	41.99	3.69	0.61	255.3	38.36	325.3
	1.5	300 x 400					2625	30.26	3.82	0.73	389.3	25.96	433.8
	2	300 x 450					2550	23.03	3.34	0.79	558.5	18.11	586.5
	2.5	300 x 500					2450	18.09	2.95	0.83	746.5	12.65	766
10	1	300 x 400	13.98	10.39	28.58	3000	2700	41.99	3.34	0.61	265.5	38.22	337.5
	1.5	300 x 450					2625	30.26	3.49	0.73	403.3	25.83	447.3
	2	300 x 500					2550	23.03	3.09	0.79	576.5	17.94	607
	2.5	300 x 550					2450	18.09	2.74	0.83	768	12.51	786.3



Table 3.6: Properties of infill frame having window opening

No. of Story	Aspect Ratio	Column size (mm x mm)	Value of						$\lambda_i H$	$R_i$	$a$ , mm	$\theta_{column}$	$l_{Columns}$ , mm		
			$f'_m$ , MPa	$E_m$ , GPa	$E_c$ , GPa	$H$ , mm	$h_{ws}$ , mm	$\theta$							
4	1	300 x 300	13.98	10.39	28.58	3000	2700	2700	2700	2700	2700	2700	2700		
	1.5	300 x 350					2625	2625	2625	2625	2625	2625	2625	2625	2625
	2	300 x 400					2550	2550	2550	2550	2550	2550	2550	2550	2550
	2.5	300 x 450					2450	2450	2450	2450	2450	2450	2450	2450	2450
7	1	300 x 350	13.98	10.39	28.58	3000	2700	2700	2700	2700	2700	2700	2700		
	1.5	300 x 400					2625	2625	2625	2625	2625	2625	2625	2625	
	2	300 x 450					2550	2550	2550	2550	2550	2550	2550	2550	
	2.5	300 x 500					2450	2450	2450	2450	2450	2450	2450	2450	
10	1	300 x 400	13.98	10.39	28.58	3000	2700	2700	2700	2700	2700	2700	2700		
	1.5	300 x 450					2625	2625	2625	2625	2625	2625	2625	2625	
	2	300 x 500					2550	2550	2550	2550	2550	2550	2550	2550	
	2.5	300 x 550					2450	2450	2450	2450	2450	2450	2450	2450	

### 3.10 Comparison of the Experimental Results for Parametric Study

The geometry of the three specimens i.e. two storied single bay RC bare frame, infill frame having opening of door and window which were tested in the laboratory, was developed in STAAD.Pro to verify the results. The ultimate load obtained from the experiment was applied for each model of the specimen in the software and then the lateral displacement obtained from STAAD.Pro was compared with the experimental deflection. The models of specimens are shown in Figure 3.7 below.

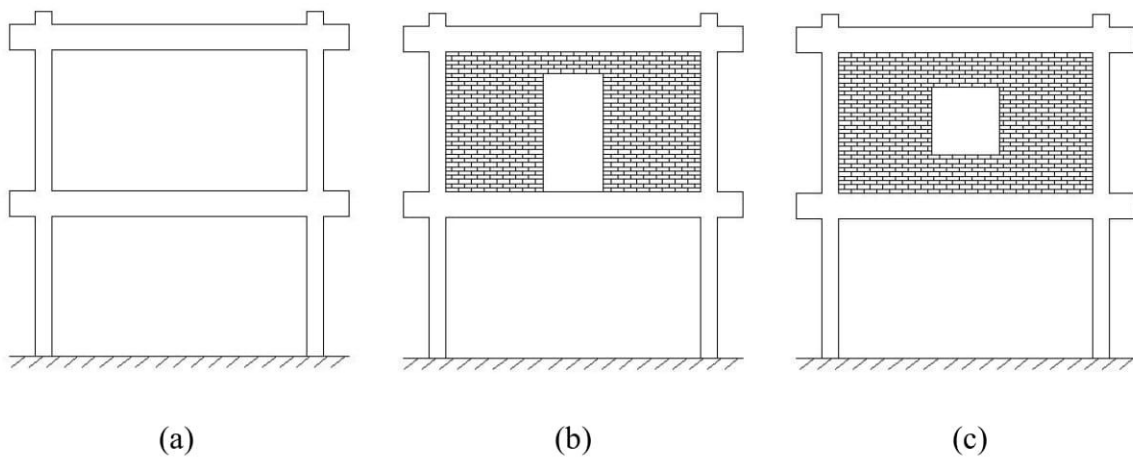


Figure 3.7: Model of two storied single bay RC (a) bare frame (b) infill frame having door opening and (c) infill frame having window opening

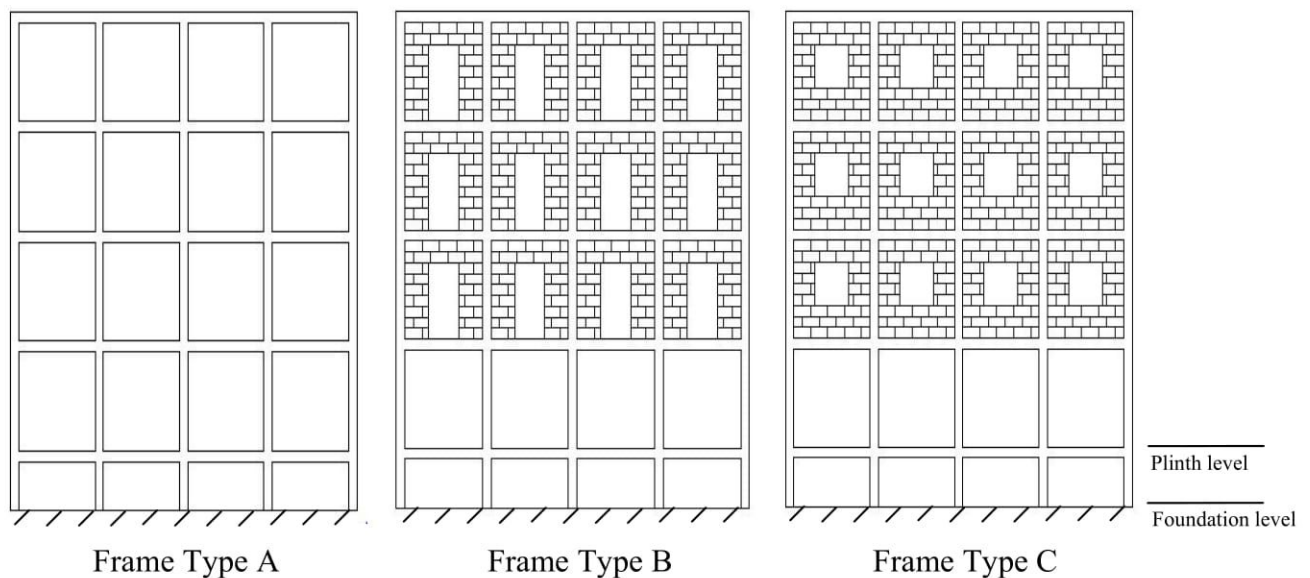


Figure 3.8: Model of 4 bays 4 storied building frame

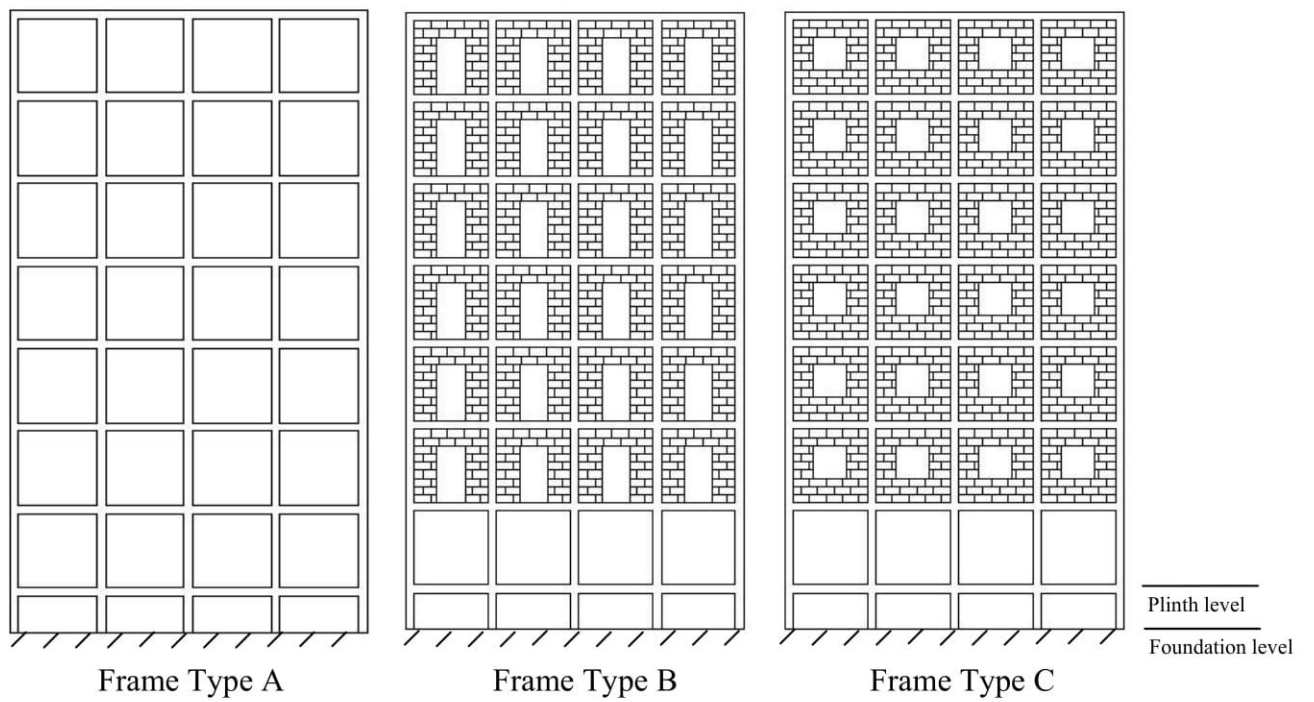


Figure 3.9: Model of 4 bays 7 storied building frame

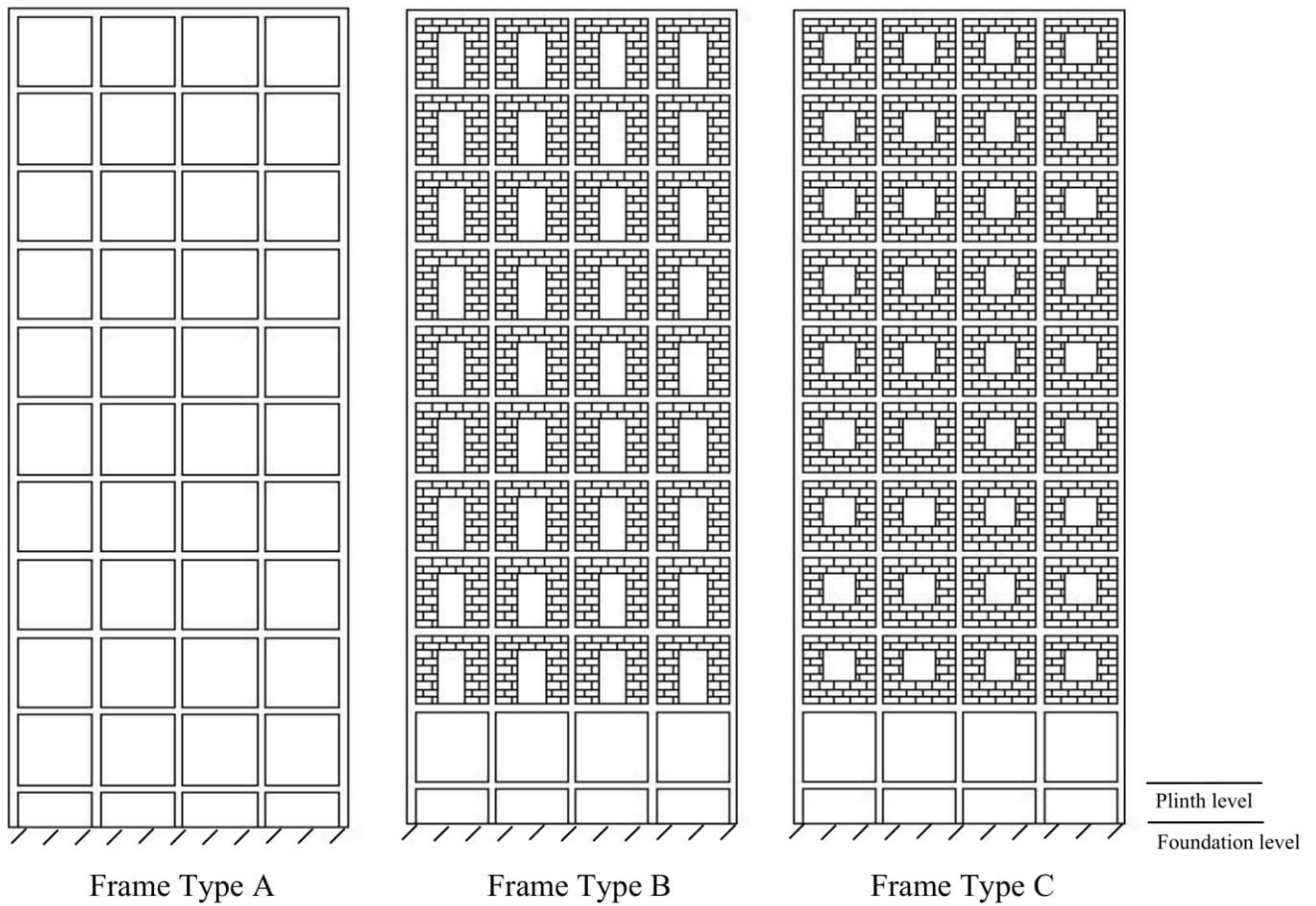


Figure 3.10: Model of 4 bays 10 storied building frame

Type A: Four bay RC bare frame, no effects of infill components are considered.

Type B: Four bay RC infill frame having door opening.

Type C: Four bay RC infill frame having window opening.

### **3.11 Observed Parameters**

The observed parameters which can influence the behavior of RC infill frame having opening due to lateral loading are given below:

- a. Panel aspect ratio
- b. Number of story in the frame
- c. Nature of infill wall opening in the panel

#### **3.11.1 Panel Aspect Ratio**

Panel aspect ratio is the direct indication of the effect of frame sway characteristics when the frame is modeled with infill having door and window opening or without considering the effect of infill. It is an important parameter for analysis of infill frame having opening as the infill stiffness greatly depends on panel aspect ratio. The panel aspect ratio depends on floor height " $h$ " and span length " $l$ " of the frame. In this analysis the floor height,  $h$  was 3000 mm for all floors. The span length,  $l$  varied such as 3000 mm, 4500 mm, 6000 mm and 7500 mm and models were analyzed for aspects of 1:1, 1:1.5, 1:2 and 1:2.5.

#### **3.11.2 Number of Story in Vertical Direction**

Another important parameter is number of story in vertical direction for analysis of infill frame having opening. It has a great influence on deflection and flexural behavior of the RC frame. To find out the effect of number of story, three types of 4, 7 and 10 storied building frames had been studied in this work.

### **3.11.3 Nature of Infill Wall having Opening in the Panel**

Variation of nature of infill having opening changes the structural behavior of building due to lateral loading. The parametric study was carried out for three types of frame without considering effect of infill and with considering infill having door and window opening.

### **3.12 Modeling Technique**

The linear analysis for each model was performed through three different conditions. Equivalent Static Analysis and Response Spectrum Analysis had been performed to generate the modeling considering UBC (1994) parameters. The boundary conditions were specified for each model type as fixed and hinged. The strut members were pin connected to the column. The results from analyses were very important in terms of understanding the structural behavior and in locating the position of maximum shear and moment. A script was developed and provided in Appendix B3 which can be used to generate a generic parametric model for such an application.

## CHAPTER IV

### RESULTS AND DISCUSSION

#### 4.1 Introduction

In this chapter load deflection response, stiffness and crack formation of each specimen is presented by experimental work. The outcomes of parametric study analyzed by STAAD.Pro are also described here considering parameters such as panel aspect ratios, number of story in vertical direction and nature of infill having opening.

Parameters such as deflection, strain with respect to load, ultimate load and displacement of the specimens were measured and also stiffness were calculated to investigate the behavior of reinforced concrete (RC) frame with masonry infill wall having opening due to lateral loading. Other parameters such as crack formation, first crack and crack pattern were also observed for each specimen.

From the parametric study, the behavior of top deflection, story wise deflection, inter story drift, shear, moment and base shear were analyzed and compared for 4, 7 and 10 storied building with aspect ratios of 1:1, 1:1.5, 1:2, 1:2.5. All these parameters are presented here for identifying the behavior of these RC frames with considering the effect of infill wall having opening due to lateral loading by both Equivalent Static Analysis and Response Spectrum Analysis.

#### 4.2 Experimental Investigation

#### 4.3 Two Storied Single Bay Bare Frame (Specimen 1)

The two storied single bay bare frame, Specimen 1, was tested and its instrumentation is shown in Figure 4.1. Cracks began forming at the bottom of windward and top of leeward side of ground floor beam at early loading. The first crack visually appeared in the

windward side of ground floor beam and beam column joint at 6.4 mm of lateral deformation and 19% of ultimate loading. The first crack was then followed by a number of cracks. One shear crack formed at the windward beam-column joints of ground floor following the first crack. These cracks would then be expanded following the first crack in the crack formation zone from tension to compression in windward and leeward side of ground floor beam. Al-Chaar (2002) observed that cracks began forming near the beam-column joints at early loading and the first crack visually appeared in the windward joint for single-bay, single-story bare frame due to in-plane loading.

Two tension cracks formed in ground floor beam at a distance  $2d$  and  $3d$  from the windward beam column joint. On the other hand, one shear crack formed at a distance  $3d$  from the leeward beam column joint of ground floor. All these cracks formed at 28 mm of lateral deformation and 58% of ultimate loading. At this loading, also two tension cracks formed at the top and one tension crack formed at the bottom of 1<sup>st</sup> floor windward column. The formation of these cracks would be expected to result in stress release in the RC frame, with a consequent redistribution of loads. The load distribution in the frame obviously changed as new cracks formed and the old cracks propagated.

At 54.58 mm of lateral deformation and 96% of ultimate loading, some additional cracks were also formed such as one shear crack at the bottom of leeward ground floor beam, two tension cracks at the bottom of leeward ground floor column, five tension cracks at bottom of windward 1<sup>st</sup> floor beam, three tension cracks at bottom and five tension cracks at top of windward 1<sup>st</sup> floor column. The cracks in the Specimen 1 are shown in the Figure 4.2 indicated by number 303, 315 and 343. The failure mode of bare frame, Specimen 1 is shown in Figure 4.3. The experimental load deflection curve at the top of 1<sup>st</sup> floor windward column (LVDT-3) is presented in Figure 4.4. The experimental ultimate load for the bare frame was 13.9 kips with a maximum displacement of 62.64 mm. Analysis of the behavior of Specimen 1 subjected to in-plane lateral loading revealed that the most critical sections was top and bottom of the windward of 1<sup>st</sup> floor column. Al-Chaar (2002) concluded that most critical sections are top of windward column, top of leeward column, bottom of windward column and bottom of leeward column for the single-bay, single-story bare frame subjected to in-plane lateral loading.

The strain at bottom of windward column of ground floor is shown in Figure 4.5. The other displacements recorded in LVDTs and strain are shown in Figure A2.1 and A2.4 of Appendix A2.



Figure 4.1: Specimen 1, Instrumentation of two storied single bay bare frame



(a)



(b)



(c)





(d)



(e)

Figure 4.2: Specimen 1, Formation of cracks in two storied single bay bare frame



Figure 4.3: Specimen 1, Failure of two storied single bay bare frame

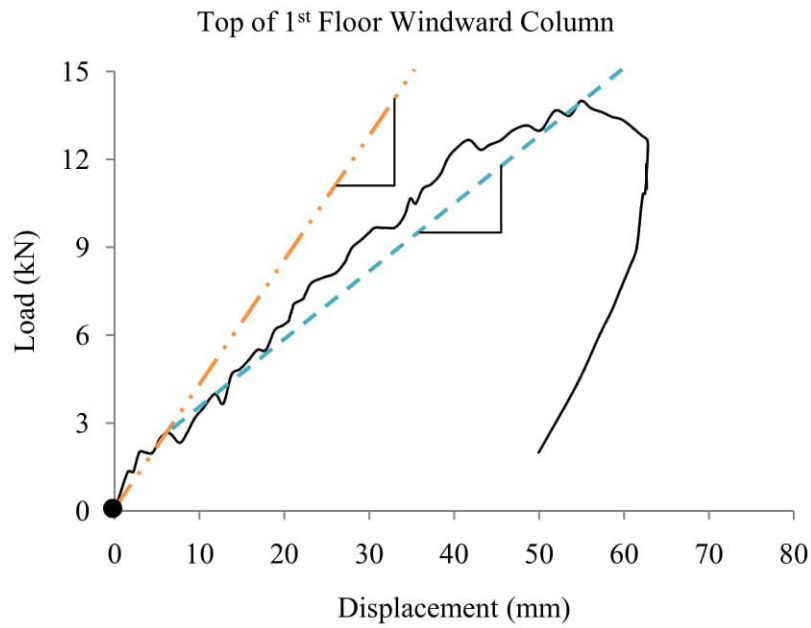


Figure 4.4: Specimen 1, Experimental load deflection curve for LVDT-3

It was found that the stiffness of two storied single bay bare frame was 0.5 kN/mm from origin to first crack and 0.23 kN/mm from first crack to ultimate load from Figure 4.4. Thus it indicated that the stiffness was higher up to first crack and then the stiffness decreased after the formation of first crack.

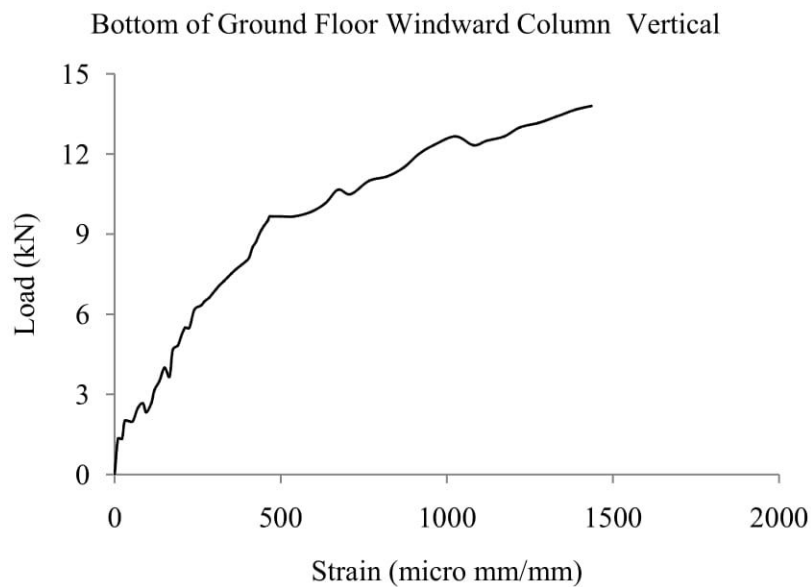


Figure 4.5: Specimen 1, Load vs strain curve for strain gauge S1

#### 4.4 Two Storied Single Bay Infill Frame having Door Opening (Specimen 2)

The instrumented side and first crack formation of the two storied single bay infill frame having door opening, Specimen 2, is shown in Figure 4.6. The cracks were surveyed at various stages of loading during the testing of the specimen. The first crack as a stair pattern was observed one course below from top of door at the windward side in the infill which is occurred at 6.5 mm of lateral deformation and 33% ultimate loading. Al-Chaar (2002) observed for single bay infill frame with concrete masonry unit that the first crack was a sudden stair crack in the infill. It occurred at 10.16 mm of deformation. At 19 mm of deformation, the first crack was followed by many cracks; specifically, a horizontal crack in the infill three courses above horizontal segment of the first crack.

Then it followed by specifically stair crack at the bottom of leeward portion in the infill and shear crack at the windward beam column joint of ground floor at 13.82 mm of lateral deformation and 56% of ultimate loading. With the increasing load, cracks propagated such as four tension cracks at the bottom of windward ground floor beam at a distance 0.5d, 2d, 3d and 4d respectively, four tension cracks at the top of leeward ground floor beam at a distance 0.25d, 0.5d, d and 2d respectively, one shear crack at the top of leeward ground floor column, five tension cracks at the bottom of windward ground floor column and stair crack at the bottom of windward side in the infill. These cracks formed at 22.28 mm of lateral deformation and 67% of ultimate loading. All cracks formed in Specimen 2 during testing were shown in the Figure 4.7 indicated by number 507, 511, 517, 527 and 546. At 38.9 mm of lateral deformation and 88% of ultimate loading, several cracks propagated such as stair crack at leeward side beside the door from lintel and mid-portion. Thus a diagonal strut was formed in the infill beside the left and right side of door opening as shown in Figure 4.8. Some cracks were also propagated such as separation of brick infill and ground floor beam at the interface between the frame and infill, three tension cracks at top of 1<sup>st</sup> floor leeward beam at ultimate loading.

The crack continued to enlarge and sudden crushing was observed at 56.61 mm of deformation with an ultimate load of 24.49 kN by shear crack at the top of leeward and by tension crack at bottom of windward ground floor column. Then the test stopped, the unsound concrete and LVDTs were removed. Al-Chaar (2002) concluded that crushing of the concrete masonry unit in the top windward corner was observed at 82.5 mm deformation for single bay infill frame with concrete masonry unit.

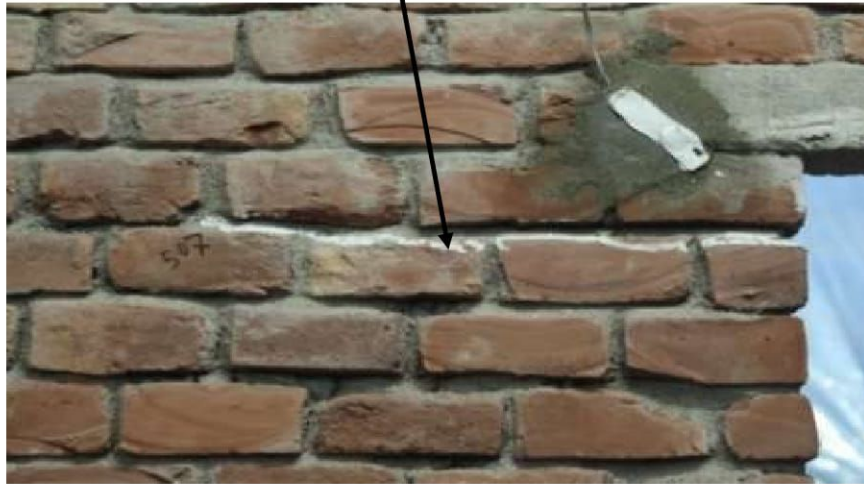


Figure 4.6: Specimen 2, Instrumentation and first crack formation of two storied single bay infill frame having door opening



(a)



(b)

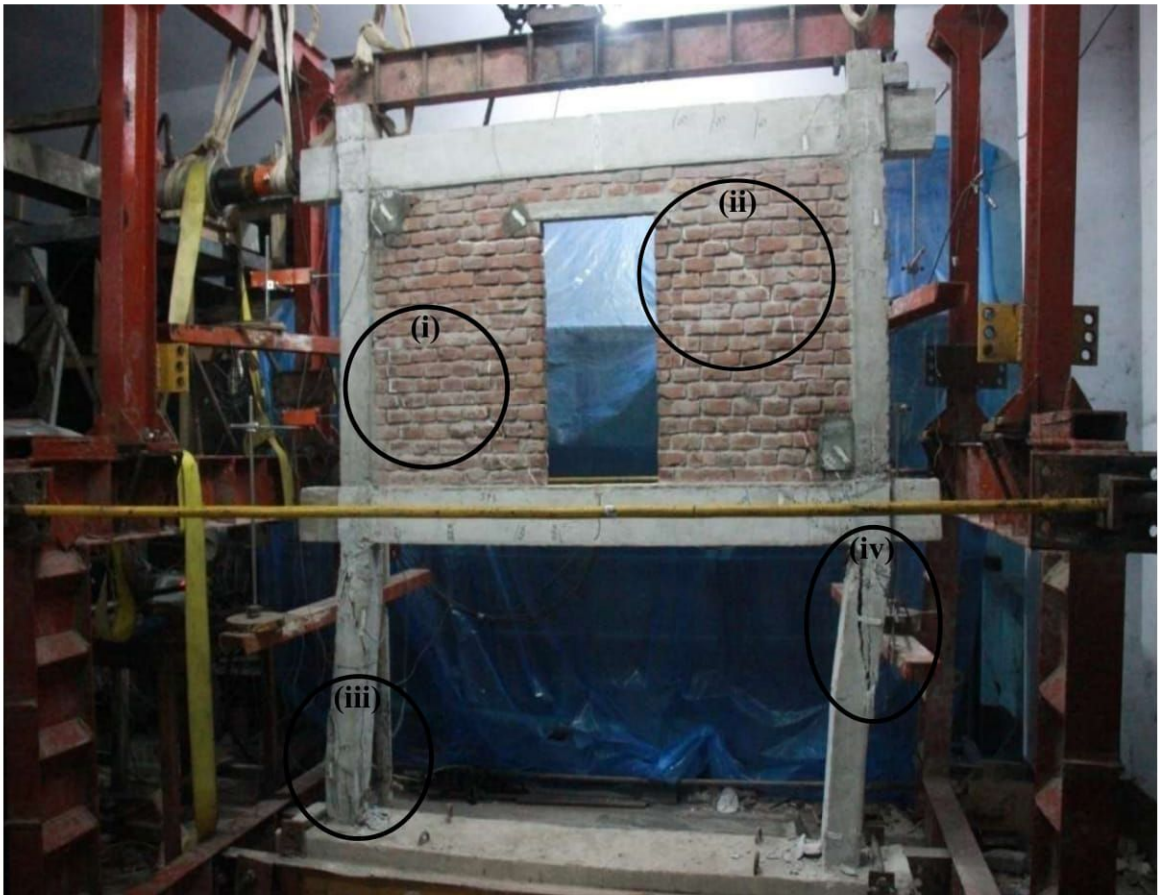


(c)



(d)

Figure 4.7: Specimen 2, Formation of cracks in two storied single bay infill frame having door opening





(i)



(ii)



(iii)



(iv)

Figure 4.8: Specimen 2, Failure of two storied single bay infill frame having door opening

The load displacement curve in Figure 4.9 shows the measured displacements with respect to loads at the top of 1<sup>st</sup> floor of windward column. The strain calculated from the strain gauge S13 is presented in Figure 4.10. The other displacements recorded in LVDTs are shown in Figure A2.2 and strain in Figure A2.5 of Appendix A2.

From the experimental load deflection curve of two storied single bay infill frame having door opening, it was observed that the stiffness was higher from origin to first crack than from first crack to ultimate load which was same as specimen 1, bare frame. From Figure

4.9, it was found that the stiffness of specimen 2 was 1.58 kN/mm from origin to first crack and 0.38 kN/mm from first crack to ultimate load. It was also observed that the stiffness of specimen 2 was three times greater than specimen 1 up to first crack and almost nearly two times greater than specimen 1 after first crack to ultimate load. The infill present at top story was mainly responsible for the increase of stiffness and higher deflection at top of ground floor compared to top of 1<sup>st</sup> floor of the frame.

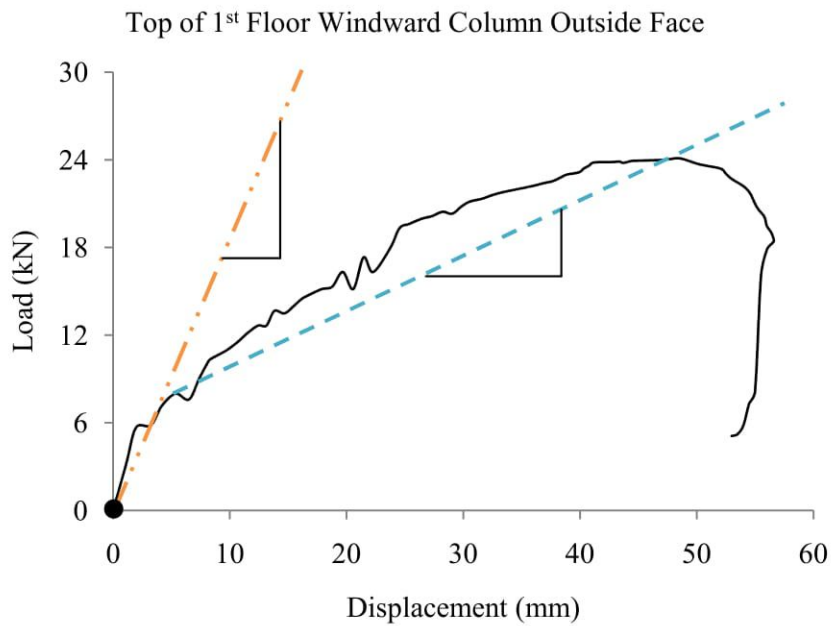


Figure 4.9: Specimen 2, Experimental load deflection curve for LVDT-3

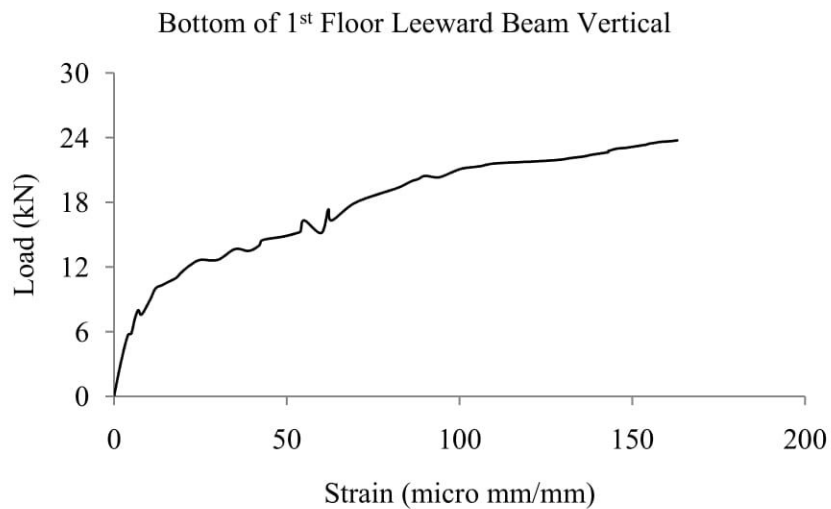


Figure 4.10: Specimen 2, Load vs strain curve for strain gauge S13

#### 4.5 Two Storied Single Bay Infill Frame having Window Opening (Specimen 3)

The instrumentation before testing and first crack formation of the two storied single bay infill frame having window opening, Specimen 3, is shown in Figure 4.11. The specimen was loaded gradually and first crack was visually appeared at the infill wall along left to right as stair crack below three courses of window opening. The first crack in the infill initiated at 3.24 mm of lateral deformation and 29% of ultimate loading. Al-Chaar (2002) observed that the first crack appeared in the top of leeward column for single bay infill frame with brick,. The first crack in the infill initiated at 15.24 mm of deformation. This stair crack appeared almost along the diagonal of the infill.

The first crack was then followed three tension cracks at top of ground floor beam at a distance 0.25d, 1.5d, 2.75d from leeward beam column joint, three tension cracks at bottom of ground floor beam at a distance d, 2.5d, 3.5d from windward beam column joint, two tension cracks at bottom of leeward and three tension cracks at top of windward ground floor column. All these cracks formed at 12.38 mm of lateral deformation and 61% of ultimate loading indicated by number 727 and 746 are shown in Figure 4.12.

The stair crack appeared almost along the diagonal of the infill at the left side of the window. Then this crack extended to horizontally at the bottom of the window and merged with the tension crack formed at top of leeward ground floor beam. Thus a diagonal strut was formed in the infill from left to right as shown in Figure 4.12 (e).

As the specimen was further loaded, stair crack forming was prolonged at the windward and leeward side in the infill; size of tension cracks in the beam was increased following their path. One shear crack formed at the windward beam column joint of ground floor, four tension cracks formed at the top of leeward 1<sup>st</sup> floor beam at a spacing 1.5d, 2.5d, 3.5d and 4.5d respectively, two shear cracks formed at top of 1<sup>st</sup> floor windward column and one shear crack formed at top of ground floor windward column. All these cracks formed at 30.88 mm of lateral deformation and 91% of ultimate loading.

It has been observed that there was physical formation of obvious diagonal strut in both Specimen 2 and 3. In Specimen 2, diagonal strut was formed at both left and right side of the door opening. On the other hand, diagonal strut was formed at the left side, bottom and right side of the window opening in Specimen 3. Al-Chaar (2002) concluded that there was the physical formation of an obvious diagonal strut in single bay infill frame with brick.



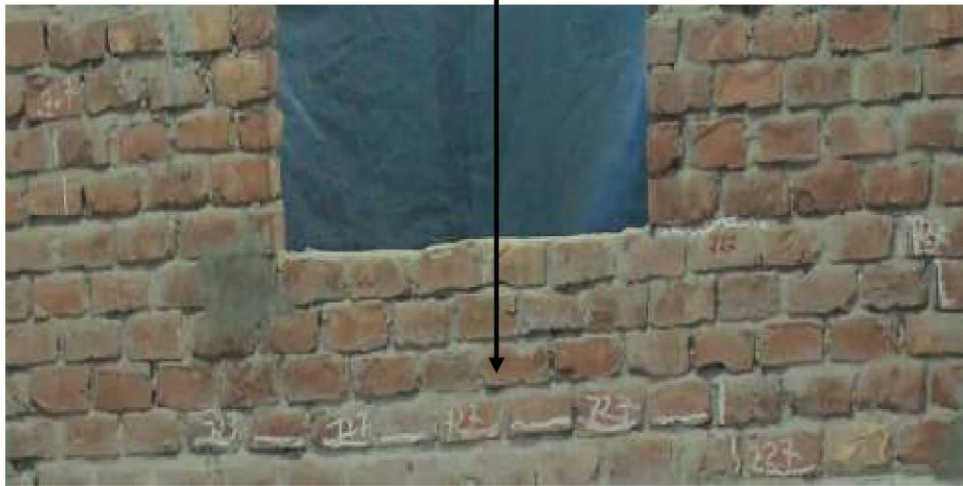


Figure 4.11: Specimen 3, Instrumentation and first crack formation of two storied single bay infill frame having window opening



(a)



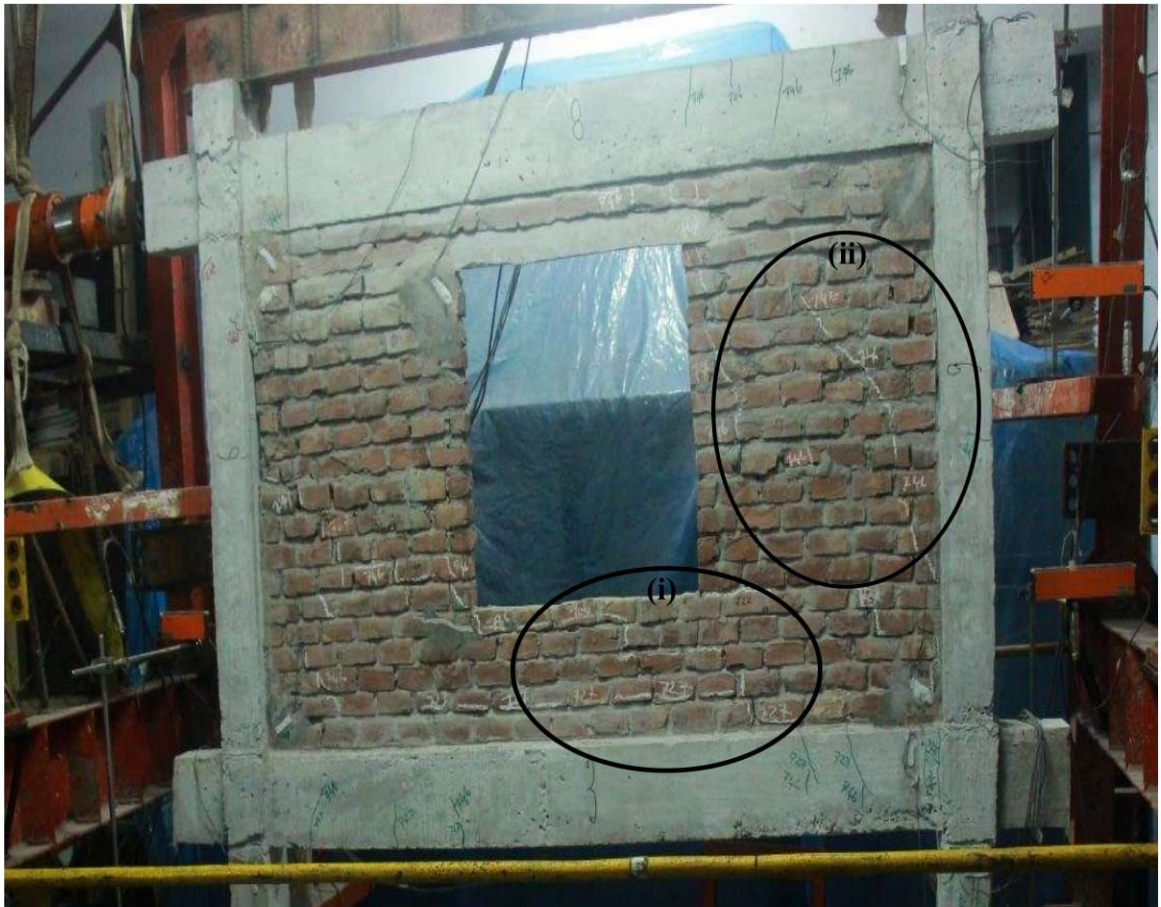
(b)



(c)



(d)



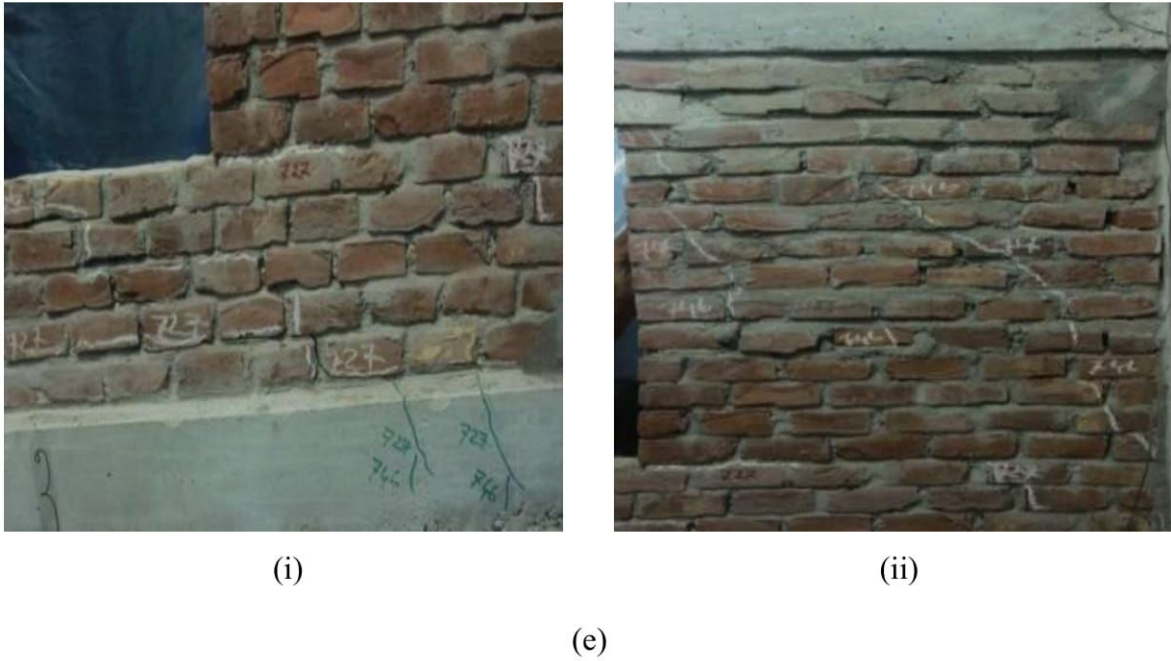


Figure 4.12: Specimen 3, Formation of cracks of two storied single bay infill frame having window opening

The experimental ultimate load for the infill frame having window opening was 23.65 kips with a maximum displacement of 56.74 mm. The load displacement curve of the top of 1<sup>st</sup> floor of windward column (LVDT-3) is shown in Figure 4.13.

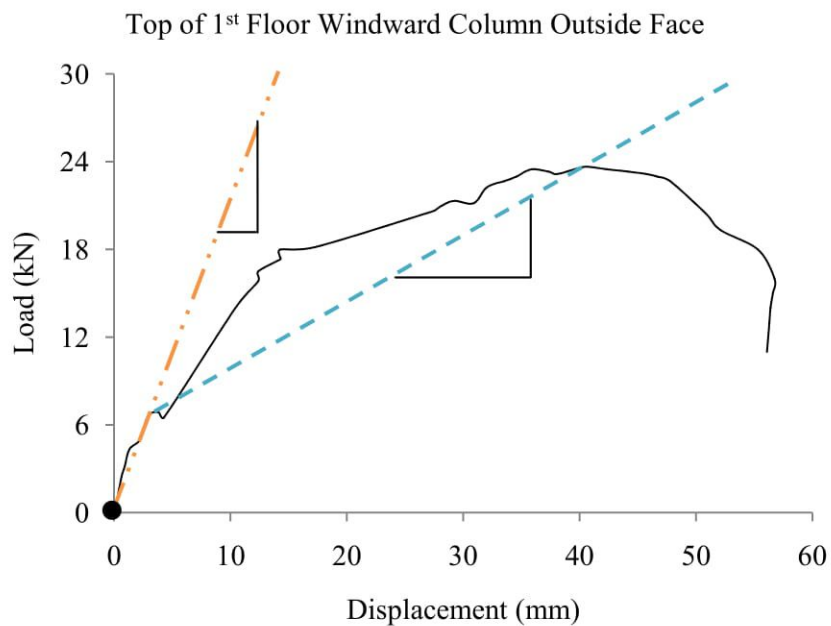


Figure 4.13: Specimen 3, Experimental load deflection curve for LVDT-3

It was found that the stiffness of specimen 3 was 2.06 kN/mm from origin to first crack and 0.48 kN/mm from first crack to ultimate load from Figure 4.13. So the stiffness of specimen 3 was four times greater than specimen 1 up to first crack and two times greater than specimen 1 after first crack to ultimate load.

The strain calculated from the strain gauge S2 is presented in Figure 4.14. The other displacements recorded in LVDTs and strain are shown in Figure A2.3 and A2.6 of Appendix A2.

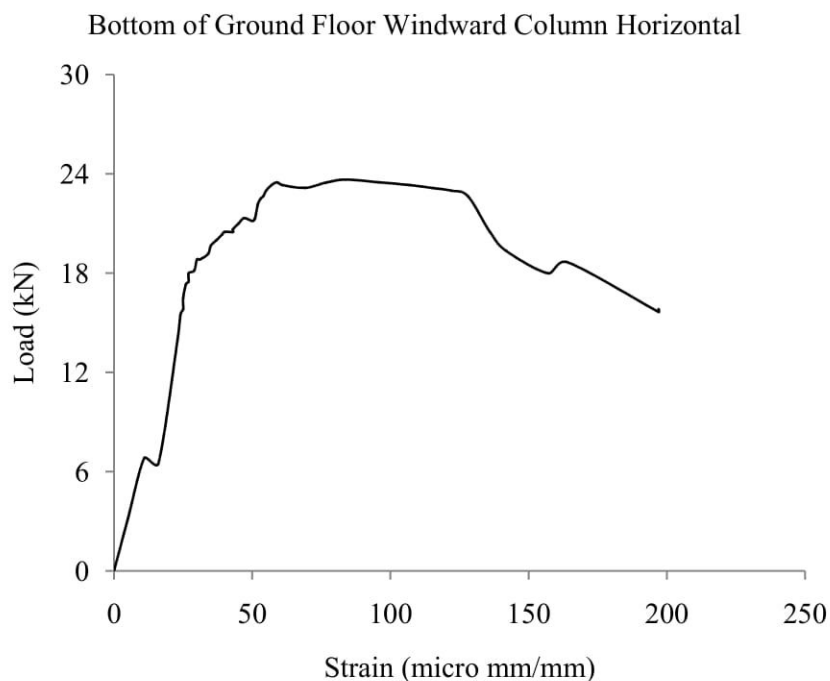


Figure 4.14: Specimen 3, Load vs strain curve for strain gauge S2

#### 4.6 Comparison of Theoretical Results in STAAD.Pro with the Experimental Results

Two storied single bay bare frame, Specimen 1:

The experimental ultimate load was 13.99 kN and deflection up to first crack was 6.4 mm and linear deflection of load deflection curve was 41.7 mm. The deflection up to linear analysis by STAAD.Pro software was found 4.75 mm.

Two storied single bay infill frame having door opening, Specimen 2:

The experimental ultimate load was 24.49 kN and deflection up to first crack was 6.5 mm and linear deflection of load deflection curve was 28.24 mm. The deflection up to linear analysis by STAAD.Pro software was found 3.48 mm.

Two storied single bay infill frame having window opening, Specimen 3:

The experimental ultimate load was 23.65 kN and deflection up to first crack was 3.24 mm and linear deflection of load deflection curve was 14.28 mm. The deflection up to linear analysis by STAAD.Pro software was found 3.35 mm.

#### **4.7 Theoretical Investigation**

#### **4.8 Results of Parametric Study**

A number of total 36 numbers of building frames representing different structural configurations including bare frame, infill frame having door and window opening keeping ground floor open at the bottom level due to lateral loading were modeled and analyzed. The results of these analyses are presented in this section and comparisons are made of all models by both static and dynamic points of view with varying parameters.

#### **4.9 Effect of Infill having Opening on Story Sway**

##### **4.9.1 Top Deflection of Frames**

Top deflection of bare frame (Type A), infill frame having door opening (Type B) and infill frame having window opening (Type C) of all models have been summarized in table 4.1-4.3 for both fixed and hinged support. From tables, it has been noticed that Equivalent Static Analysis gives higher values of top deflection for all models than Response Spectrum Analysis and top deflection is higher in hinged support than fixed support of 4, 7 and 10 storied building with all aspect ratios of 1:1, 1:1.5, 1:2 and 1:2.5.

Table 4.1: Top deflection of 4 storied building

Story No.	Type of Frame	Aspect Ratio	Top Deflection (mm)			
			Fixed Support		Hinged Support	
			RSA	ESA	RSA	ESA
4 Storied Building	A	1:1	5.44	5.51	6.32	6.60
	B		1.68	1.70	2.54	2.62
	C		1.78	1.83	2.69	2.77
	A	1:1.5	5.61	5.69	6.55	6.86
	B		1.80	1.83	2.77	2.84
	C		1.88	1.93	2.90	2.97
	A	1:2	5.59	5.66	6.58	6.88
	B		1.85	1.93	2.87	2.97
	C		1.93	2.01	2.97	3.07
	A	1:2.5	5.13	5.23	6.02	6.32
	B		1.85	1.93	2.79	2.92
	C		1.93	2.01	2.87	3.00

Table 4.2: Top deflection of 7 storied building

Story No.	Type of Frame	Aspect Ratio	Top Deflection (mm)			
			Fixed Support		Hinged Support	
			RSA	ESA	RSA	ESA
7 Storied Building	A	1:1	12.24	12.95	13.41	14.50
	B		2.06	2.13	3.23	3.35
	C		2.21	2.31	3.45	3.58
	A	1:1.5	12.75	13.49	14.05	15.21
	B		2.24	2.34	3.58	3.71
	C		2.36	2.49	3.76	3.91
	A	1:2	12.80	13.56	14.15	15.34
	B		2.41	2.54	3.81	3.99
	C		2.54	2.69	3.96	4.17
	A	1:2.5	11.68	12.40	12.88	13.97
	B		2.54	2.72	3.81	4.04
	C		2.67	2.87	3.96	4.22

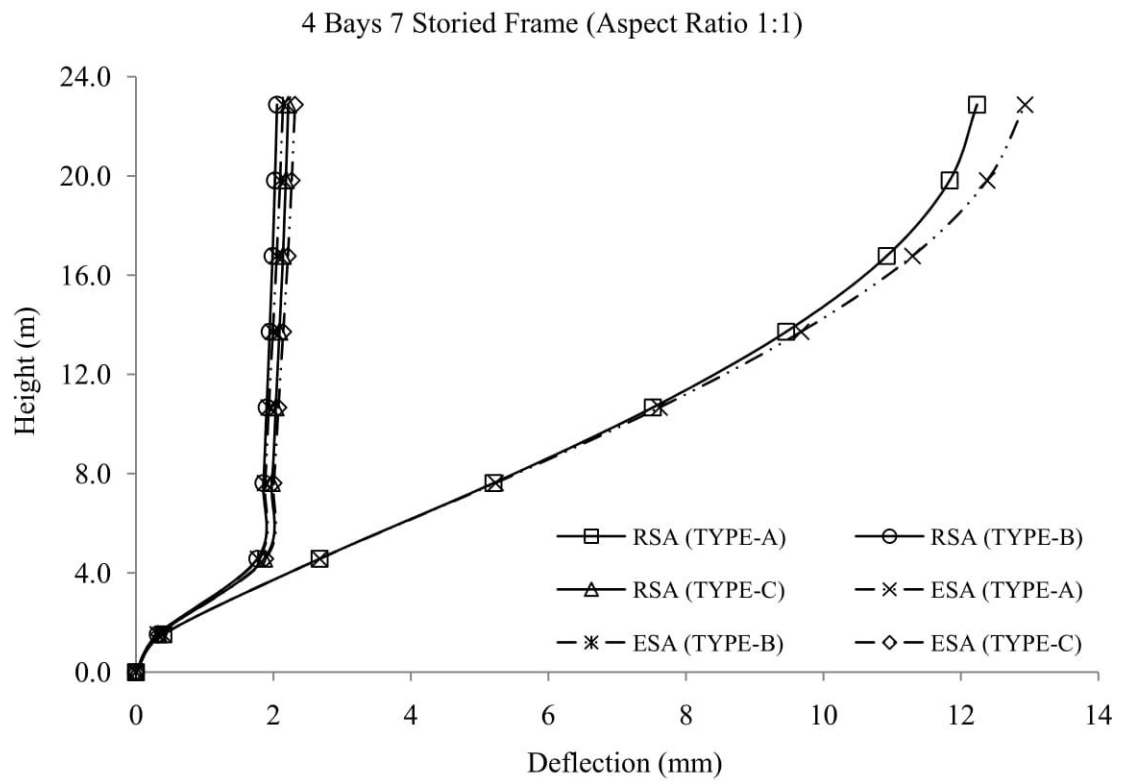
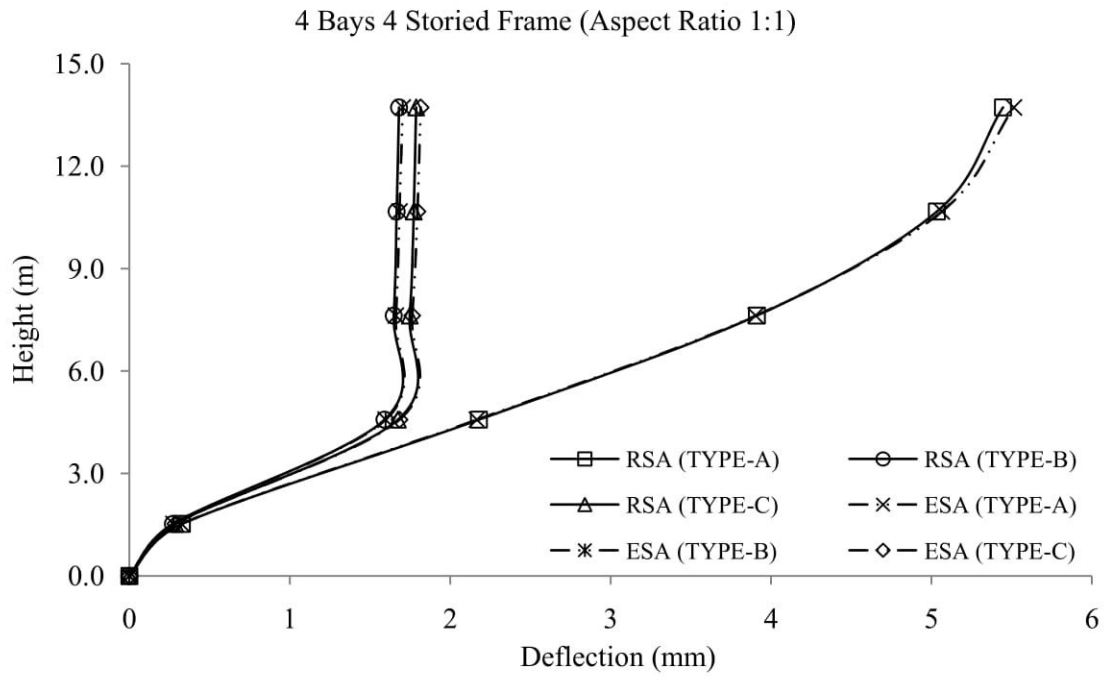
Table 4.3: Top deflection of 10 storied building

Story No.	Type of Frame	Aspect Ratio	Top Deflection (mm)			
			Fixed Support		Hinged Support	
			RSA	ESA	RSA	ESA
10 Storied Building	A	1:1	20.47	22.17	22.00	24.26
	B		2.41	2.59	3.81	4.04
	C		2.64	2.84	4.11	4.39
	A	1:1.5	21.18	22.99	22.86	25.25
	B		2.59	2.77	4.19	4.42
	C		2.77	2.97	4.42	4.67
	A	1:2	21.29	23.11	23.01	25.45
	B		2.84	3.07	4.52	4.83
	C		3.02	3.28	4.75	5.05
	A	1:2.5	19.35	21.01	20.83	23.01
	B		3.15	3.45	4.67	5.05
	C		3.35	3.68	4.90	5.31

#### 4.9.2 Story wise Deflection of Frames

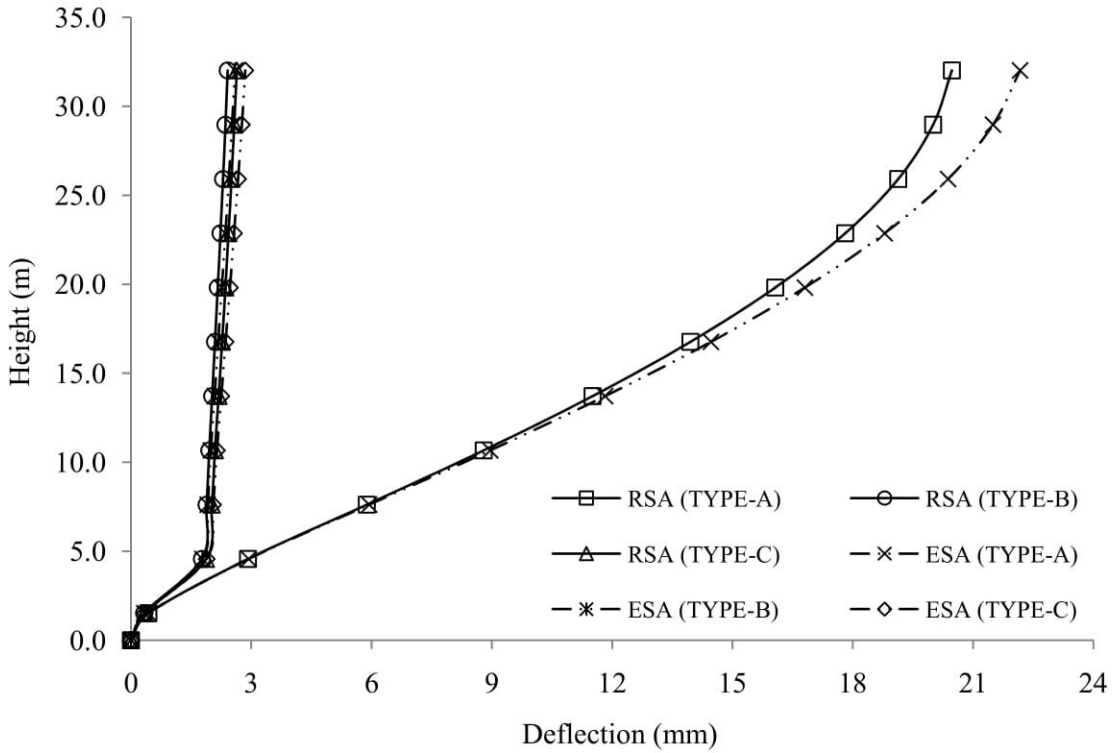
Story wise total deflection of all models with all aspect ratios for fixed and hinged support is summarized. Then graphs are plotted using these results which are shown in Figure 4.15 and 4.16 for aspect ratio of 1:1. From the graphs it is found that story wise deflection is greater in Equivalent Static Analysis than Response Spectrum Analysis for bare frame (Type A) and infill frame having opening (Type B and Type C) for 4, 7 and 10 storied building. It is also observed that deflection reduces gradually with the increase of infill having opening (Type B and Type C) due to increased stiffness of the story for the presence of infill having opening. Here, the infill is acting as equivalent diagonal strut which is actually responsible for increase of story stiffness. The deflection in infill having window opening is slightly higher than infill having door opening. The displacement profiles for both Equivalent Static Analysis (ESA) and Response Spectrum Analysis (RSA) have a sudden change of slope at 4.6 m i.e. at top of ground floor. The stiffness irregularity between the ground floor and immediate upper floor is responsible for the sudden changes in the slope of the profile. Thus higher movement of building can be observed in the ground floor if the consideration of infill in frame is not made, which can lead to large damage in the columns at the ground floor due to lateral loading. The other

graphs of story wise deflection of frames with beam-column aspect ratios of 1:1.5, 1:2 and 1:2.5 are shown in Figure B4.4, B4.5 and B4.6 of Appendix B4.





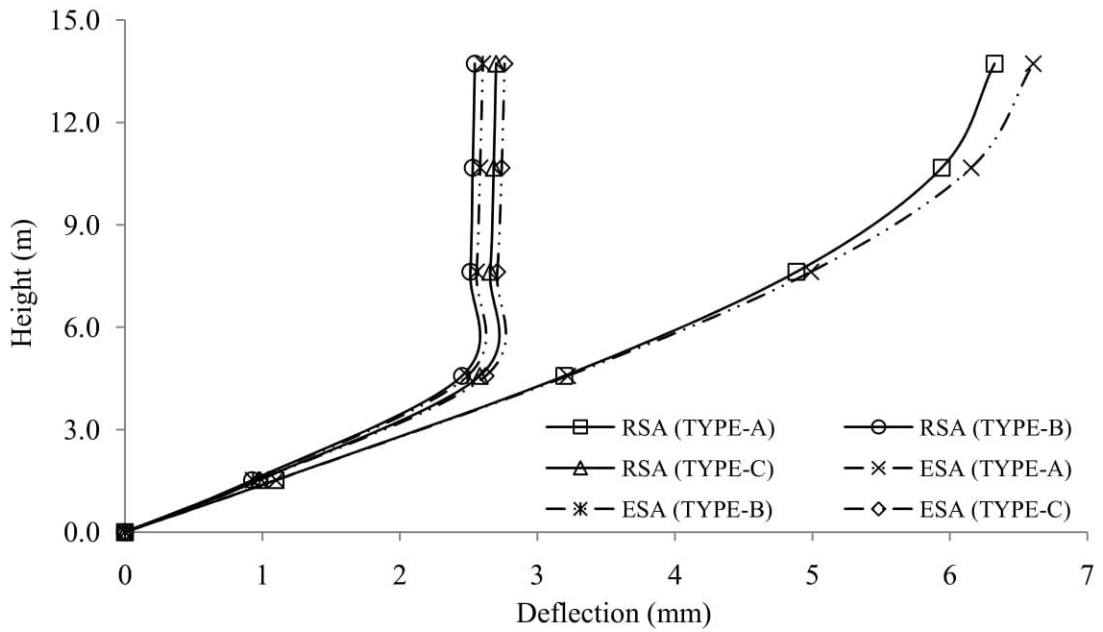
4 Bays 10 Storied Frame (Aspect Ratio 1:1)



(c)

Figure 4.15: Story wise deflection of (a) 4 storied (b) 7 storied and (c) 10 storied building frames for fixed support with aspect ratio of 1:1

4 Bays 4 Storied Frame (Aspect Ratio 1:1)



(a)

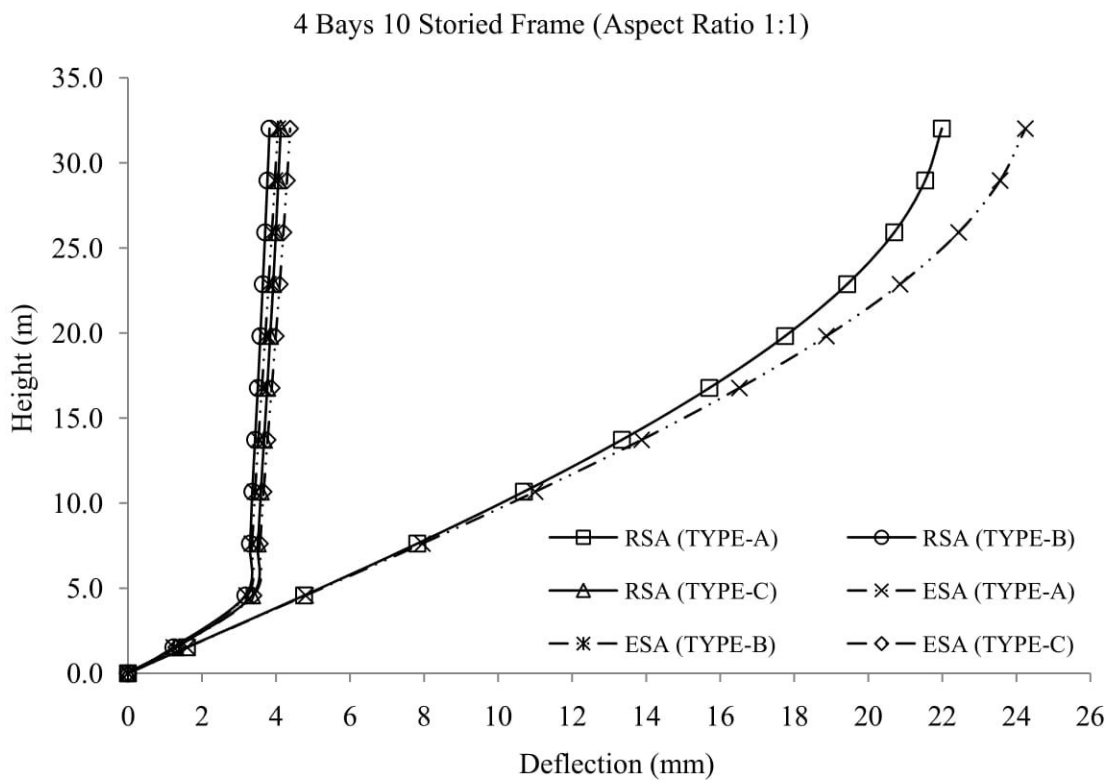
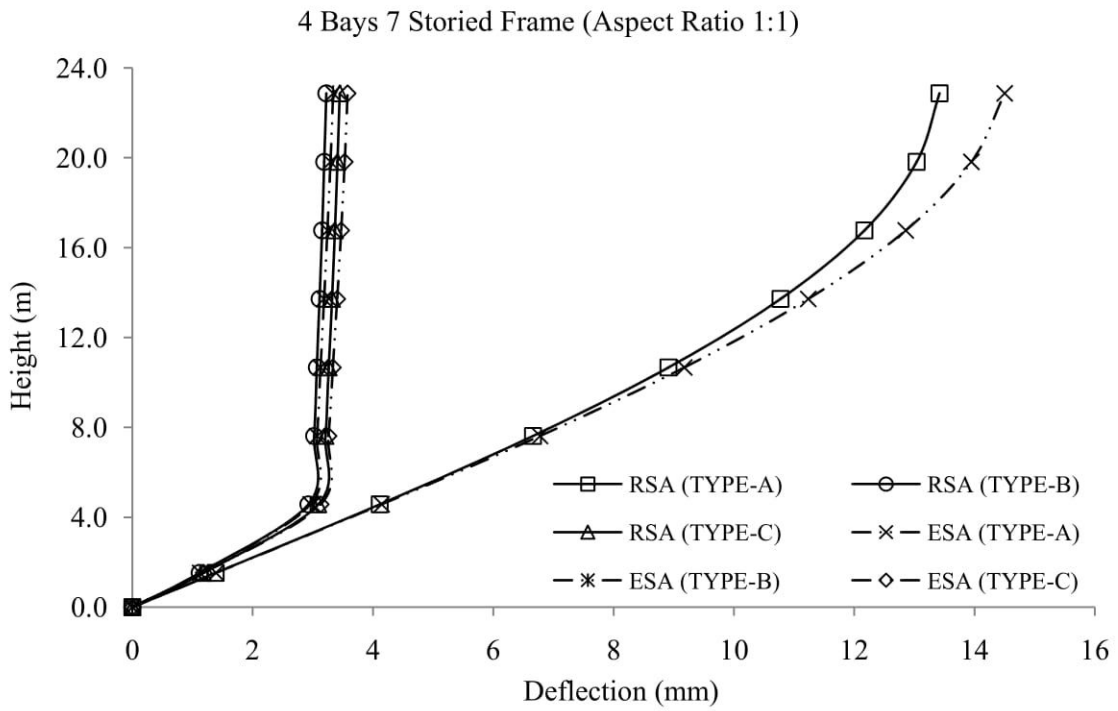
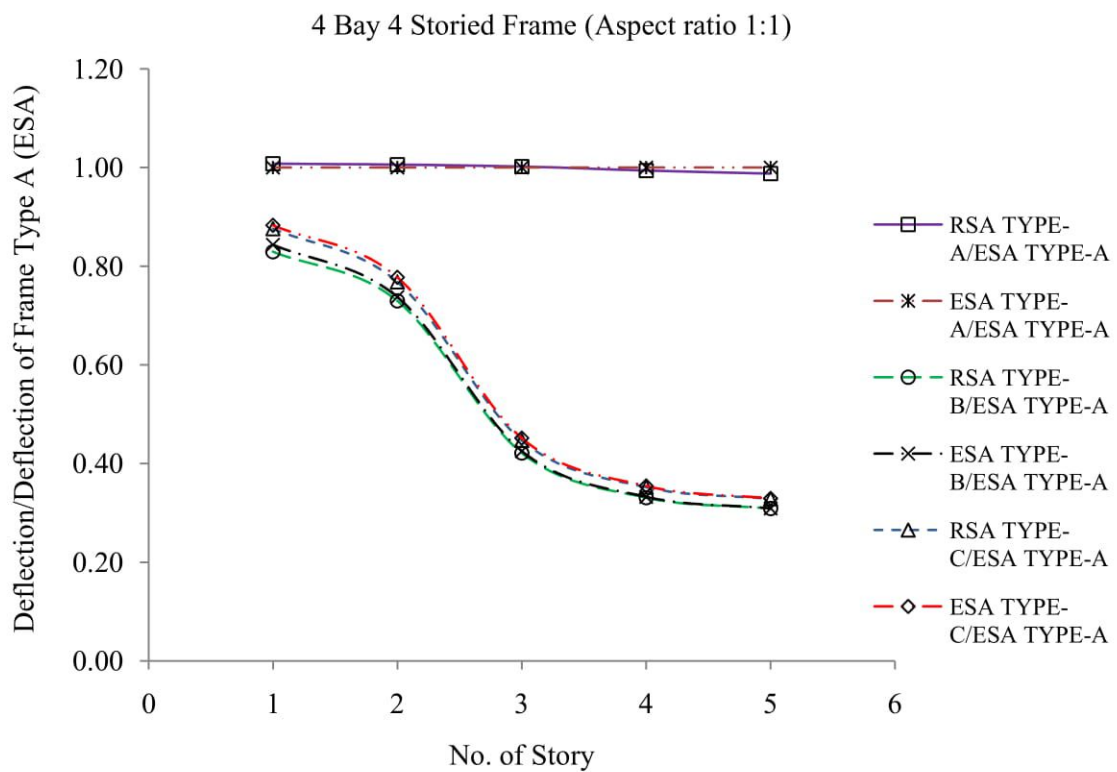


Figure 4.16: Story wise deflection of (a) 4 storied (b) 7 storied and (c) 10 storied building frames for hinged support with aspect ratio of 1:1

### 4.9.3 Story Wise Deflection Pattern with respect to ESA Deflection of Bare Frame

Storey wise deflection pattern of frames with respect to ESA deflection of bare frame (Type A) for both supports is shown in Figure 4.17 and 4.18 for aspect ratio of 1:1. For fixed support, it is found that the deflection of all frames with respect to ESA deflection of bare frame (Type A) decreases with story height for both ESA and RSA in all cases except RSA of bare frame (Type A). For hinged support, the storey wise deflection value also decreases with increasing the story height after 1.5 m. That represents that Equivalent Static Analysis gives higher story wise deflection values compared to Response Spectrum Analysis with respect to bare frame. The other graphs of story wise deflection pattern of frames with respect to ESA deflection of bare frame (Type A) is shown in Figure B4.7, B4.8 and B4.9 of Appendix B4.



(a)

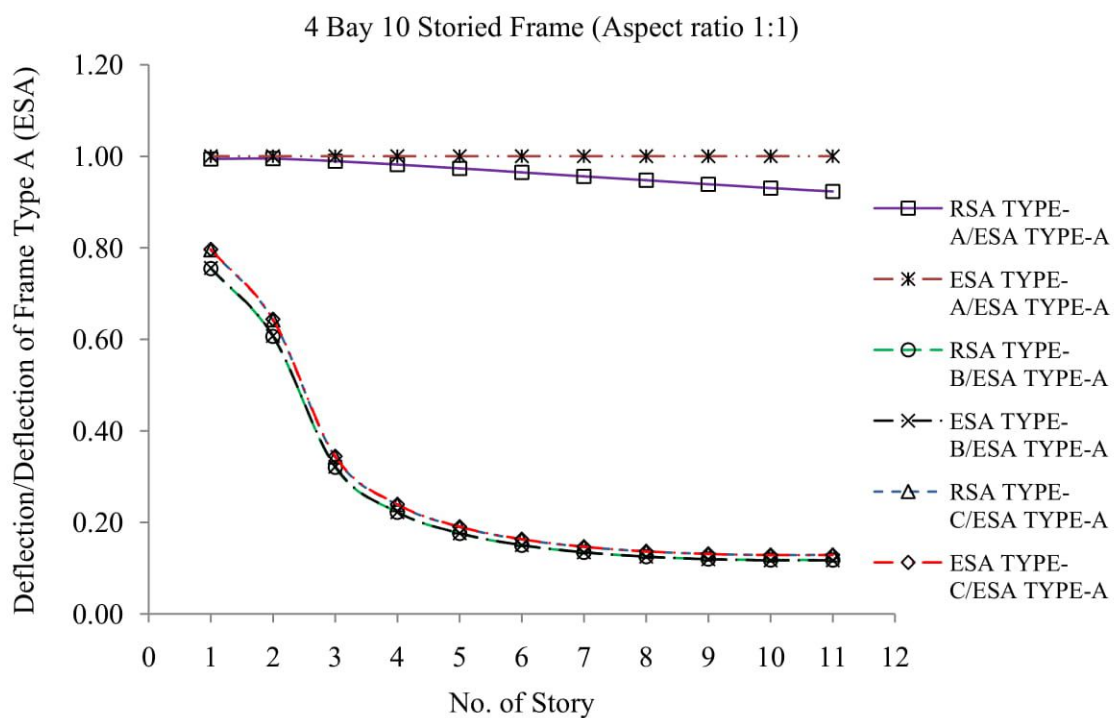
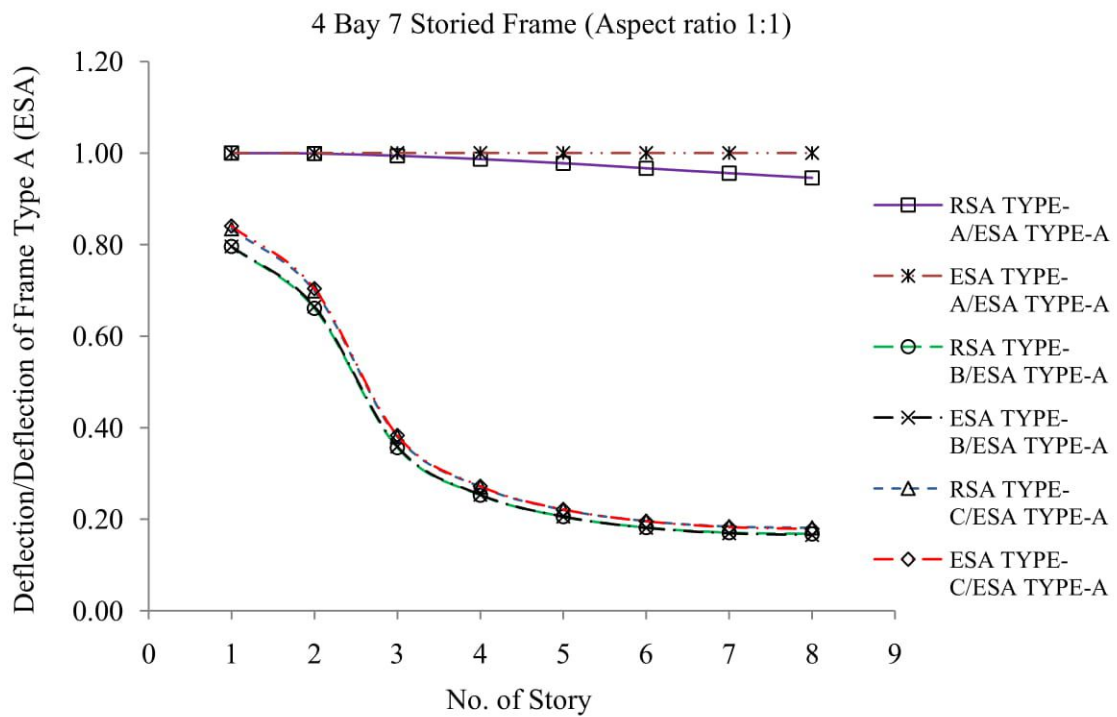
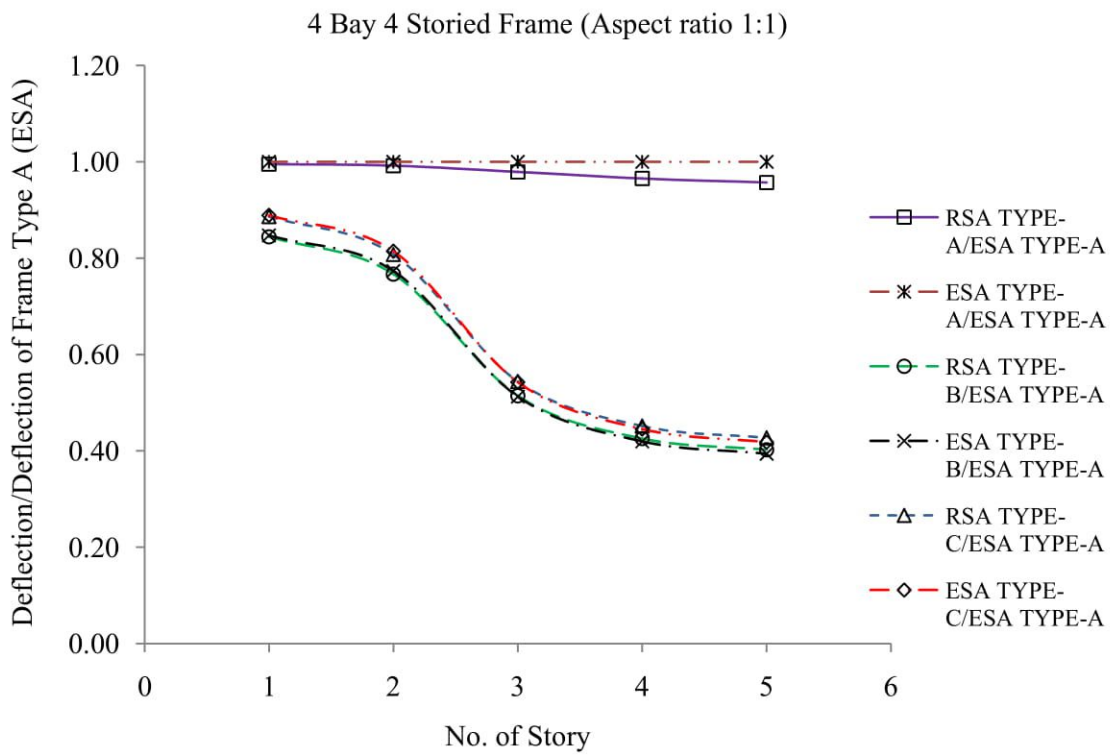
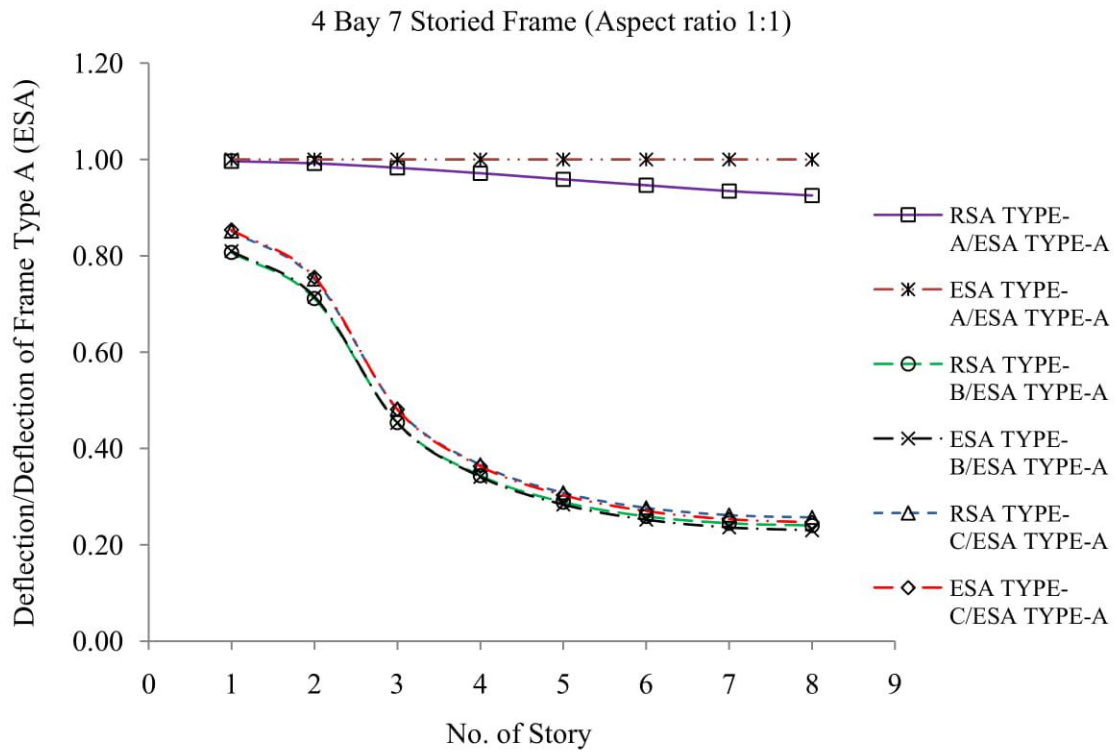


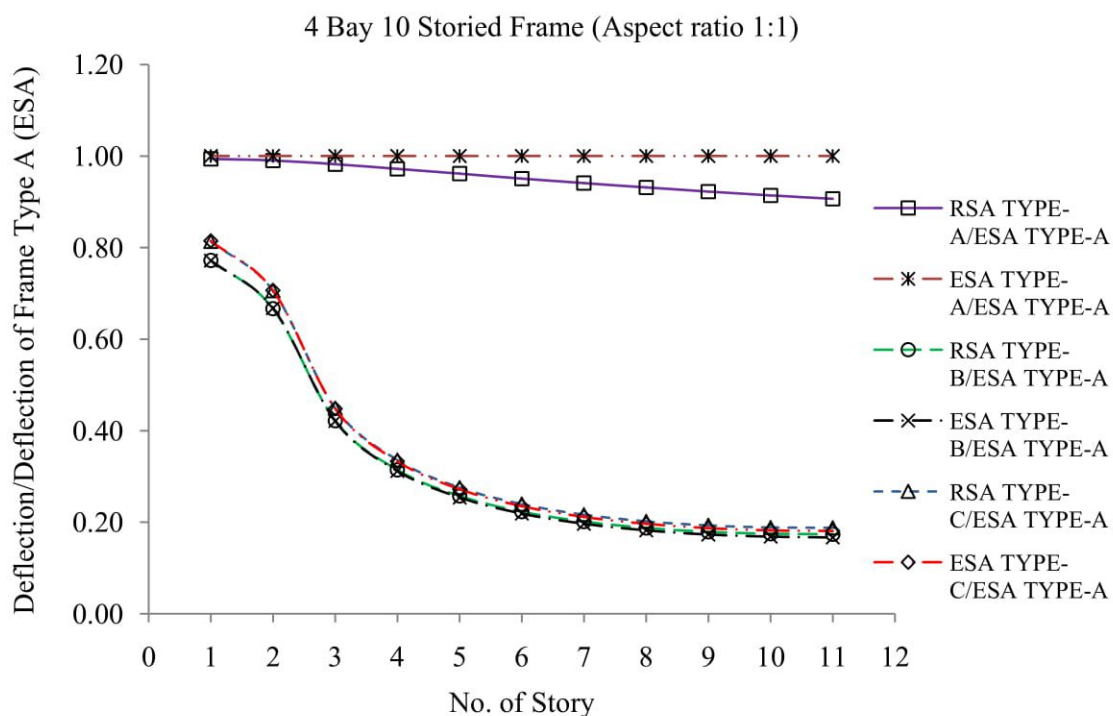
Figure 4.17: Story wise deflection pattern of (a) 4 storied (b) 7 storied and (c) 10 storied building frames for fixed support with respect to ESA deflection of bare frame with aspect ratio of 1:1



(a)



(b)



(c)

Figure 4.18: Story wise deflection pattern of (a) 4 storied (b) 7 storied and (c) 10 storied building frames for hinged support with respect to ESA deflection of bare frame with aspect ratio of 1:1

#### 4.9.4 Inter Story Drift

Inter story drift (ID) for all models with aspect ratios of 1:1, 1:1.5, 1:2, 1:2.5 at ground floor level are determined in Equivalent Static Analysis and Response Spectrum Analysis and summarized in Table 4.4-4.6. From Tables, it has been observed that the inter story drift value is almost same in RSA and ESA for fixed and hinged support. The inter story drift value of all models is higher for hinged support than fixed support. The inter story drift value becomes less in frame Type B and C than Type A for both supports. This is caused due to the presence of infill having opening in frame Type B and C and consideration of the effect of equivalent strut i.e. infill having opening in the frame. Here, the inter story drift is considered at ground floor level because load concentration occurs at ground floor level since infill is located on the upper stories keeping the ground floor open.

Table 4.4: Inter story drift at ground floor level of 4 storied building

Story No.	Type of Frame	Aspect Ratio	Inter Story Drift			
			Fixed Support		Hinged Support	
			RSA	ESA	RSA	ESA
4 Storied Building	A	1:1	1.85	1.84	2.10	2.12
	B		1.32	1.32	1.53	1.56
	C		1.39	1.40	1.61	1.65
	A	1:1.5	1.88	1.87	2.17	2.20
	B		1.39	1.39	1.65	1.69
	C		1.44	1.45	1.71	1.75
	A	1:2	1.84	1.83	2.16	2.19
	B		1.39	1.40	1.68	1.71
	C		1.42	1.44	1.72	1.76
	A	1:2.5	1.68	1.67	1.97	1.99
	B		1.32	1.33	1.58	1.62
	C		1.35	1.36	1.61	1.65

Table 4.5: Inter story drift at ground floor level of 7 storied building

Story No.	Type of Frame	Aspect Ratio	Inter Story Drift			
			Fixed Support		Hinged Support	
			RSA	ESA	RSA	ESA
7 Storied Building	A	1:1	2.27	2.28	2.73	2.76
	B		1.45	1.46	1.81	1.84
	C		1.53	1.55	1.91	1.95
	A	1:1.5	2.36	2.36	2.88	2.91
	B		1.57	1.59	2.01	2.04
	C		1.64	1.65	2.09	2.12
	A	1:2	2.35	2.36	2.91	2.94
	B		1.61	1.62	2.09	2.11
	C		1.66	1.67	2.14	2.17
	A	1:2.5	2.16	2.16	2.64	2.67
	B		1.56	1.57	1.98	2.01
	C		1.60	1.61	2.03	2.06

Table 4.6: Inter story drift at ground floor level of 10 storied building

Story No.	Type of Frame	Aspect Ratio	Inter Story Drift			
			Fixed Support		Hinged Support	
			RSA	ESA	RSA	ESA
10 Storied Building	A	1:1	2.48	2.50	3.16	3.20
	B		1.44	1.45	1.94	1.97
	C		1.53	1.54	2.06	2.09
	A	1:1.5	2.61	2.62	3.36	3.40
	B		1.59	1.61	2.18	2.20
	C		1.66	1.67	2.27	2.30
	A	1:2	2.62	2.63	3.41	3.45
	B		1.66	1.67	2.29	2.31
	C		1.71	1.72	2.35	2.38
	A	1:2.5	2.41	2.42	3.09	3.12
	B		1.63	1.65	2.19	2.22
	C		1.68	1.69	2.25	2.28

#### 4.10 Effect of Infill having Opening on Maximum Bending Moment

Equivalent Static Analysis and Response Spectrum Analysis have been carried out to study the flexural effect on frames having infill walls due to lateral loading. The value of maximum bending moment of 4, 7 and 10 storied building frames with all aspect ratios is summarized in Table 4.7-4.9 for fixed support. From Tables, it is noticed that the value of bending moment increases for all types of frame in ESA than RSA. The bending moment is less for Type B and Type C than Type A in both RSA and ESA. The bending moment in Type B and Type C i.e. infill frame having door and window opening is reduced due to the acting of infill as a diagonal strut in the frame which actually stiffens the structure. The value of maximum moment also increases with the increase of story height and aspect ratio. In ESA, the maximum moment for all types of frame governs at ground floor presented by 2-B location. On the other hand, maximum moment in RSA for frame Type B and Type C governs at ground floor location presented by 2-B and Type A governs at ground floor location presented by 1-B for all models.



Table 4.7: Maximum moment and their governing location for 4 storied building for fixed support

Story No.	Type of Frame	Aspect Ratio	Maximum Moment (N-m)		Location	
			RSA	ESA	RSA	ESA
4 Storied Building	A	1:1	13426	19272	1-B	2-B
	B		10846	10883	2-B	2-B
	C		11359	11406	2-B	2-B
	A	1:1.5	20149	34889	1-B	2-B
	B		16947	20163	2-B	2-B
	C		17492	20900	2-B	2-B
	A	1:2	27722	56308	1-B	2-B
	B		23724	32929	2-B	2-B
	C		24240	33443	2-B	2-B
	A	1:2.5	36338	85685	1-B	2-B
	B		31585	49638	2-B	2-B
	C		32098	50220	2-B	2-B

Table 4.8: Maximum moment and their governing location for 7 storied building for fixed support

Story No.	Type of Frame	Aspect Ratio	Maximum Moment (N-m)		Location	
			RSA	ESA	RSA	ESA
7 Storied Building	A	1:1	21177	26829	1-B	2-B
	B		16162	16265	2-B	2-B
	C		16949	17056	2-B	2-B
	A	1:1.5	31323	44757	1-B	2-B
	B		24814	25012	2-B	2-B
	C		25604	25807	2-B	2-B
	A	1:2	42647	67786	1-B	2-B
	B		34197	35719	2-B	2-B
	C		34976	36628	2-B	2-B
	A	1:2.5	54957	99865	1-B	2-B
	B		44911	53802	2-B	2-B
	C		45688	54614	2-B	2-B

Table 4.9: Maximum moment and their governing location for 10 storied building for fixed support

Story No.	Type of Frame	Aspect Ratio	Maximum Moment (N-m)		Location	
			RSA	ESA	RSA	ESA
10 Storied Building	A	1:1	28786	33301	1-B	2-B
	B		20797	20897	2-B	2-B
	C		21781	21896	2-B	2-B
	A	1:1.5	41945	54192	1-B	2-B
	B		31421	31637	2-B	2-B
	C		32404	32625	2-B	2-B
	A	1:2	56501	80446	1-B	2-B
	B		43140	43478	2-B	2-B
	C		44284	44629	2-B	2-B
	A	1:2.5	71707	114785	1-B	2-B
	B		55655	57237	2-B	2-B
	C		56580	57745	2-B	2-B

The value of maximum bending moment for hinged support of all models is summarized in Table 4.10-4.12. From Tables, it is found that the moment for hinged support also increases for all types of frame in ESA than RSA and also less for Type B and Type C than Type A in both RSA and ESA like fixed support. The governing location of maximum moment for both fixed and hinged support is same i.e. at ground floor level in ESA presented by location 2-B. On the other hand, maximum moment for hinged support in RSA governs at ground floor location presented by 1-A for frame Type A for all models. But maximum moment of frame Type B and Type C for hinged support governs at ground floor level presented by location 2-B in RSA similar to the governing location for fixed support. Also the moment increases in hinged support for all frames than fixed support with the increase of story height and aspect ratio. Alam (2014) concluded from his study that bending moment increased in the first ground floor whereas reduced in upper floors after placement of infill. Infill was placed as diagonal strut which stiffened the structure. As a result, bending moment decreased in those stories where infill was placed.

Table 4.10: Maximum moment and their governing location for 4 storied building for hinged support

Story No.	Type of Frame	Aspect Ratio	Maximum Moment (N-m)		Location	
			RSA	ESA	RSA	ESA
4 Storied Building	A	1:1	15460	19791	1-A	2-B
	B		12865	14280	2-B	2-B
	C		13525	14955	2-B	2-B
	A	1:1.5	22522	35910	1-A	2-B
	B		19426	23253	2-B	2-B
	C		20085	23916	2-B	2-B
	A	1:2	30282	57912	1-A	2-B
	B		26593	34576	2-B	2-B
	C		27232	35220	2-B	2-B
	A	1:2.5	39888	87782	1-A	2-B
	B		35792	51248	2-B	2-B
	C		36455	51870	2-B	2-B

Table 4.11: Maximum moment and their governing location for 7 storied building for hinged support

Story No.	Type of Frame	Aspect Ratio	Maximum Moment (N-m)		Location	
			RSA	ESA	RSA	ESA
7 Storied Building	A	1:1	22207	28070	1-A	2-B
	B		18587	19073	2-B	2-B
	C		19508	20035	2-B	2-B
	A	1:1.5	32183	46384	1-A	2-B
	B		28984	30401	2-B	2-B
	C		29940	31366	2-B	2-B
	A	1:2	43087	70723	1-A	2-B
	B		40470	44343	2-B	2-B
	C		41412	45307	2-B	2-B
	A	1:2.5	56271	103896	1-A	2-B
	B		52673	63777	2-B	2-B
	C		53605	64779	2-B	2-B

Table 4.12: Maximum moment and their governing location for 10 storied building for hinged support

Story No.	Type of Frame	Aspect Ratio	Maximum Moment (N-m)		Location	
			RSA	ESA	RSA	ESA
10 Storied Building	A	1:1	27695	34234	1-A	2-B
	B		25401	25686	2-B	2-B
	C		26656	26941	2-B	2-B
	A	1:1.5	39813	55316	1-A	2-B
	B		38883	39344	2-B	2-B
	C		40145	40605	2-B	2-B
	A	1:2	53071	81779	1-A	2-B
	B		53509	54077	2-B	2-B
	C		54749	55314	2-B	2-B
	A	1:2.5	68924	116113	1-A	2-B
	B		68530	72864	2-B	2-B
	C		69739	74103	2-B	2-B

#### 4.11 Effect of Infill having Opening on Maximum Shear Force

The shear force of all types of frame with all aspect ratios is summarized in Table 4.13-4.15 for both fixed and hinged support. From Tables, it is found that the maximum shear force of all models occurs at ground floor presented by 1-B location in Response Spectrum Analysis and 2-B location in Equivalent Static Analysis for both supports. The shear force at Type A i.e. bare frame is higher than Type B and Type C i.e. infill frame having door or window opening in both RSA and ESA. Also the value of shear is greater in ESA than RSA for all models with all aspect ratios. Although the governing location of maximum shear for both fixed and hinged support is same, the value of maximum shear is higher in all models for hinged support rather than fixed support. Alam (2014) also concluded that as shear force increased in the open ground floor due to presence of infill in upper floors, consequently bending moment showed same pattern of change. Due to pendulum effect deflection was concentrated in ground floors so the moment was also concentrated.

Table 4.13: Maximum shear and their governing location for 4 storied building

Story No.	Type of Frame	Aspect Ratio	Maximum Shear (kN)				Location	
			Fixed Support		Hinged Support			
			RSA	ESA	RSA	ESA	RSA	ESA
4 Storied Building	A	1:1	8.75	22.57	9.59	22.92	1-B	2-B
	B		7.76	12.85	7.95	13.10	1-B	2-B
	C		8.13	13.65	8.35	13.92	1-B	2-B
	A	1:1.5	12.93	30.70	13.24	31.13	1-B	2-B
	B		11.92	18.87	12.18	19.18	1-B	2-B
	C		12.30	19.48	12.57	19.80	1-B	2-B
	A	1:2	17.50	39.77	18.07	40.28	1-B	2-B
	B		16.47	25.08	16.99	25.06	1-B	2-B
	C		16.84	24.50	17.37	24.81	1-B	2-B
	A	1:2.5	22.91	50.65	23.71	51.19	1-B	2-B
	B		21.84	31.81	22.62	31.79	1-B	2-B
	C		22.21	31.18	23.00	31.16	1-B	2-B

Table 4.14: Maximum shear and their governing location for 7 storied building

Story No.	Type of Frame	Aspect Ratio	Maximum Shear (kN)				Location	
			Fixed Support		Hinged Support			
			RSA	ESA	RSA	ESA	RSA	ESA
7 Storied Building	A	1:1	12.74	26.53	14.00	27.35	1-B	2-B
	B		11.17	14.16	11.51	14.17	1-B	2-B
	C		11.73	14.51	12.10	15.08	1-B	2-B
	A	1:1.5	18.54	34.32	19.38	35.28	1-B	2-B
	B		16.90	22.98	17.60	22.99	1-B	2-B
	C		17.48	22.79	18.21	22.80	1-B	2-B
	A	1:2	24.82	43.32	26.12	44.38	1-B	2-B
	B		23.12	31.58	24.28	31.57	1-B	2-B
	C		23.69	31.32	24.88	31.31	1-B	2-B
	A	1:2.5	32.20	54.25	33.88	55.30	1-B	2-B
	B		30.41	40.06	32.02	40.04	1-B	2-B
	C		30.98	39.64	32.61	39.62	1-B	2-B

Table 4.15: Maximum shear and their governing location for 10 storied building

Story No.	Type of Frame	Aspect Ratio	Maximum Shear (kN)				Location	
			Fixed Support		Hinged Support			
			RSA	ESA	RSA	ESA	RSA	ESA
10 Storied Building	A	1:1	16.27	30.73	17.64	31.35	1-B	2-B
	B		13.99	16.53	14.64	16.53	1-B	2-B
	C		14.64	17.08	15.41	17.07	1-B	2-B
	A	1:1.5	23.49	38.03	22.92	38.55	1-B	2-B
	B		20.83	26.56	22.07	26.60	1-B	2-B
	C		21.55	26.53	22.84	26.56	1-B	2-B
	A	1:2	31.35	46.58	32.77	47.42	1-B	2-B
	B		28.30	36.21	30.18	36.22	1-B	2-B
	C		29.01	36.14	30.94	36.15	1-B	2-B
	A	1:2.5	40.45	57.02	42.20	58.30	1-B	2-B
	B		39.73	46.04	42.55	46.77	1-B	2-B
	C		44.68	47.97	47.81	51.66	1-B	2-B

The governing location of maximum moment and shear of all types of frame for both fixed and hinged support is shown in Figure 4.19-4.21 in both RSA and ESA.

For moment,

ESA = Equivalent Static Analysis for all types of frame (fixed and hinged support)

RSA (O) = Response Spectrum Analysis for infill frame having opening (fixed and hinged support)

RSA (B-F) = Response Spectrum Analysis for Type A, bare frame (fixed support)

RSA (B-H) = Response Spectrum Analysis for Type A, bare frame (hinged support)

For shear,

ESA = Equivalent Static Analysis for all types of frame (fixed and hinged support)

RSA = Response Spectrum Analysis for all types of frame (fixed and hinged support)

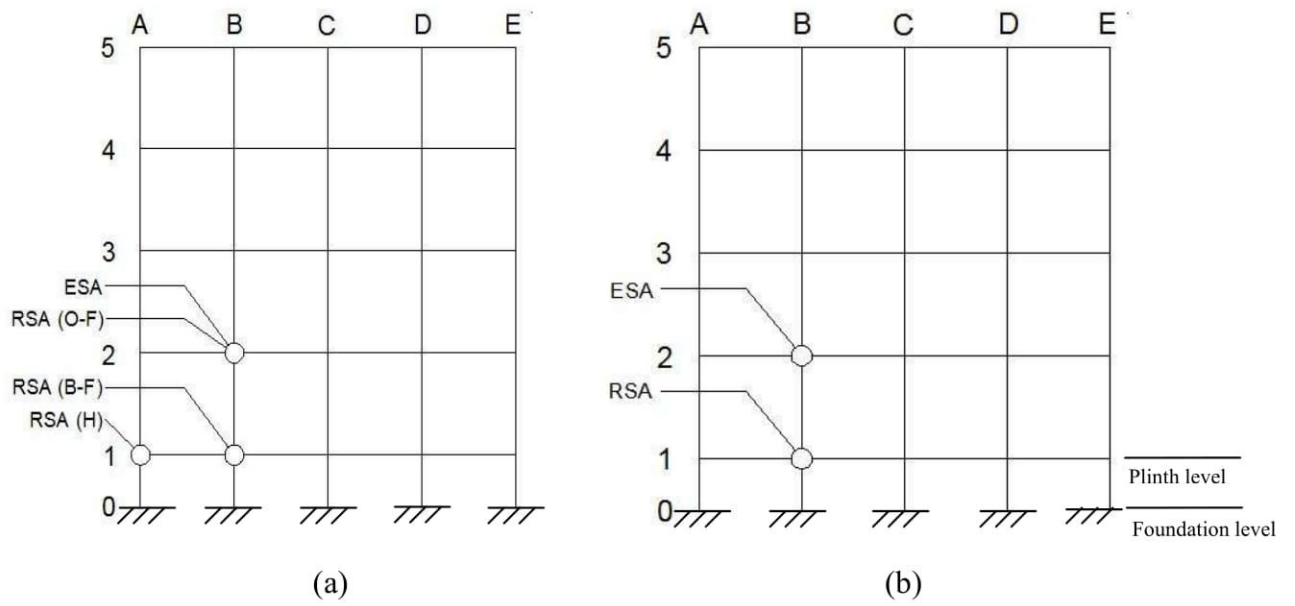


Figure 4.19: Governing location of (a) maximum moment and (b) maximum shear for 4 storied building

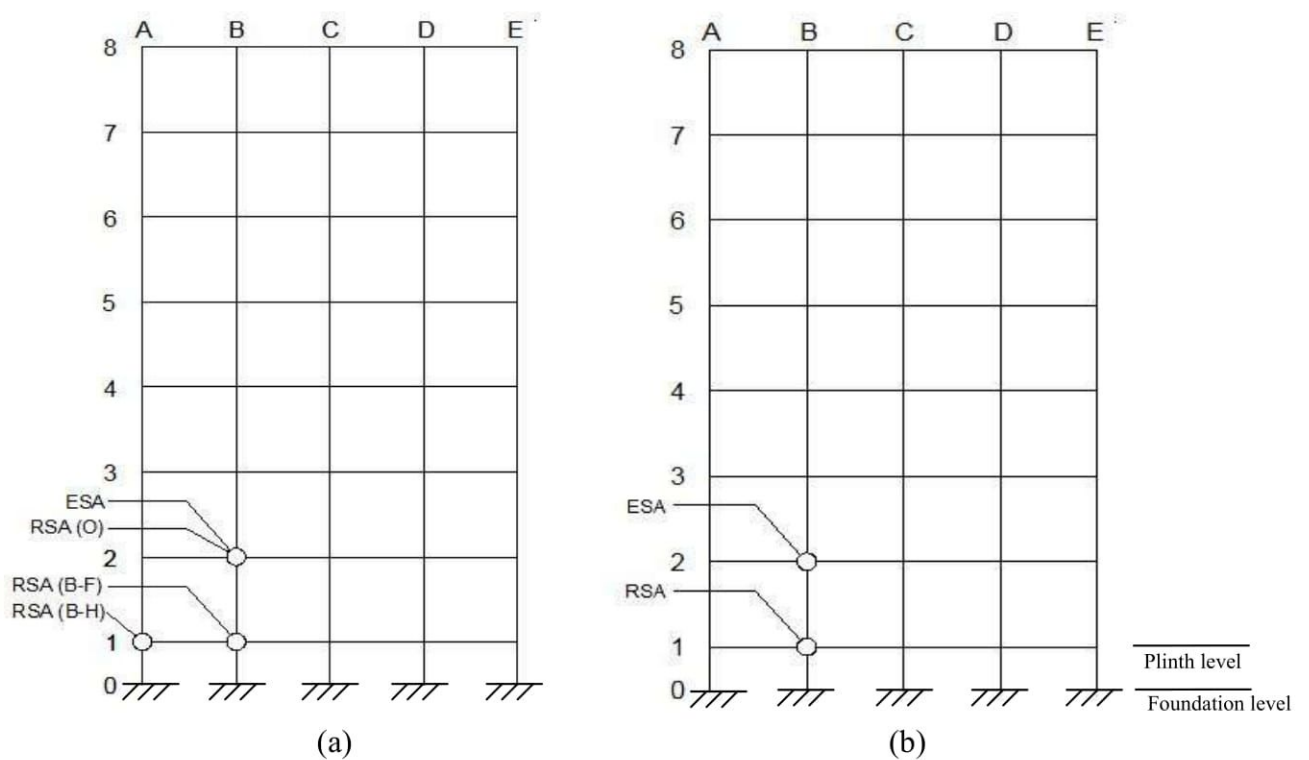


Figure 4.20: Governing location of (a) maximum moment and (b) maximum shear for 7 storied building

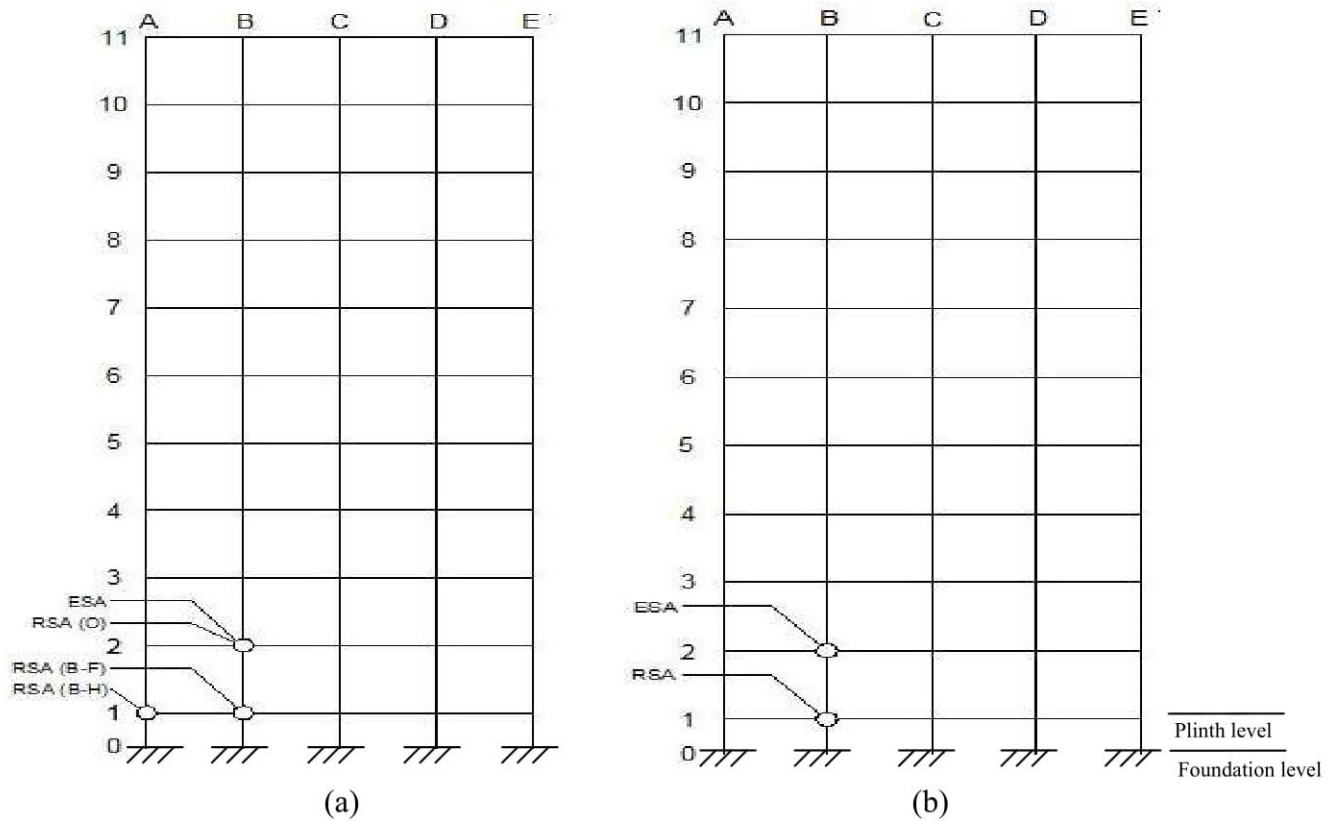


Figure 4.21: Governing location of (a) maximum moment and (b) maximum shear for 10 storied building

The maximum moment and shear of all types of frames of 4, 7 and 10 storied building frames with aspect ratios of 1:1, 1:1.5, 1:2 and 1:2.5 governs at ground floor level in both Equavalent Static Analysis and Response Spectrum Analysis. The absence of infill in the ground floor level of these frames is responsible for this. Also soft floor forms at ground floor level due to stiffness irregularity between ground floor and upper floor in the building frames. Although the value of inter story drift is almost same in both Equavalent Static Analysis and Response Spectrum Analysis, it decreases in infill frames having opening due to consideration of effect of infill in the frames.

It has been observed that the value of maximum moment and shear is always greater in Equavalent Static Analysis than Response Spectrum Analysis. Also the governing location of maximum moment and shear for some frames is not same in the ground floor level. Another thing is noticeable that the variation of moment between ESA and RSA significantly decreases for infill frames having opening of 10 storied building compared to 4 and 7 storied building frames.



Actually, the load distribution in Response Spectrum Analysis is quite different from Equivalent Static Analysis. Equivalent Static Analysis is based on a cantilever type of load distribution which does not consider significant impact of higher mode of structure and offered quite large moment demands for these models. In Response Spectrum Analysis, multiple mode shapes and modal mass participation of the structure for different building frequencies are considered. Thus Response Spectrum Analysis gives better insight into these building frames performance and demands on the structure in terms of moment and shear.

#### 4.12 Effect of Infill having Opening on Base Shear

Base shear of all types of frames for 4, 7 and 10 storied building with all aspect ratios is summarized in Table 4.16. The base shear in frame Type B and C i.e. infill frame having door and window opening is lower than Type A i.e. bare frame due to opening in infill frame.

Table 4.16: Base shear of all types of frames

Type of Frame	Aspect Ratio	Base Shear (kN) in RSA and ESA		
		4 Storied Building	7 Storied Building	10 Storied Building
A	1:1	36.80	54.16	68.98
B		32.26	47.13	60.03
C		33.82	49.53	63.15
A	1:1.5	54.56	79.12	99.55
B		50.06	72.13	90.69
C		51.66	74.58	93.81
A	1:2	74.27	106.53	132.97
B		69.82	99.64	124.20
C		71.38	102.04	127.27
A	1:2.5	97.54	138.35	171.50
B		93.14	131.45	162.78
C		94.70	133.90	165.90

### 4.13 Mode Shapes of Frames

Since Response Spectrum Analysis has been performed hence different mode shapes for probable vibration pattern are encountered. Different frequencies of vibration arise for different mode shapes. Here some well distinguished mode shapes are given to get some ideas about the different modes of vibration in dynamic analysis. The first three mode shapes of 4 bays 7 storied building frame with aspect ratio 1:1 is shown in Figure 4.22.

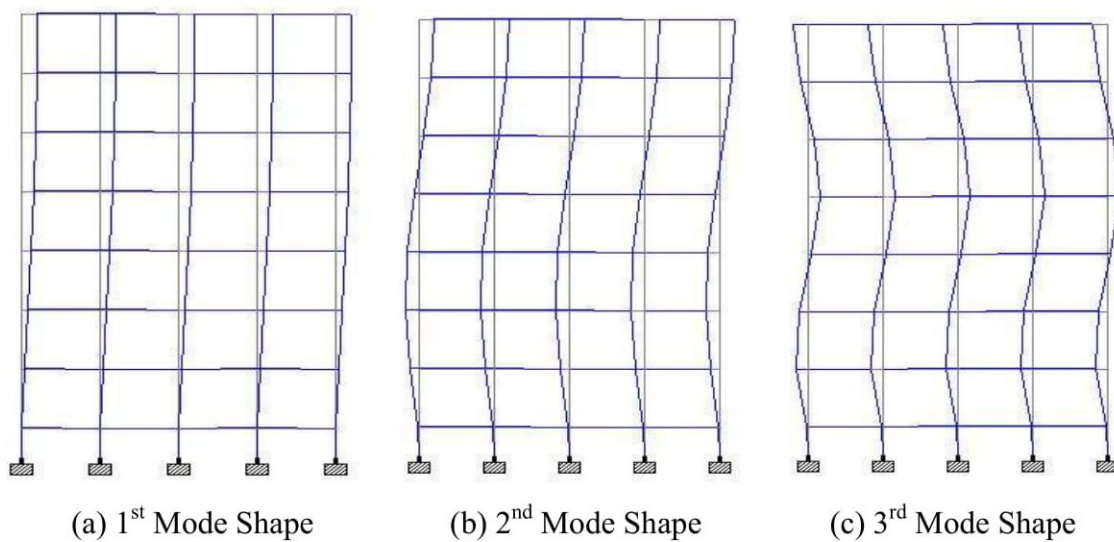


Figure 4.22: Mode shapes of 4 bays 7 storied building

## CHAPTER V

### CONCLUSIONS AND RECOMMENDATIONS

#### 5.1 General

In this study, experimental analysis has been done in the laboratory and computational analysis has been performed by both Equivalent Static Analysis (ESA) and Response Spectrum Analysis (RSA) on reinforced concrete (RC) frames considering the effect of without infill and with infill having opening on upper floors keeping open ground floor due to lateral loading. Generally the effect of infill having opening is not considered for the design of building. So a comparison can be made by the experimental and parametric study to understand the actual behavior of reinforced concrete frame with masonry infill walls having opening with the current design practice.

#### 5.2 Conclusions

The findings of the study are summarized below:

- i. From the experimental analysis, it is found that the failure load and stiffness for two storied single bay reinforced concrete infill frame having opening was greater than bare frame. The failure load increased by 75% and 69%, however, the displacement reduced by 9.74% and 9.53% for infill frame having door and window opening respectively with respect to bare frame. The stiffness of infill frame having door and window opening was three and four times greater than bare frame up to first crack.
- ii. Equivalent Static Analysis gave higher value of the maximum moment and shear than Response Spectrum Analysis for all types of frames. These values were lower in infill frame having opening than bare frame due to consideration of effect of infill and difference of load distribution of ESA and RSA in the frame. The maximum bending moment and shear governed at ground floor level where infill was absent and increased than other floors in both RSA and ESA. The value of maximum

bending moment and shear also increased with the increase of story height and aspect ratio for all frames.

- iii. Sway increased suddenly at ground floor, whereas it decreased on upper floor for infill frames having opening and formed soft floor at ground floor level due to stiffness variation between ground and upper floor. The consideration of presence of infill walls having opening in the frame with open ground floor made the upper floor rigid and as a result major deflection concentrated in ground floor. The inter story drift value in the ground floor also decreased in infill frames having opening due to consideration of effect of infill in the frames.
- iv. Equivalent Static Analysis gave conservative results compared to Response Spectrum Analysis for conventional design of regular buildings.

### **5.3 Recommendations**

The following recommendations can be made for future works:

- i. The scope of the present investigation can be expanded by including more infill thickness, no of stories and bays under investigation.
- ii. The analysis can be carried out for different infill orientation and presence of openings at different story in the frame.
- iii. The elements in the model were considered to be two dimensional. To be more realistic with the results three dimensional elements for analysis can be used.
- iv. The frame can be studied under cyclic-loading to evaluate its performance.

## REFERENCES

Alam, M. T., 2014, “Behaviour of Randomly Infilled RC Frames with Soft Ground Floor subjected to Seismic Loading, M.Sc. Thesis, Bangladesh University of Engineering and Technology.

Al-Chaar, G., 2002, “Evaluating Strength and Stiffness of Unreinforced Masonry Infill Structures”, US Army Corps of Engineers, Engineer Research and Development Center, ERDC/CERL TR-02-1, January.

Al-Chaar, G., 1998, “Non-Ductile Behavior of Reinforced Concrete Frames with Masonry Infill Panels Subjected to In-Plane Loading”, U.S. Army Corps of Engineers, Construction Engineering Research Laboratories, Technical Manuscript 99/18/ADA 360129, December.

Al-Chaar, G., and Mehrabi, A., 2008, “Constitutive Models for Nonlinear Finite Element Analysis of Masonry Prisms and Infill Walls”, US Army Corps of Engineers, Engineer Research and Development Center, ERDC/CERL TR- 08-19, March.

Al-Chaar, G., Sweeney, S., and Brady, P., 1996, “Push Over Laboratory Testing of Unreinforced Masonry Infills”, Wind and Seismic Effects, NIST SP 904, August.

Amerhein J. E., 2000, “Reinforced Masonry Engineering Handbook, Clay and Concrete Masonry”, 5<sup>th</sup> Edition, Masonry Institute of America, CRC Press, Boca Raton, New York.

American Concrete Institute (ACI) & American Society of Civil Engineers (ASCE), 1992, Building Code Requirements for Concrete Masonry Structures (AU 530-921, ASCE 5-921, TMS 402-92) and Specifications for Masonry Structures (ACI 530.1-921, ASCE 6-921, TMS 602- 92).

American Concrete Institute (ACI 318), 2008, “Building Code Requirements for Structural Concrete”, ACI Committee, Farmington Hills, MI.

American Society for Testing and Materials (ASTM) A615, 1995, “Annual Book of ASTM Standards”. Vol. 03. Philadelphia, USA. pp. 3-499.

American Society for Testing and Materials (ASTM) C 39, 1994, “Annual Book of ASTM Standards”. Vol. 04.05. Philadelphia, USA. pp. 4-47.

American Society for Testing and Materials (ASTM) C 62, 1994, “Annual Book of ASTM Standards”, Vol. 04.05. Philadelphia.

American Society for Testing and Materials (ASTM) C 67, 2008, “Annual Book of ASTM Standards”, Philadelphia.

American Society for Testing and Materials (ASTM) C 109, 1994, “Annual Book of ASTM Standards”, Vol. 04.01. Philadelphia.

American Society for Testing and Materials (ASTM) C 270, 1994, Standard Specification for Mortar for Unit Masonry, “Annual Book of ASTM Standards”.

American Society for Testing and Materials (ASTM) E8, 1995, “Annual Book of ASTM Standards”. Vol. 02. Philadelphia, USA. pp. 2-68.

Angel, R., Abram, D. P., Shapiro, D., J. Uzarski, D. and Webster, M., 1994, “Behavior of Reinforced Concrete Frames with Masonry Infills”, Structural Research Series No. 589, UILU-ENG-94-2005, University of Illinois at Urbana, Illinois, March.

Bangladesh National Building Code (BNBC), 1993, 1<sup>st</sup> Edition, Housing and Building Research Institute, Mirpur and Bangladesh Standard and Testing Institute, Tejgaon, Dhaka.

Benjamin, J.R., and Williams, H.A., 1958, “The Behavior of One-Story Shear Walls”, Journal of the Structural Division, Proceedings of the American Society of Civil Engineers, vol. 84, no. ST4, July.

Bennett, R.M., Flanagan, R.D., Adham, S., Fischer, W.L. and Tenbus, MA., 1996, "Evaluation and Analysis of the Performance of Masonry Infills During the Northridge Earthquake", Oak Ridge National Laboratory, February.

Bertero, V., and Brokken, S., 1983, "Infills in Seismic Resistant Building", Journal of the Structural Engineering, ASCE, Vol. 109, No 6, June, pp 1337-1361.

Colangelo, F., 2005, "Pseudo-dynamic Seismic Response of Reinforced Concrete Frames Infilled with Non-structural Brick Masonry", Earthquake Engng Struct. Dyn. 34:1219–1241.

EERI, 2001, "Annotated Images from the Bhuj, India Earthquake of January 26", (CD). Earthquake Engineering Research Institute, Oakland, CA.

Fiorato, A.E., Sozen, M.A. and Gamble. W.L., 1970, "An Investigation of the Interaction of Reinforced Concrete Frames with Masonry Filler Walls", Civil Engineering Studies, Structural Research Series No. 370, University of Illinois, Urbana, November.

Haque, S., 2007, "Behavior of Multistoried RC Framed Buildings with Open Ground Floor under Seismic Loading, M.Sc. Degree Dissertation, Bangladesh University of Engineering and Technology (BUET), Dhaka, Bangladesh.

Holm, T.A., 1978, "Structural Properties of Block Concrete", Proceedings of the North American Masonry Conference, Boulder: The Masonry Society, paper # 5.

Holmes, M., 1961, "Steel Frames with Brickwork and Concrete Infilling", Proceedings of the Institution of Civil Engineers, vol. 19, pp. 473-4 7S.

International Building Code (IBC), 2000, Building Officials and Code Administrators International, International Conference of Building Officials and Southern Building Code Congress International, U.S.A.

Klingner, R. E., and Bertero, V. V., 1978, "Earthquake Resistance of Infilled Frames", *Journal of the Structural Engineering*, ASCE, Vol. 104, No. ST6, June, pp. 973-989.

Mainstone, R. J., 1971, "On the Stiffness and Strengths of Infilled Frames", *Proceedings of the Institution of Civil Engineers*, Supplement IV, UK, pp 57-90.

Mallick, D.V. and Garg, R.P., 1971, "Effects of Openings on the Lateral Stiffness of Infilled Frames", *Proceedings of the Institution of Civil Engineers*, vol. 49, no. 7371, June.

Mehrabi, A. B., Shing, P. B., Schuller, M. P. and Noland, J. L., 1996, "Experimental Evaluation of Masonry-Infilled RC Frames", *Journal of Structural Engineering*, ASCE, Vol. 122, No. 3, March, pp 228-237.

Moghaddam, H. A. and Dowling, P. J., 1987, "The State of the Art in Infilled Frames", Imperial College of Science and Technology, Civil Eng. Department, London, U.K, ESEE Research Report No. 87-2.

Mohyeddin-Kermani, A., 2011, "Modelling and Performance of RC Frames with Masonry Infill under In-Plane and Out-of-Plane Loading", PhD. Thesis, The University of Melbourne.

Mondal, G., and Jain, S. K., 2008, "Lateral Stiffness of Masonry Infilled Reinforced Concrete (RC) Frames with Central Opening", *Earthquake Spectra*, Volume 24, No. 3, pages 701–723, August; Earthquake Engineering Research Institute.

Murty, C. V. R. and Jain, S. K., 2000, "Beneficial Influence of Masonry Infills on Seismic Performance of RC Frame Buildings", *Proceedings, 12<sup>th</sup> World Conference on Earthquake Engineering*, New Zealand, Paper No. 1790.

Paulay, T., and Priestley, M. J. N., 1992, "Seismic Design of Reinforced Concrete and Masonry Buildings", John Wiley & Sons.



Polyakov, S.V., 1956, "On the Interactions between Masonry Filler Walls and Enclosing Frame When Loaded in the Plane of the Wall", (English translation by G.L. Cairns, 1963) Translations in Earthquake Engineering Research Institute, Moscow, Russia.

Rashid, M. H., 2005, "Effect of Infill Walls on Frames due to Seismic Loading", M.Sc. Degree Dissertation, Bangladesh University of Engineering and Technology (BUET), Dhaka, Bangladesh.

Riddington, J. R., 1984, "The Influence of Initial Gaps on Infilled Frame Behavior", Proceedings of the Institution of Civil Engineers, part 2, vol. 77, paper 8767, September.

Rosenblueth, E., 1951, "A Basis for Seismic Design," Ph.D. Thesis, University of Illinois, Urbana.

Smith, B. S., 1962, "Lateral Stiffness of Infilled Frames", Journal of the Structural Division, Proceedings of American Society of Civil Engineers, vol. 88, no. 3355, December.

Smith, B.S., 1966, "Behavior of Square Infilled Frames", Journal of the Structural Division, Proceedings of American Society of Civil Engineers, vol. 92, no. ST1, February.

Smith, B.S. and Carter, C., 1969, "A Method of Analysis for Infilled Frames", Proceedings of the Institution of Civil Engineers, vol. 44, paper 7218.

Smith, B. S. and Coull, 1991, "An Infilled-Frame Structures, Tall Building Structures Analysis and Design", John Wiley & Sons, inc. 168-174.

Sonmez, E., 2013, "Effect of Infill Wall Stiffness Variations on the Behavior of Reinforced Concrete Frames under Earthquake Demands", M.Sc. Thesis, Izmir Institute of Technology.

Stavridis, A., 2009, “Analytical and Experimental Study of Seismic Performance of Reinforced Concrete Frames Infilled with Masonry Walls.” Ph.D. Thesis, Univ. of California, San Diego, CA.

Uniform Building Code (UBC) Standards, 2000, “International Conference of Building Officials”, Whittier: ICBO.

Uniform Building Code (UBC) Standards, 1994, “International Conference of Building Officials”, Whittier: ICBO.

Uniform Building Code (UBC) Standards, 1994, “International Conference of Building Officials”, Section: 2105.3.2-2105.3.4, Whittier: ICBO.

Uniform Building Code (UBC) Standards, 1967, “International Conference of Building Officials”, Whittier: ICBO.

Wilson, E. L., Der Kiureghian, A. and Bayom, E. R., 1981, “A Replacement for the SRSS Method in Seismic Analysis”, *Earthquake Engineering and Structural Dynamics*, Vol. 9. pp. 187-192.

Wilson, E. L., 2002, “Three-Dimensional Static and Dynamic Analysis of Structures, A Physical Approach with Emphasis on Earthquake Engineering”, Third Edition, Computers and Structures, Inc. Berkeley, California, USA, ISBN 0-923907-00-9.

## APPENDIX A1

Table A1.1: Instrumentation plan for Specimen 1, RC bare frame

Channel No.	Sensor No.	Scale Factor	Type	Gauge Length (mm)	Location	Ordinate (x,y,z) (mm)
1	L1	2	Load Cell	N/A	Horizontal	(-150,2100,75)
2	L2	1	Load Cell	N/A	Vertical	(1000,2525,75)
3	R1	2	LVDT-1	100	Top of 1st floor leeward column Collar	(1700,2212.5,75)
4	R2	2	LVDT-2	100	Top of 1st floor leeward column	(1700,1818.75,75)
5	R3	2	LVDT-3	100	Top of 1st floor windward column	(0,1818.75,75)
6	R4	1	LVDT-4	50	Top of ground floor leeward column	(1700,843.75,75)
7	R5	1	LVDT-5	50	Bottom of 1st floor windward column	(0,1406.25,75)
8	R6	1	LVDT-6	50	Bottom of 1st floor leeward column	(1700,1181.25,75)
9	S1	1	Strain on concrete	30	Bottom of ground floor windward column vertical	(25,300,150)
10	S2	1	Strain on concrete	30	Bottom of ground floor windward column horizontal	(25,300,0)
11	S3	1	Strain on concrete	30	Top of ground floor windward column vertical	(75,975,150)
12	S4	1	Strain on concrete	30	Top of ground floor windward column horizontal	(75,975,0)

Channel No.	Sensor No.	Scale Factor	Type	Gauge Length (mm)	Location	Ordinate (x,y,z) (mm)
13	S5	1	Strain on concrete	30	Bottom of ground floor leeward column vertical	(1625,300,0)
14	S6	1	Strain on concrete	30	Bottom of ground floor leeward column horizontal	(1625,300,150)
15	S7	1	Strain on concrete	30	Top of ground floor leeward column vertical	(1675,975,0)
16	S8	1	Strain on concrete	30	Top of ground floor leeward column horizontal	(1675,975,150)
17	S9	1	Strain on concrete	30	Top of ground floor leeward beam vertical	(1550,1175,125)
18	S10	1	Strain on concrete	30	Top of ground floor leeward beam horizontal	(1550,1175,25)
19	S11	1	Strain on concrete	30	Top of 1st floor leeward column vertical	(1675,1950,150)
20	S12	1	Strain on concrete	30	Top of 1st floor leeward column horizontal	(1675,1950,0)
21	S13	1	Strain on concrete	30	Bottom of 1st floor leeward beam vertical	(1550,2050,125)
22	S14	1	Strain on concrete	30	Bottom of 1st floor leeward beam horizontal	(1550,2050,25)

Table A1.2: Instrumentation plan for Specimen 2, infill RC frame having door opening

Channel No.	Sensor No.	Scale Factor	Type	Gauge Length (mm)	Location	Ordinate (x,y,z) (mm)
1	L1	2	Load Cell	N/A	Horizontal	(-150,2100,75)
2	L2	1	Load Cell	N/A	Vertical	(1000,2525,75)
3	R1	2	LVDT-1	100	Top of 1st floor leeward column Collar	(1700,2212.5,75)
4	R2	2	LVDT-2	100	Top of 1st floor leeward column	(1700,1818.75,75)
5	R3	2	LVDT-3	100	Top of 1st floor windward column	(0,1818.75,75)
6	R4	1	LVDT-4	50	Top of ground floor leeward column	(1700,843.75,75)
7	R5	1	LVDT-5	50	Bottom of 1st floor windward column	(0,1406.25,75)
8	R6	1	LVDT-6	50	Bottom of 1st floor leeward column	(1700,1181.25,75)
9	S1	1	Strain on concrete	30	Bottom of ground floor windward column vertical	(25,300,150)
10	S2	1	Strain on concrete	30	Bottom of ground floor windward column horizontal	(25,300,0)
11	S3	1	Strain on concrete	30	Top of ground floor windward column vertical	(75,975,150)
12	S4	1	Strain on concrete	30	Top of ground floor windward column horizontal	(75,975,0)
13	S5	1	Strain on concrete	30	Bottom of ground floor leeward column vertical	(1625,300,0)

14	S6	1	Strain on concrete	30	Bottom of ground floor leeward column horizontal	(1625,300,150)
15	S7	1	Strain on concrete	30	Top of ground floor leeward column vertical	(1675,975,0)
16	S8	1	Strain on concrete	30	Top of ground floor leeward column horizontal	(1675,975,150)
17	S9	1	Strain on concrete	30	Top of ground floor leeward beam vertical	(1550,1175,125)
18	S10	1	Strain on concrete	30	Top of ground floor leeward beam horizontal	(1550,1175,25)
19	S11	1	Strain on concrete	30	Top of 1st floor leeward column vertical	(1675,1950,150)
20	S12	1	Strain on concrete	30	Top of 1st floor leeward column horizontal	(1675,1950,0)
21	S13	1	Strain on concrete	30	Bottom of 1st floor leeward beam vertical	(1550,2050,125)
22	S14	1	Strain on concrete	30	Bottom of 1st floor leeward beam horizontal	(1550,2050,25)
23	S15	1	Strain on wall	30	Top of 1st floor windward infill diagonal	(150,1950,150)
24	S16	1	Strain on wall	30	Bottom of 1st floor leeward infill diagonal	(1550,1275,150)
25	S17	1	Strain on wall	30	Top of 1st floor infill beside door diagonal	(600,1900,150)

Table A1.3: Instrumentation plan for Specimen 3, infill RC frame having window opening

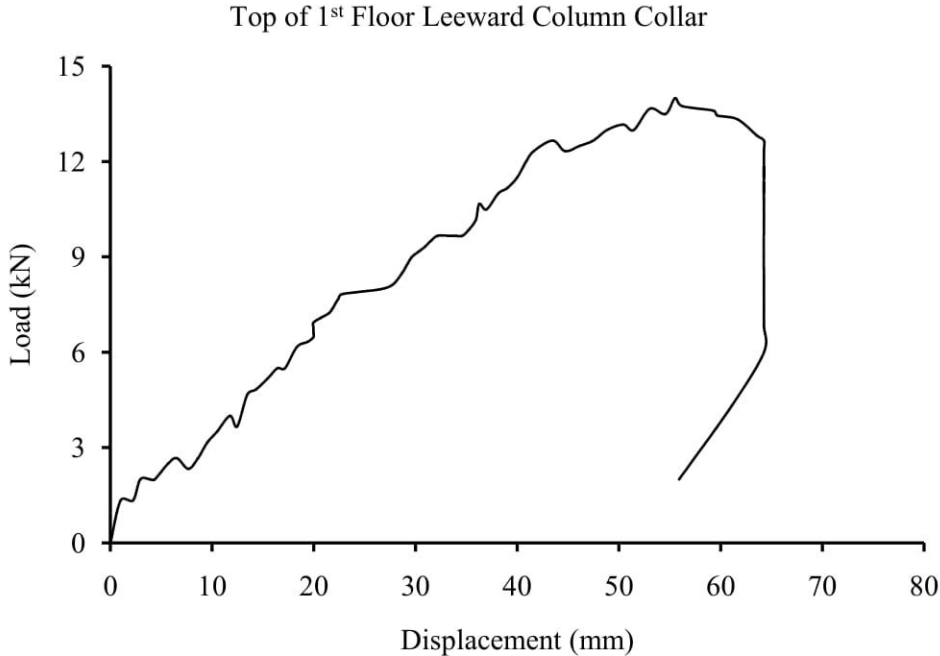
Channel No.	Sensor No.	Scale Factor	Type	Gauge Length (mm)	Location	Ordinate (x,y,z) (mm)
1	L1	2	Load Cell	N/A	Horizontal	(-150,2100,75)
2	L2	1	Load Cell	N/A	Vertical	(1000,2525,75)
3	R1	2	LVDT-1	100	Top of 1st floor leeward column Collar	(1700,2212.5,75)
4	R2	2	LVDT-2	100	Top of 1st floor leeward column	(1700,1818.75,75)
5	R3	2	LVDT-3	100	Top of 1st floor windward column	(0,1818.75,75)
6	R4	1	LVDT-4	50	Top of ground floor leeward column	(1700,843.75,75)
7	R5	1	LVDT-5	50	Bottom of 1st floor windward column	(0,1406.25,75)
8	R6	1	LVDT-6	50	Bottom of 1st floor leeward column	(1700,1181.25,75)
9	S1	1	Strain on concrete	30	Bottom of ground floor windward column vertical	(25,300,150)
10	S2	1	Strain on concrete	30	Bottom of ground floor windward column horizontal	(25,300,0)
11	S3	1	Strain on concrete	30	Top of ground floor windward column vertical	(75,975,150)
12	S4	1	Strain on concrete	30	Top of ground floor windward column horizontal	(75,975,0)
13	S5	1	Strain on concrete	30	Bottom of ground floor leeward column vertical	(1625,300,0)

Channel No.	Sensor No.	Scale Factor	Type	Gauge Length (mm)	Location	Ordinate (x,y,z) (mm)
14	S6	1	Strain on concrete	30	Bottom of ground floor leeward column horizontal	(1625,300,150)
15	S7	1	Strain on concrete	30	Top of ground floor leeward column vertical	(1675,975,0)
16	S8	1	Strain on concrete	30	Top of ground floor leeward column horizontal	(1675,975,150)
17	S9	1	Strain on concrete	30	Top of ground floor leeward beam vertical	(1550,1175,125)
18	S10	1	Strain on concrete	30	Top of ground floor leeward beam horizontal	(1550,1175,25)
19	S11	1	Strain on concrete	30	Top of 1st floor leeward column vertical	(1675,1950,150)
20	S12	1	Strain on concrete	30	Top of 1st floor leeward column horizontal	(1675,1950,0)
21	S13	1	Strain on concrete	30	Bottom of 1st floor leeward beam vertical	(1550,2050,125)
22	S14	1	Strain on concrete	30	Bottom of 1st floor leeward beam horizontal	(1550,2050,25)
23	S15	1	Strain on wall	30	Top of 1st floor windward infill diagonal	(150,1950,150)

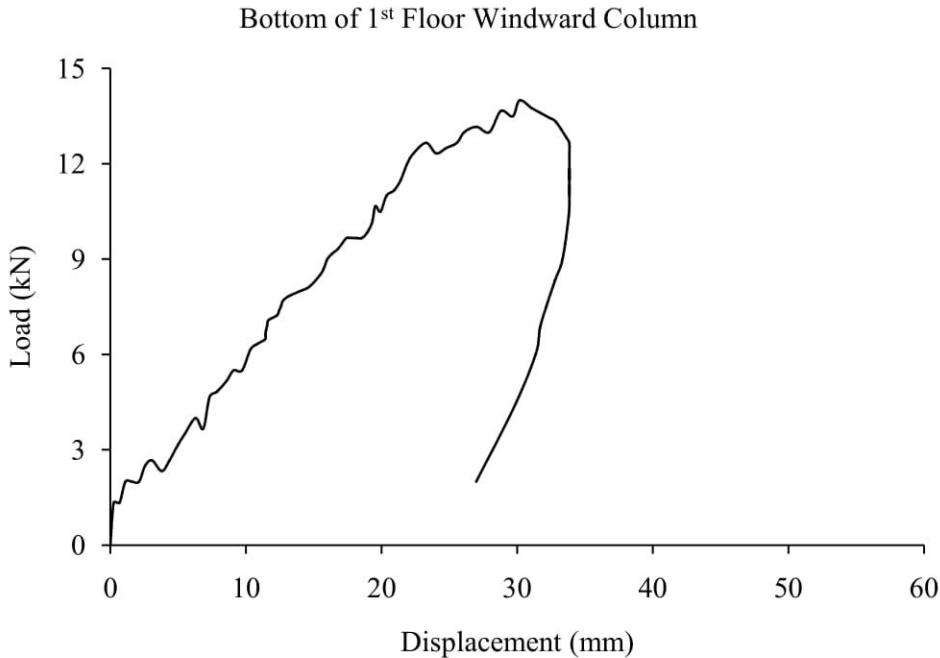


Channel No.	Sensor No.	Scale Factor	Type	Gauge Length (mm)	Location	Ordinate (x,y,z) (mm)
24	S16	1	Strain on wall	30	Bottom of 1st floor leeward infill diagonal	(1550,1275,150)
25	S17	1	Strain on wall	30	Top of 1st floor infill beside window diagonal	(600,1900,150)
26	S18	1	Strain on wall	30	Bottom of 1st floor windward infill diagonal	(6,267,6)

**APPENDIX A2**

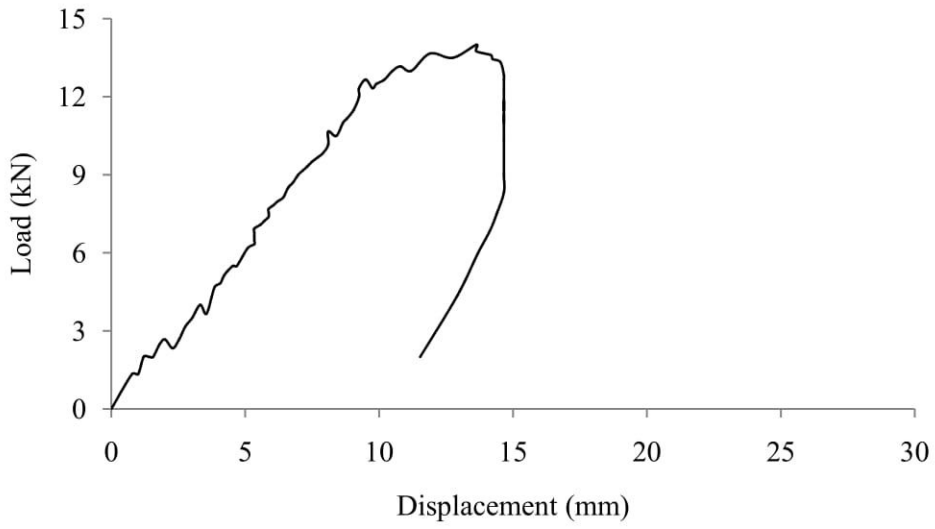


(a)



(b)

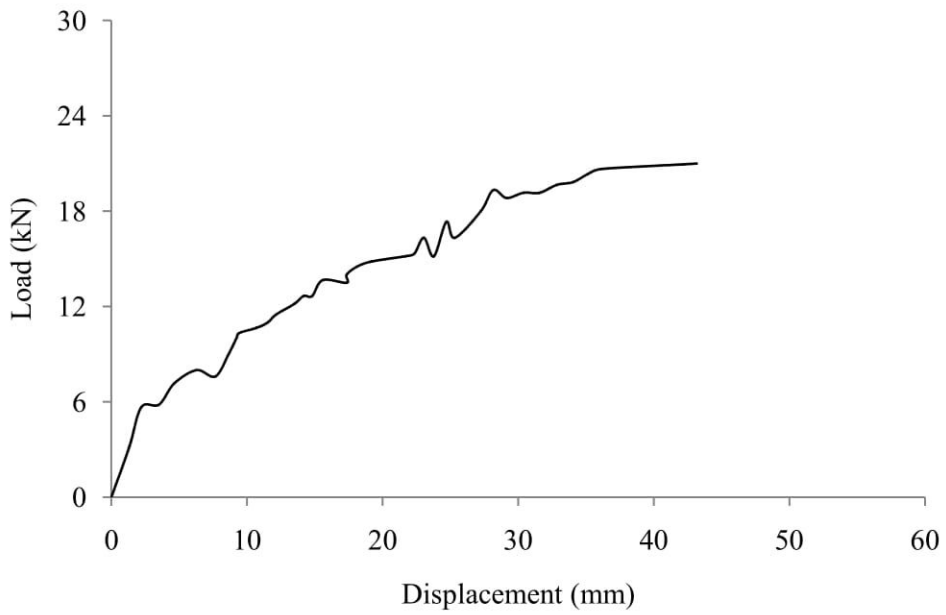
Top of Ground Floor Leeward Column



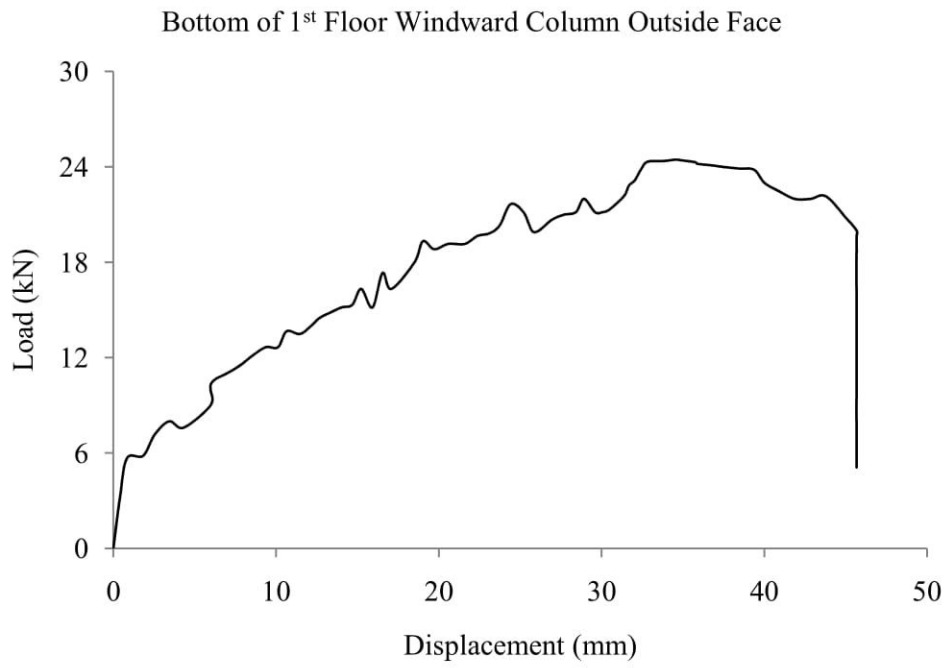
(c)

Figure A2.1: Specimen 1, Experimental load deflection curve for (a) LVDT-1, (b) LVDT-5 and (c) LVDT-4

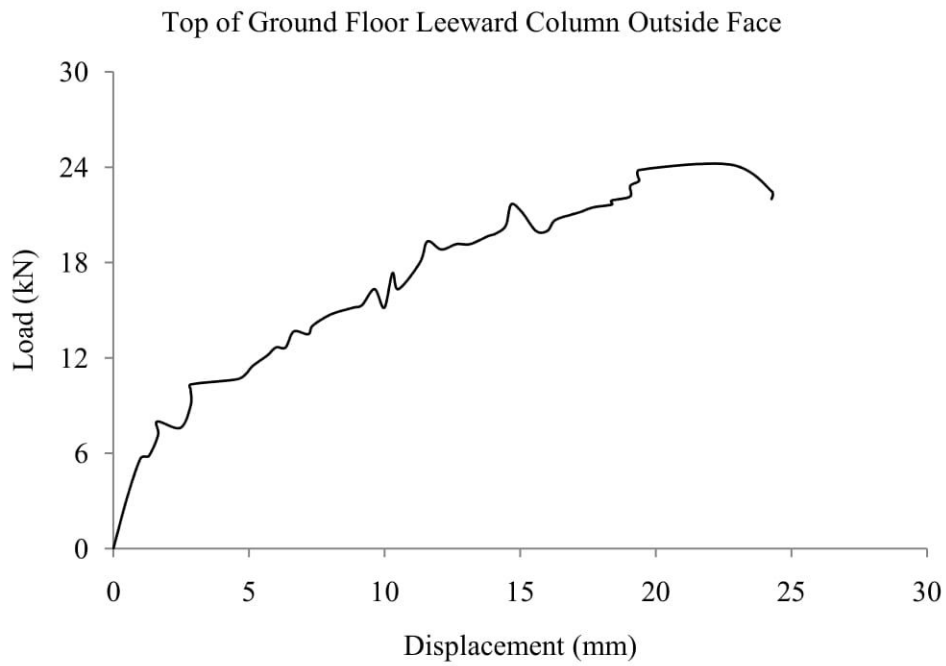
Top of 1<sup>st</sup> Floor Leeward Column Collar Outside Face



(a)

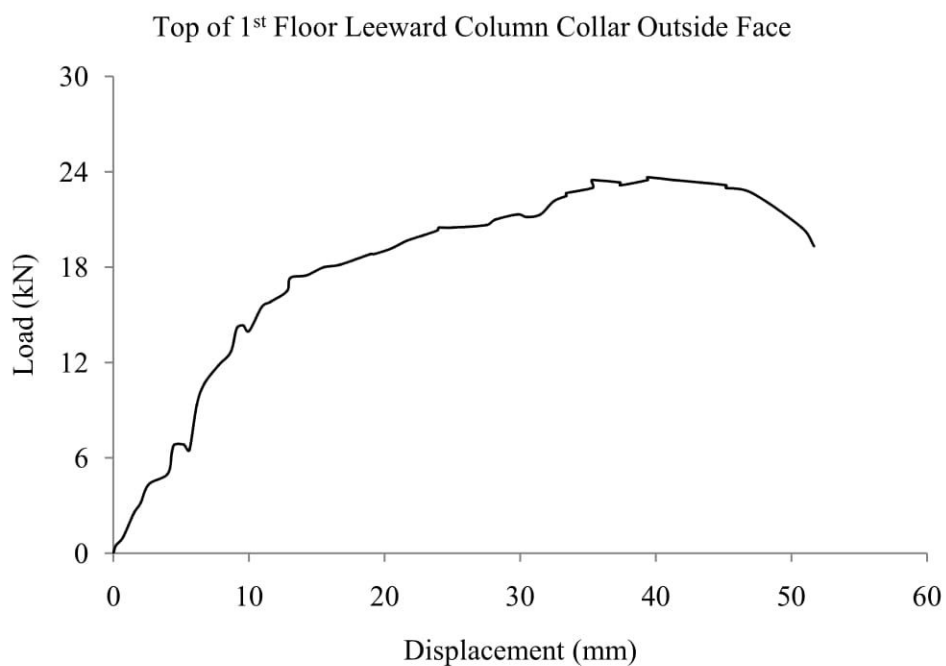


(b)

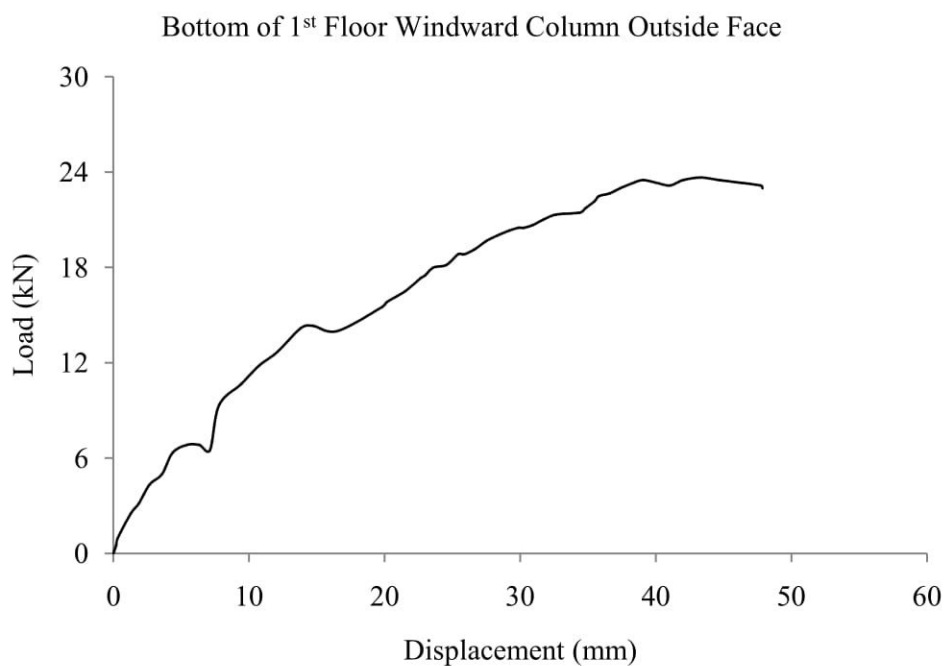


(c)

Figure A2.2: Specimen 2, Experimental load deflection curve for (a) LVDT-1,  
(b) LVDT-5 and (c) LVDT-4

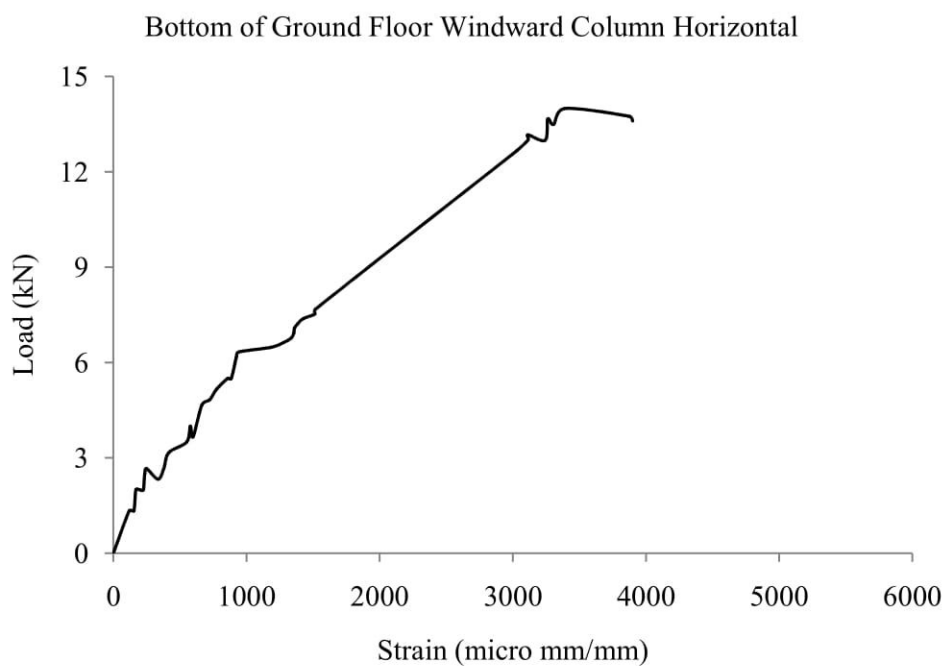


(a)

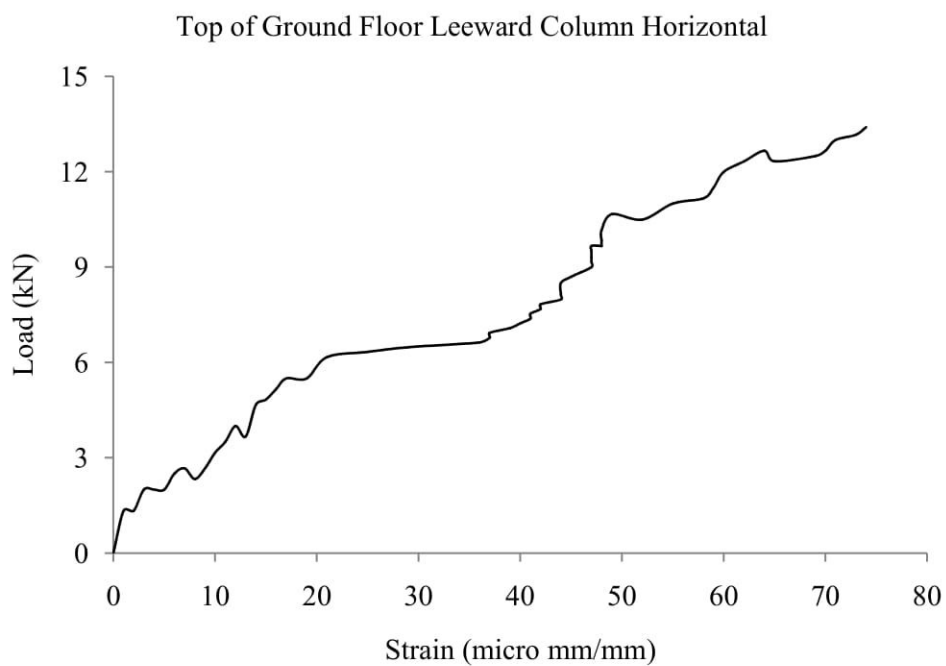


(b)

Figure A2.3: Specimen 3, Experimental load deflection curve for (a) LVDT-1 and (b) LVDT-5

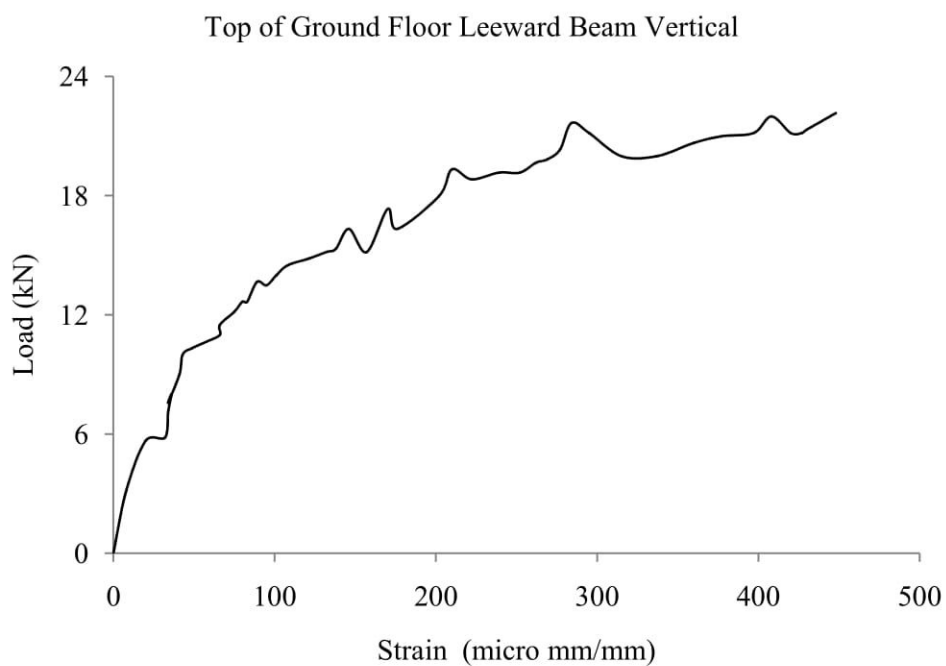


(a)

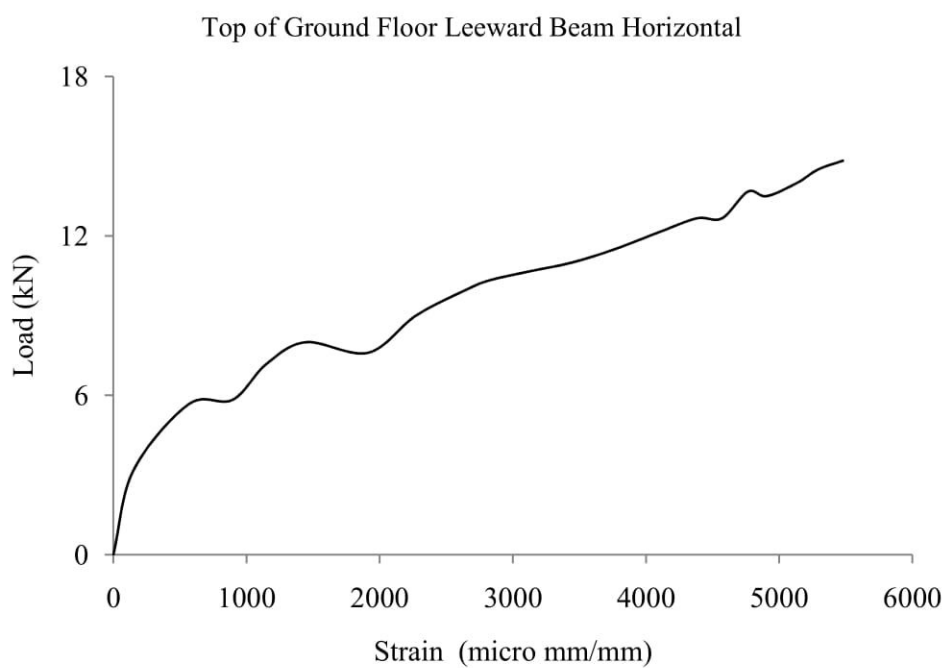


(b)

Figure A2.4: Specimen 1, Load vs strain for strain gauge (a) S1 and (b) S8

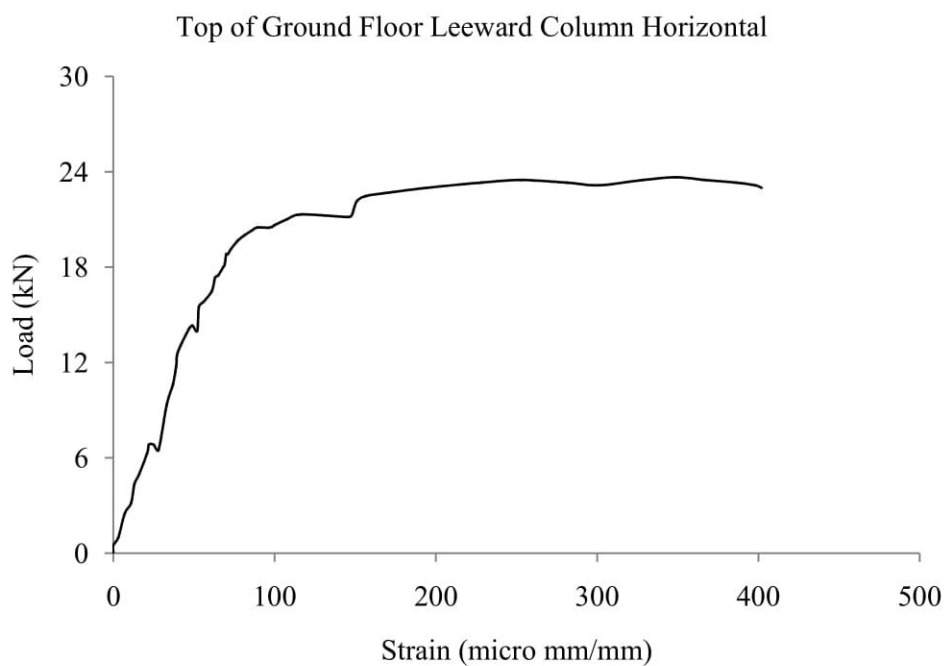


(a)

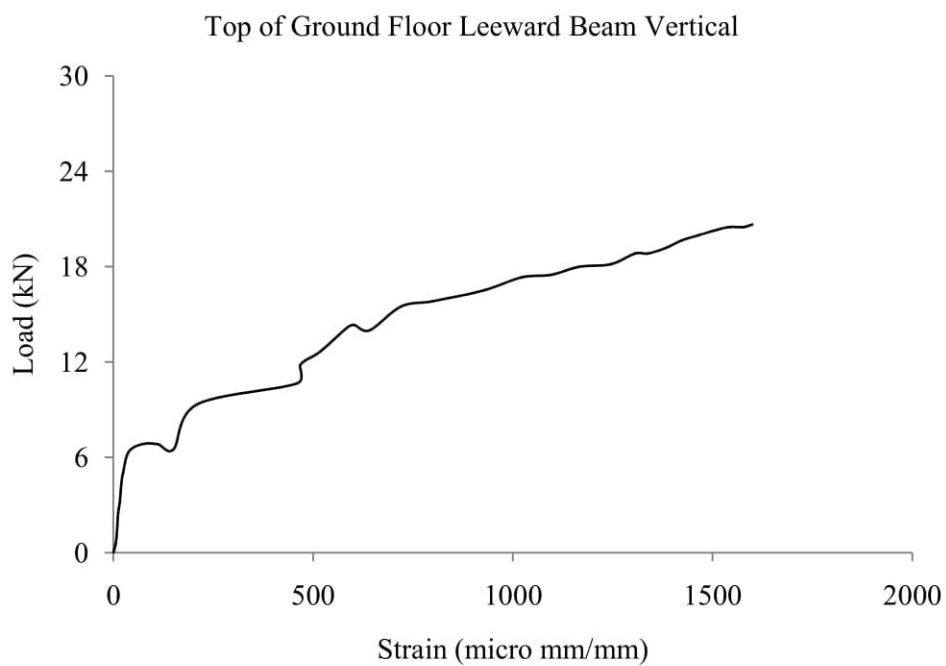


(b)

Figure A2.5: Specimen 2, Load vs strain for strain gauge (a) S9 and (b) S10



(a)



(b)

Figure A2.6: Specimen 3, Load vs strain for strain gauge (a) S8 and (b) S9



## APPENDIX B1

### Verification of STAAD.Pro UBC, 1994 Base Shear Generation with Bangladesh National Building Code, 1993:

A typical calculation is carried out to verify the base shear generation by BNBC, 1993 with UBC, 1994 by STAAD.Pro. For this checking, a four bay four storied bare frame was taken for base shear calculation.

According to BNBC, Base Shear,  $V = ZIC*W / R$

Where,

Z = Seismic zone coefficient (BNBC Table 6.2.22) = 0.15 (zone – 2);

I = Structure importance factor (BNBC Table 6.2.23) = 1.0 (Category – III);

R = Response reduction factor which depends on the type of structural system (BNBC Table 6.2.24) = 5 (Ordinary concrete moment resisting frames);

$$C = 1.25 \times S / (T)^{2/3}$$

S = Soil factor which depends on site class (BNBC Table 6.2.25) = 1.2;

$$\text{Structure Period, } T = C_t \times (h_n)^{3/4}$$

$C_t$  = Time Period coefficient = 0.073 (for reinforced concrete moment resisting frames)

$h_n$  = Height of building from foundation or from top of rigid basement = 13.72 m

$$\text{Structure Period, } T = C_t \times (h_n)^{3/4} = 0.073 \times (13.72)^{3/4} = 0.5204$$

$$C = 1.25 \times S / (T)^{2/3} = 1.25 \times 1.2 / (0.5204)^{2/3} = 2.32 < 2.75 \text{ (OK)}$$

W = Weight of the Frame = (Column Weight) + (Beam Weight) + (Foundation Short

Column) + (Open Ground Floor Infill Frame Wall Load)

$$\begin{aligned} \text{Weight of the Frame, } W &= (20 \text{ nos} \times 304.8 \text{ mm} \times 304.8 \text{ mm} \times 3048 \text{ mm} \times 2.44 \times 10^{-8} \\ &\text{kN/mm}^3) + (20 \text{ nos} \times 304.8 \text{ mm} \times 254 \text{ mm} \times 3048 \text{ mm} \times 2.44 \times 10^{-8} \text{ kN/mm}^3) + (5 \text{ nos} \times \\ &304.8 \text{ mm} \times 304.8 \text{ mm} \times 1524 \text{ mm} \times 2.44 \times 10^{-8} \text{ kN/mm}^3) + (12 \text{ nos} \times 3048 \text{ mm} \times 3048 \\ &\text{mm} \times 127 \text{ mm} \times 1.856 \times 10^{-8} \text{ kN}) \\ &= 533.38 \text{ kN} \end{aligned}$$

Design Base Shear,  $V = ZIC * W / R = 37.12 \text{ kN}$

From, Base Shear by Equivalent Static Analysis (BNBC 1993),  $V = 37.12 \text{ kN}$

The STAAD.Pro UBC 1997 model generated 36.80 kN base shear for this model. The variation of base shear is less than 0.86% thus the calculation is verified.

## APPENDIX B2

### Calculation of Strut Width of Infill Frame having Door Opening:

From Mainstone (1971) and Smith and Carter (1969),

We know,

$$\lambda_1 H = H [(E_m t \sin 2\theta) / (4E_c I_c h_w)]^{1/4}$$

$$\text{and, } a = 0.175D (\lambda_1 H)^{-0.4}$$

Where,  $a$  = Equivalent strut width

$t$  = Thickness of the masonry infill panel

$H$  = Height of the confining frame

$E_m$  = Modulus of elasticity of the masonry unit

$E_c$  = Modulus of elasticity of concrete

$h$  = Height of the infill panel

$I_c$  = Moment of inertia of the column

$\theta$  = Angle produce by the strut with the horizontal

$$\text{Again, } l_{\text{column}} = a / \cos\theta_{\text{column}}$$

$$\tan\theta_{\text{column}} = \{ h - ( a / \cos\theta_{\text{column}} ) \} / l$$

$$\text{Also, Reduction factor, } (R_I)_i = 0.6 (A_{\text{open}} / A_{\text{panel}})^2 - 1.6 (A_{\text{open}} / A_{\text{panel}}) + 1$$

Where:  $A_{\text{open}}$  = Area of the opening ( $\text{mm}^2$ )

$A_{\text{panel}}$  = Area of the infill panel ( $\text{mm}^2$ ) =  $l \times h$

Height of the confining frame,  $H = 3000$  mm

The width of the infill,  $W = 3000$  mm

Height of the infill panel,  $h = 2700$  mm

Length of the beam,  $L = 3000$  mm

Diagonal length of the infill panel,  $D = \sqrt{2700^2 + 3000^2} = 4036$  mm

Effective thickness of the infill,  $t = 125$  mm

Angle of diagonal to horizontal,  $\theta = \tan^{-1}(2700/3000) = 41.99^\circ$

Column dimension =  $300$  mm  $\times$   $300$  mm

Cross-sectional area of the column,  $A_c = 90000$  mm<sup>2</sup>

Moment of inertia of the column,  $I_c = (300*300^3)/12 = 675 \times 10^6$  mm<sup>3</sup>

Beam dimension =  $250$  mm  $\times$   $300$  mm

Moment of inertia of the beam,  $I_b = (250*300^3)/12 = 562.5 \times 10^6$  mm<sup>3</sup>

Elastic modulus of the frame,  $E_c = 28578.25$  MPa

Elastic modulus of infill panel,  $E_m = 10392.71$  MPa

Door size =  $1050$  mm  $\times$   $2100$  mm

$$\text{So, } \lambda_l H = H [(E_m t \sin 2\theta) / (4E_c I_c h_w)]^{1/4}$$
$$= 4.14$$

$$a = 0.175D (\lambda_l H)^{-0.4}$$
$$= 0.175*4036 (4.14)^{-0.4}$$
$$= 400.12 \text{ mm}$$

$$\text{Reduction factor, } (R_l)_i = 0.6 (A_{\text{open}} / A_{\text{panel}})^2 - 1.6 (A_{\text{open}} / A_{\text{panel}}) + 1$$
$$= 0.6 (1050*2100 / 8100000)^2 - 1.6 (1050*2100 / 8100000) + 1$$
$$= 0.6092$$

$$\text{Final } a = 400.12*0.6092 = 243.75 \text{ mm}$$

$$\tan \theta_{\text{column}} = \{ h - (a / \cos \theta_{\text{column}}) \} / l$$
$$\theta_{\text{column}} = 38.53^\circ$$

$$l_{\text{column}} = a / \cos \theta_{\text{column}}$$
$$l_{\text{column}} = 311.25 \text{ mm}$$

### APPENDIX B3

#### Input File for Equivalent Static and Response Spectrum Analysis:

Input files for 4 bay 4 storied infill frame having door opening with aspect ratio 1:1  
(Equivalent Static Analysis and Response Spectrum Analysis):

STAAD PLANE

START JOB INFORMATION

ENGINEER DATE 25-Oct-17

END JOB INFORMATION

INPUT WIDTH 79

SET PRINT 1

UNIT FEET KIP

SET PRINT 1

JOINT COORDINATES

1 0 0 0; 2 10 0 0; 3 0 5 0; 4 10 5 0; 5 20 0 0; 6 20 5 0; 7 30 0 0; 8 30 5 0;  
9 40 0 0; 10 40 5 0; 11 0 15 0; 12 10 15 0; 13 20 15 0; 14 30 15 0; 15 40 15 0;  
16 0 25 0; 17 10 25 0; 18 20 25 0; 19 30 25 0; 20 40 25 0; 21 0 35 0;  
22 10 35 0; 23 20 35 0; 24 30 35 0; 25 40 35 0; 26 0 45 0; 27 10 45 0;  
28 20 45 0; 29 30 45 0; 30 40 45 0; 31 0 16.0375 0; 32 0 23.925 0;  
33 10 16.0375 0; 34 10 23.9625 0; 35 5 20 0; 36 10 23.925 0; 37 20 16.0375 0;  
38 20 23.9625 0; 39 15 20 0; 40 20 23.925 0; 41 30 16.0375 0; 42 30 23.9625 0;  
43 25 20 0; 44 30 23.925 0; 45 40 16.0375 0; 46 40 23.9625 0; 47 35 20 0;  
48 0 26.0375 0; 49 0 33.925 0; 50 10 26.0375 0; 51 10 33.9625 0; 52 5 30 0;  
53 10 33.925 0; 54 20 26.0375 0; 55 20 33.9625 0; 56 15 30 0; 57 20 33.925 0;  
58 30 26.0375 0; 59 30 33.9625 0; 60 25 30 0; 61 30 33.925 0; 62 40 26.0375 0;  
63 40 33.9625 0; 64 35 30 0; 65 0 36.0375 0; 66 0 43.925 0; 67 10 36.0375 0;  
68 10 43.9625 0; 69 5 40 0; 70 10 43.925 0; 71 20 36.0375 0; 72 20 43.9625 0;  
73 15 40 0; 74 20 43.925 0; 75 30 36.0375 0; 76 30 43.9625 0; 77 25 40 0;  
78 30 43.925 0; 79 40 36.0375 0; 80 40 43.9625 0; 81 35 40 0;

MEMBER INCIDENCES

1 1 3; 2 2 4; 3 3 4; 4 5 6; 5 4 6; 6 7 8; 7 6 8; 8 9 10; 9 8 10; 10 3 11;

11 4 12; 12 6 13; 13 8 14; 14 10 15; 15 11 12; 16 12 13; 17 13 14; 18 14 15;  
19 11 31; 20 12 33; 21 13 37; 22 14 41; 23 15 45; 24 16 17; 25 17 18; 26 18 19;  
27 19 20; 28 16 48; 29 17 50; 30 18 54; 31 19 58; 32 20 62; 33 21 22; 34 22 23;  
35 23 24; 36 24 25; 37 21 65; 38 22 67; 39 23 71; 40 24 75; 41 25 79; 42 26 27;  
43 27 28; 44 28 29; 45 29 30; 46 31 32; 47 32 16; 48 33 36; 49 34 17; 50 31 35;  
51 35 34; 52 32 35; 53 35 33; 54 36 34; 55 37 40; 56 38 18; 57 33 39; 58 39 38;  
59 36 39; 60 39 37; 61 40 38; 62 41 44; 63 42 19; 64 37 43; 65 43 42; 66 40 43;  
67 43 41; 68 44 42; 69 45 46; 70 46 20; 71 41 47; 72 47 46; 73 44 47; 74 47 45;  
75 48 49; 76 49 21; 77 50 53; 78 51 22; 79 53 51; 80 54 57; 81 55 23; 82 57 55;  
83 58 61; 84 59 24; 85 61 59; 86 62 63; 87 63 25; 88 48 52; 89 52 51; 90 49 52;  
91 52 50; 92 50 56; 93 56 55; 94 53 56; 95 56 54; 96 54 60; 97 60 59; 98 57 60;  
99 60 58; 100 58 64; 101 64 63; 102 61 64; 103 64 62; 104 65 66; 105 66 26;  
106 67 70; 107 68 27; 108 70 68; 109 71 74; 110 72 28; 111 74 72; 112 75 78;  
113 76 29; 114 78 76; 115 79 80; 116 80 30; 117 65 69; 118 69 68; 119 66 69;  
120 69 67; 121 67 73; 122 73 72; 123 70 73; 124 73 71; 125 71 77; 126 77 76;  
127 74 77; 128 77 75; 129 75 81; 130 81 80; 131 78 81; 132 81 79;

DEFINE MATERIAL START

ISOTROPIC CONCRETE

E 606240

POISSON 0.17

DENSITY 0.150336

ALPHA 5e-006

DAMP 0.05

G 193846

TYPE CONCRETE

STRENGTH FCU 576

ISOTROPIC WALL

E 220320

POISSON 0.215

DENSITY 0.12

ALPHA 5.5e-006

DAMP 0.05

END DEFINE MATERIAL

MEMBER PROPERTY AMERICAN

3 5 7 9 15 TO 18 24 TO 27 33 TO 36 42 TO 45 PRIS YD 1 ZD 0.833

1 2 4 6 8 10 TO 14 19 TO 23 28 TO 32 37 TO 41 46 TO 49 54 TO 56 61 TO 63 68 -  
69 TO 70 75 TO 87 104 TO 116 PRIS YD 1 ZD 1

MEMBER PROPERTY AMERICAN

50 TO 53 57 TO 60 64 TO 67 71 TO 74 88 TO 103 117 TO 131 -  
132 PRIS YD 0.8125 ZD 0.417

CONSTANTS

MATERIAL CONCRETE MEMB 1 TO 49 54 TO 56 61 TO 63 68 TO 70 75 TO 87 104  
TO 116

MATERIAL WALL MEMB 50 TO 53 57 TO 60 64 TO 67 71 TO 74 88 TO 103 117 TO  
132

MEMBER COMPRESSION

50 TO 53 57 TO 60 64 TO 67 71 TO 74 88 TO 103 117 TO 132

SUPPORTS

1 2 5 7 9 FIXED

\*SLAVE RIGID MASTER 3 JOINT 3 4 6 8 10

\*SLAVE RIGID MASTER 11 JOINT 11 TO 15

\*SLAVE RIGID MASTER 16 JOINT 16 TO 20

\*SLAVE RIGID MASTER 21 JOINT 21 TO 25

\*SLAVE RIGID MASTER 26 JOINT 26 TO 30

SLAVE FX FY MASTER 35 JOINT 31 TO 47

SLAVE FX FY MASTER 52 JOINT 48 TO 64

SLAVE FX FY MASTER 69 JOINT 65 TO 81

CUT OFF MODE SHAPE 4

DEFINE UBC LOAD

ZONE 0.15 I 1 RWX 5 RWZ 5 CT 0.03 PX 0.5204 S 1.2

SELFWEIGHT 1

MEMBER WEIGHT

15 TO 18 24 TO 27 33 TO 36 UNI 0.2738

LOAD 1 LOADTYPE DL TITLE STATIC

SELFWEIGHT Y -1

MEMBER LOAD

15 TO 18 24 TO 27 33 TO 36 UNI GY -0.2738  
UBC LOAD X 1  
PERFORM ANALYSIS PRINT ALL  
CHANGE  
MEMBER COMPRESSION  
50 TO 53 57 TO 60 64 TO 67 71 TO 74 88 TO 103 117 TO 132  
PRINT STORY DRIFT  
CHANGE  
LOAD 2 LOADTYPE DL TITLE DYNAMIC  
MEMBER LOAD  
15 TO 18 24 TO 27 33 TO 36 UNI GY -0.2738  
JOINT LOAD  
3 FX 1.754  
4 FX 2.38  
6 FX 2.38  
8 FX 2.38  
10 FX 1.754  
11 FX 3.857  
12 FX 6.218  
13 FX 6.218  
14 FX 6.218  
15 FX 3.865  
16 FX 4.01  
17 FX 6.53  
18 FX 6.53  
19 FX 6.53  
20 FX 4.024  
21 FX 4.007  
22 FX 6.53  
23 FX 6.53  
24 FX 6.53  
25 FX 4.026  
26 FX 1.533



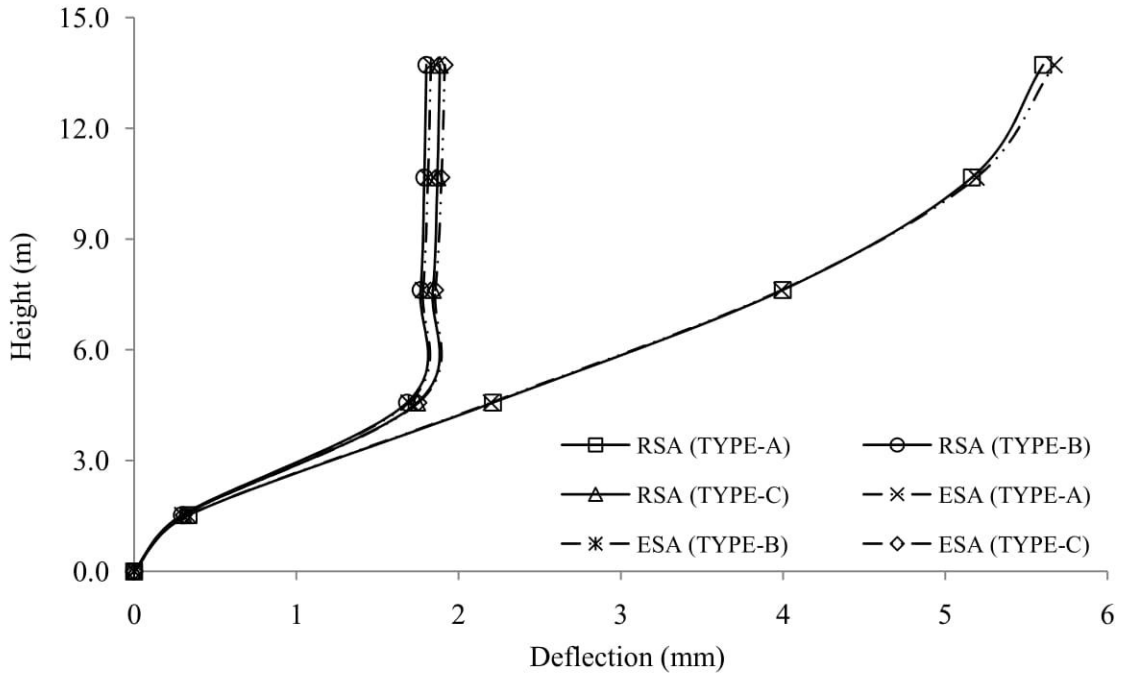
27 FX 2.316  
28 FX 2.316  
29 FX 2.316  
30 FX 1.535  
3 FY 1.754  
4 FY 2.38  
6 FY 2.38  
8 FY 2.38  
10 FY 1.754  
11 FY 3.857  
12 FY 6.218  
13 FY 6.218  
14 FY 6.218  
15 FY 3.865  
16 FY 4.01  
17 FY 6.53  
18 FY 6.53  
19 FY 6.53  
20 FY 4.024  
21 FY 4.007  
22 FY 6.53  
23 FY 6.53  
24 FY 6.53  
25 FY 4.026  
26 FY 1.533  
27 FY 2.316  
28 FY 2.316  
29 FY 2.316  
30 FY 1.535

SPECTRUM CQC X 0.012716 ACC SCALE 32.2 DAMP 0.05 LIN SAVE  
0.00358811 2.48929; 0.133217 2.48982; 0.259754 2.49645; 0.364698 2.49076;  
0.444944 2.49109; 0.528284 2.48531; 0.57458 2.4855; 0.614868 2.32665;  
0.658224 2.18615; 0.704666 2.04567; 0.766572 1.87467; 0.834625 1.72816;

0.908845 1.58779; 0.998503 1.44137; 1.06649 1.35602; 1.16847 1.23411;  
1.29205 1.11841; 1.4434 1.00282; 1.56076 0.93602; 1.67194 0.869195;  
1.82632 0.808663;  
1.97145 0.748093; 2.11038 0.705847; 2.24315 0.651343; 2.36356 0.615137;  
PERFORM ANALYSIS  
CHANGE  
MEMBER COMPRESSION  
50 TO 53 57 TO 60 64 TO 67 71 TO 74 88 TO 103 117 TO 132  
PRINT MODE SHAPES  
PRINT STORY DRIFT  
FINISH

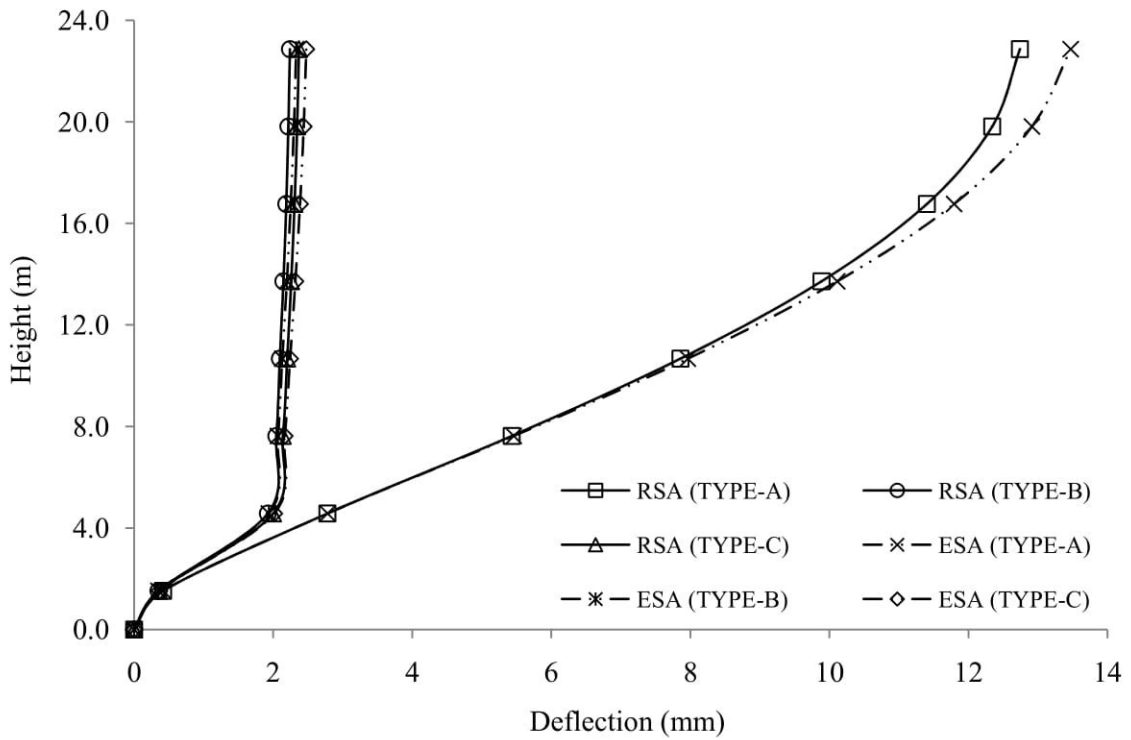
## APPENDIX B4

4 Bay 4 Storied Frame (Aspect Ratio 1:1.5)



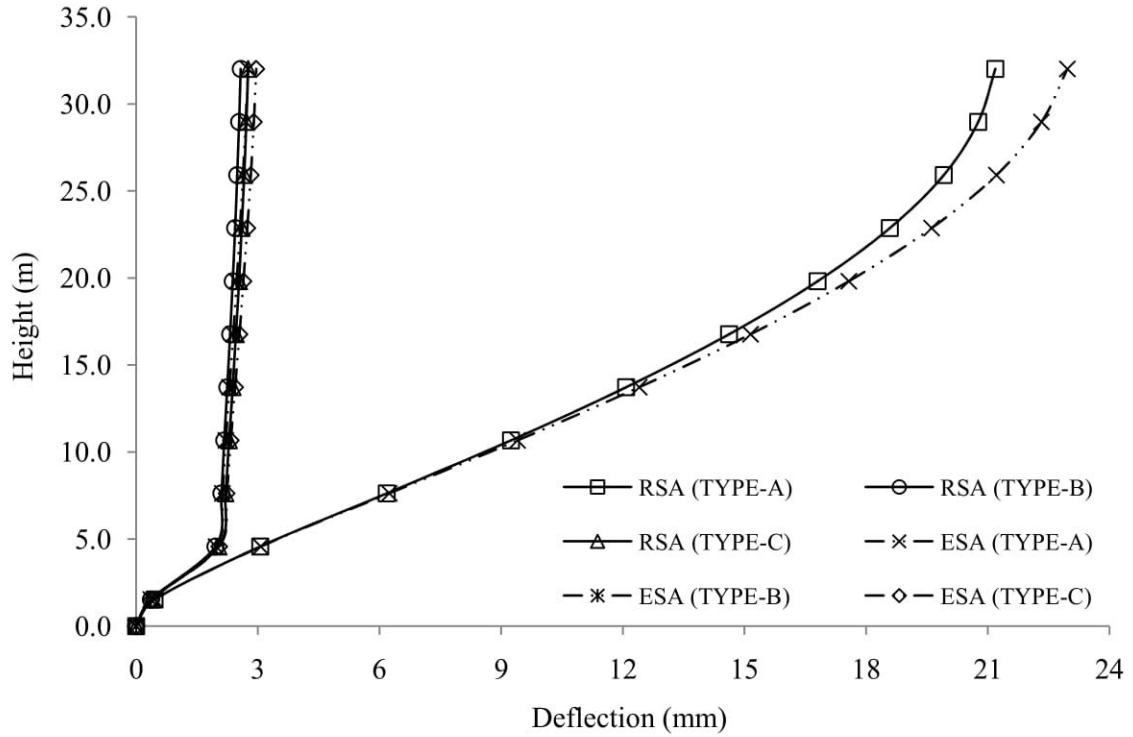
(a)

4 Bay 7 Storied Frame (Aspect Ratio 1:1.5)



(b)

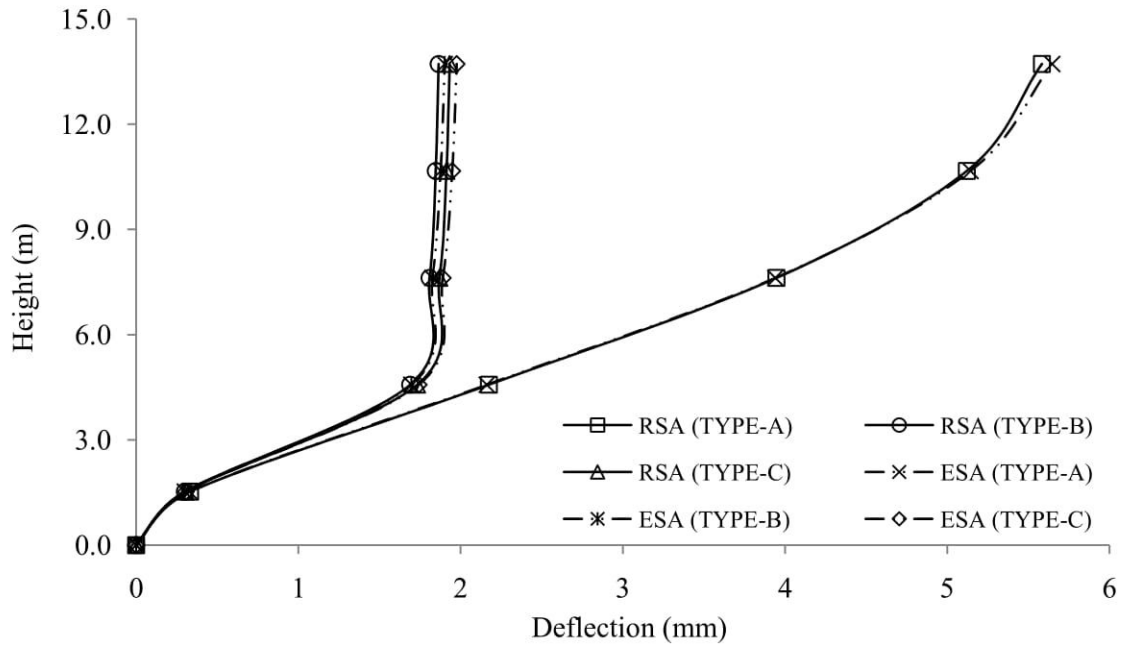
4 Bay 10 Storied Frame (Aspect Ratio 1:1.5)



(c)

Figure B4.1: Story wise deflection of (a) 4 storied (b) 7 storied and (c) 10 storied building frames for fixed support with aspect ratio of 1:1.5

4 Bay 4 Storied Frame (Aspect Ratio 1:2)



(a)

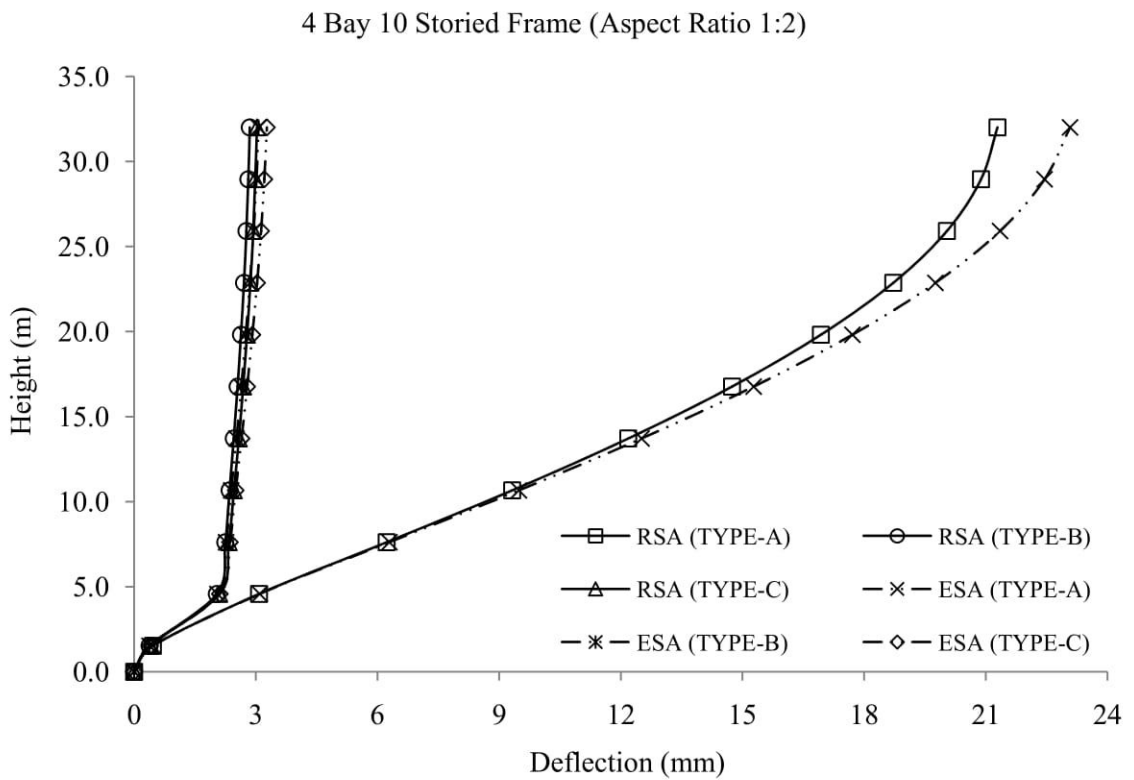
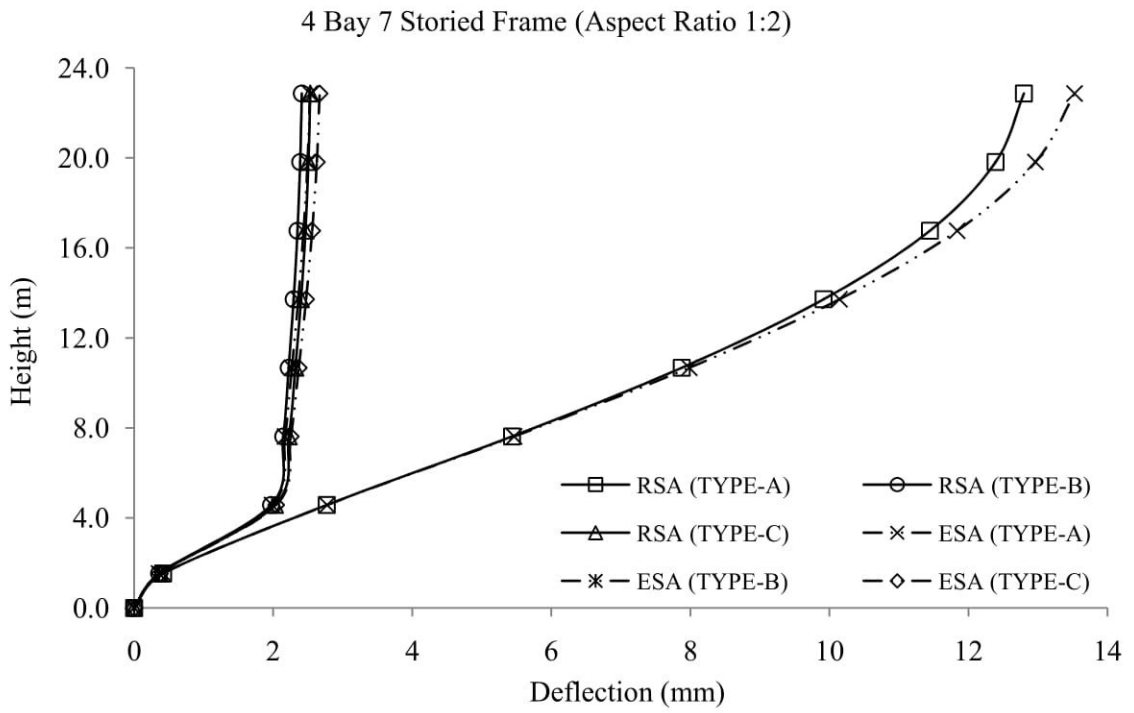
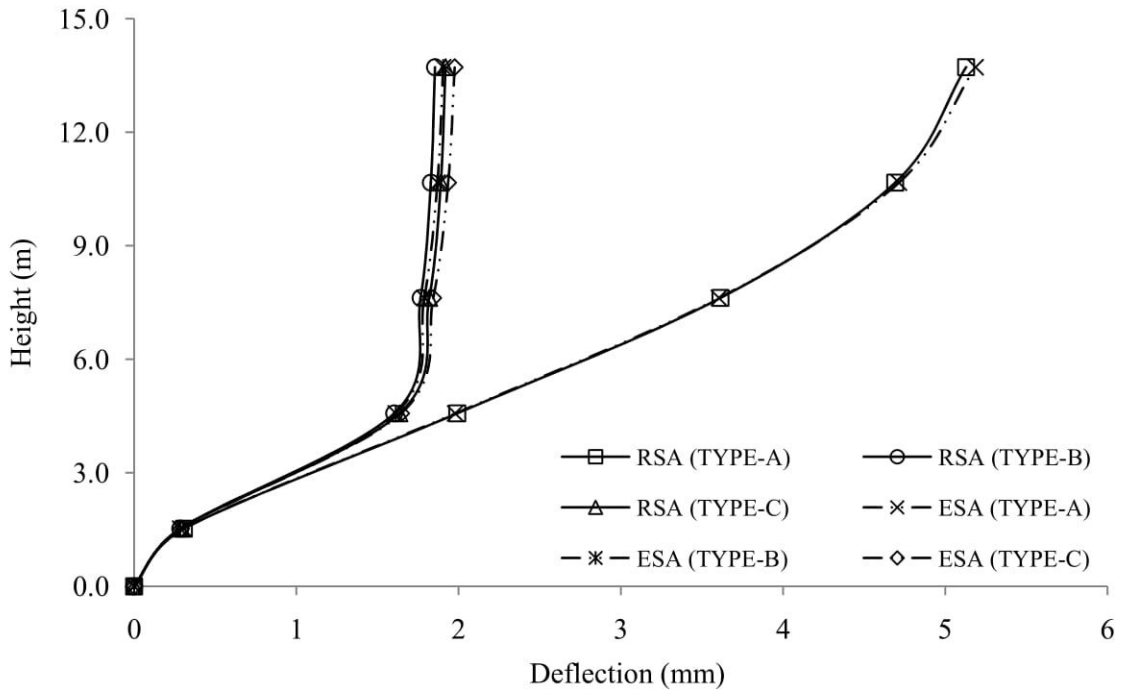


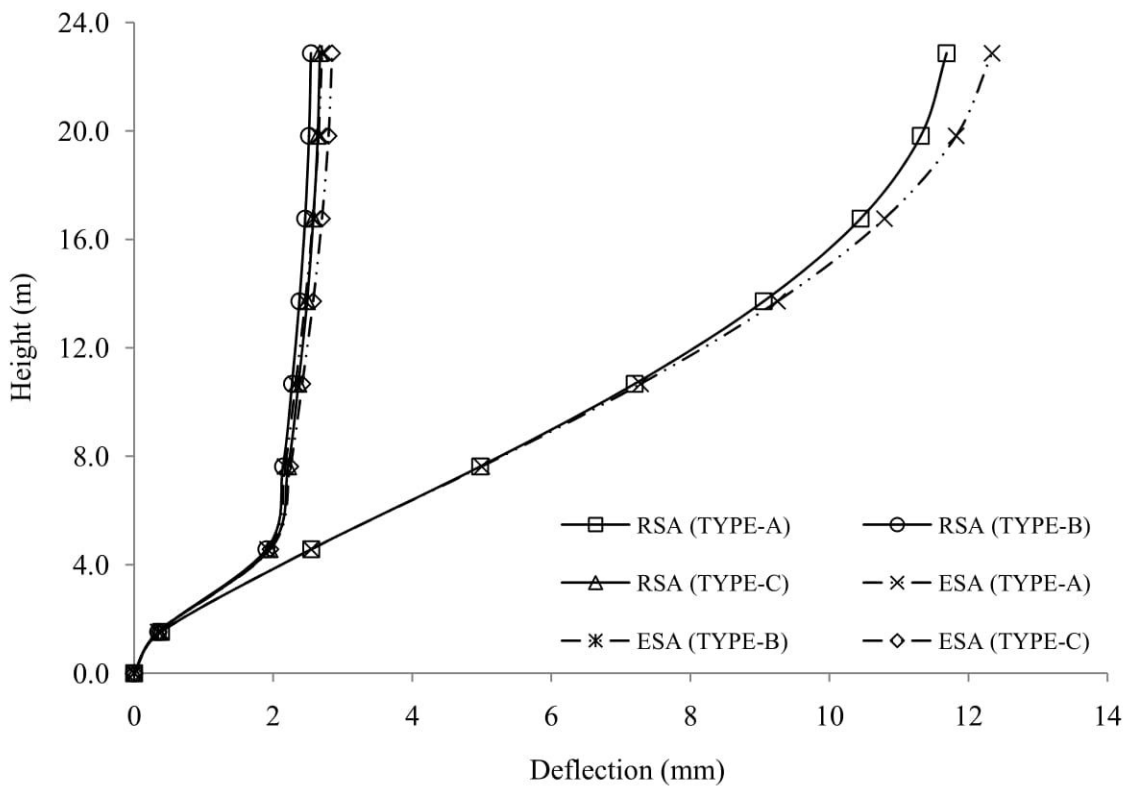
Figure B4.2: Story wise deflection of (a) 4 storied (b) 7 storied and (c) 10 storied building frames for fixed support with aspect ratio of 1:2

4 Bay 4 Storied Frame (Aspect Ratio 1:2.5)



(a)

4 Bay 7 Storied Frame (Aspect Ratio 1:2.5)



(b)

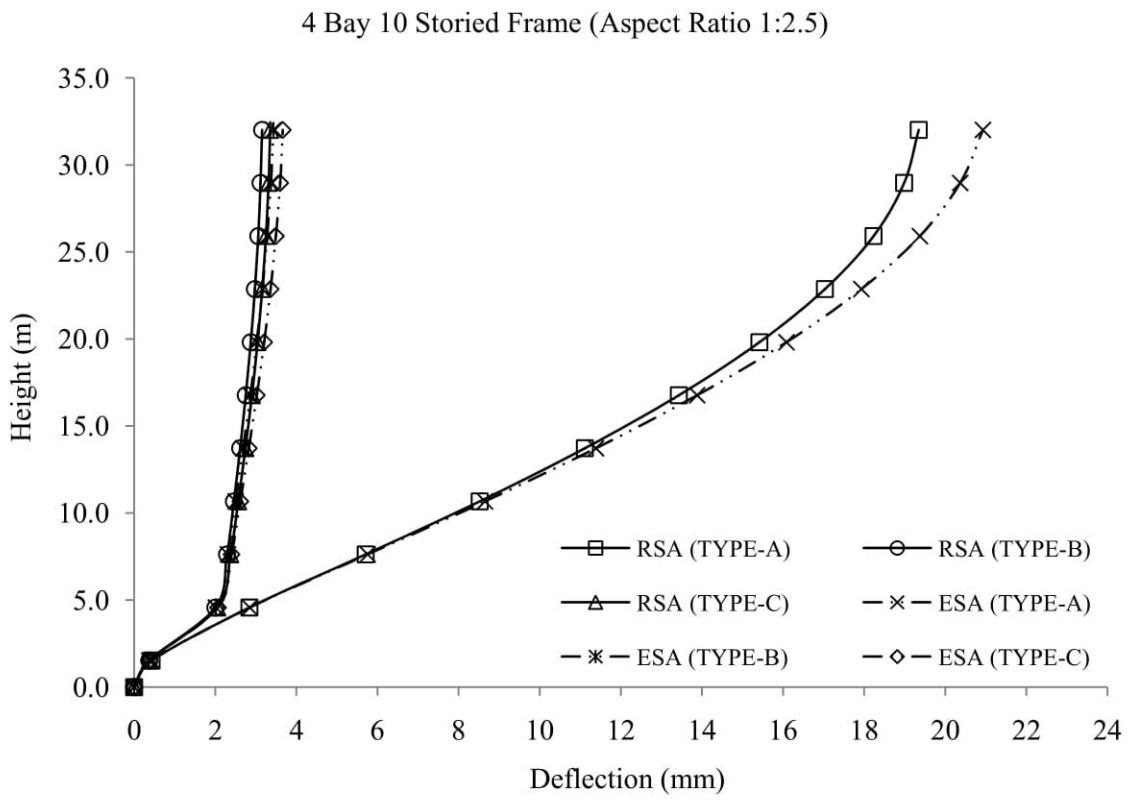
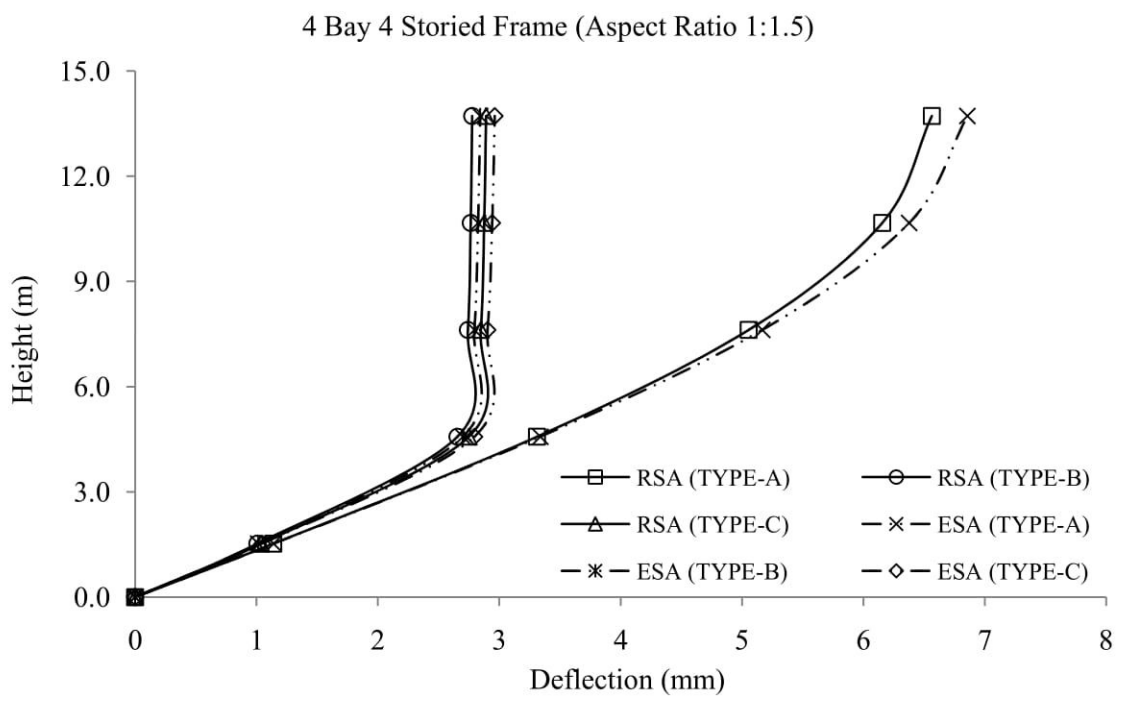


Figure B4.3: Story wise deflection of (a) 4 storied (b) 7 storied and (c) 10 storied building frames for fixed support with aspect ratio of 1:2.5



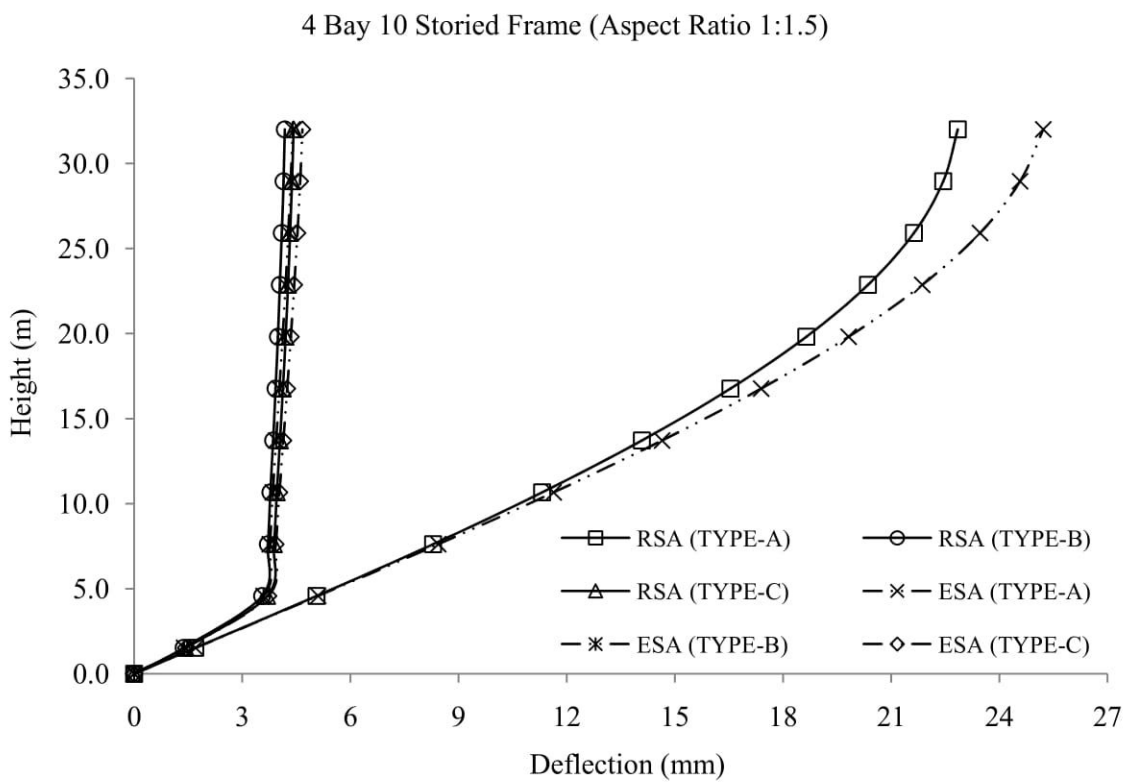
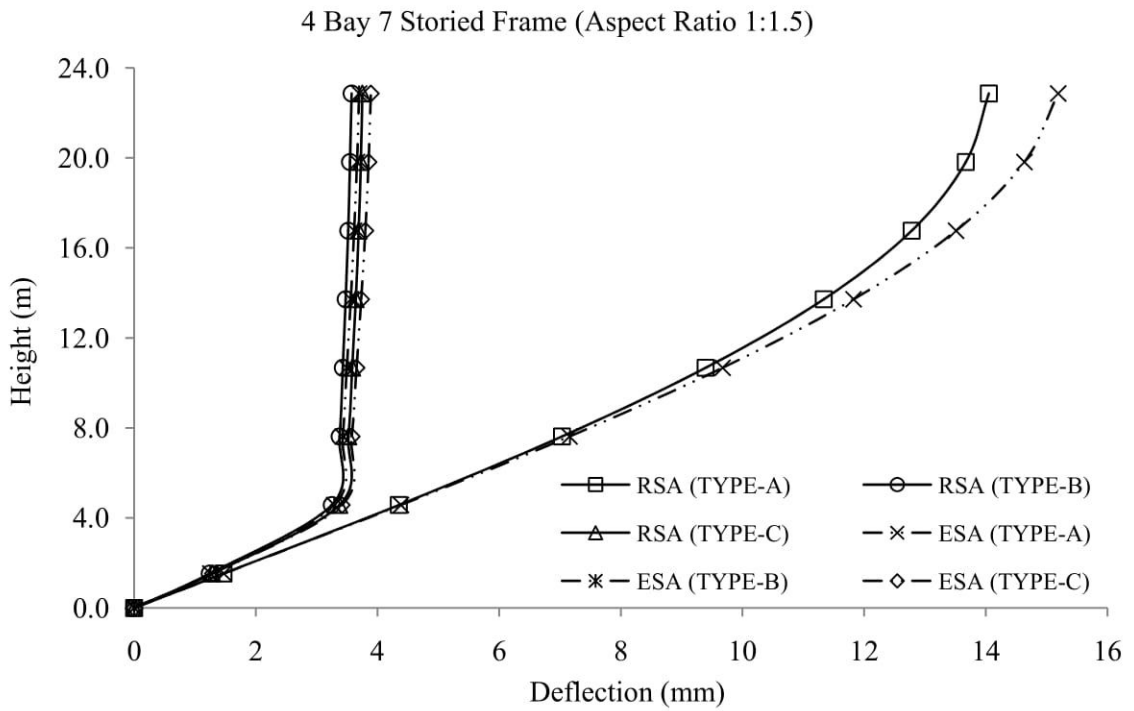
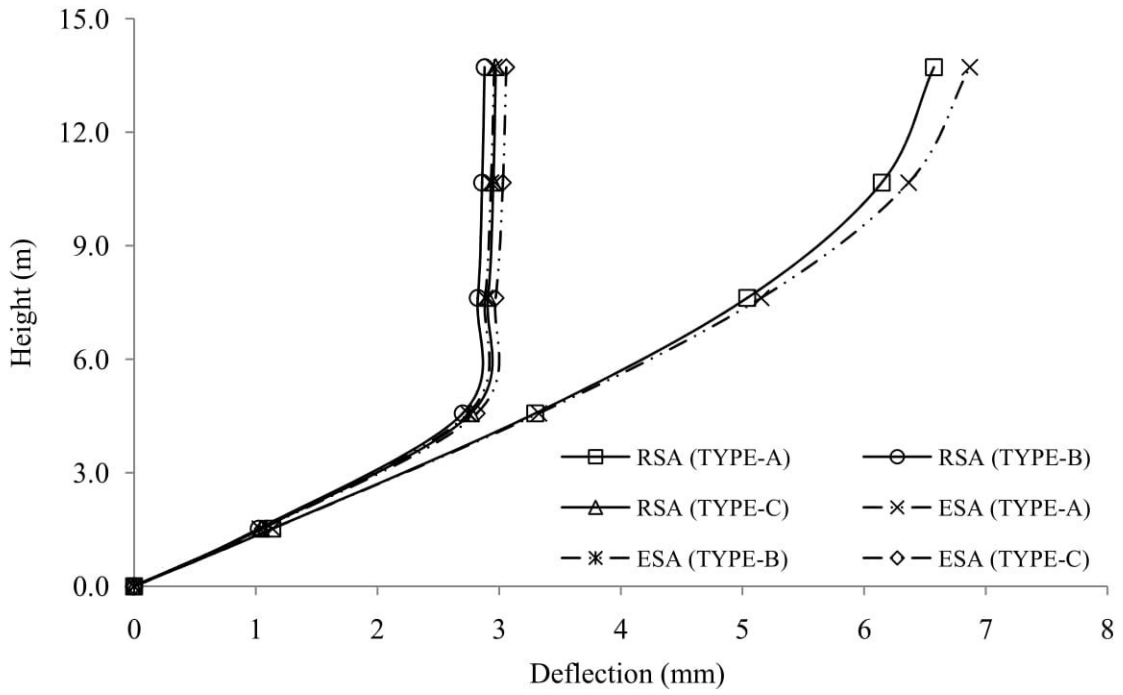


Figure B4.4: Story wise deflection of (a) 4 storied (b) 7 storied and (c) 10 storied building frames for hinged support with aspect ratio of 1:1.5

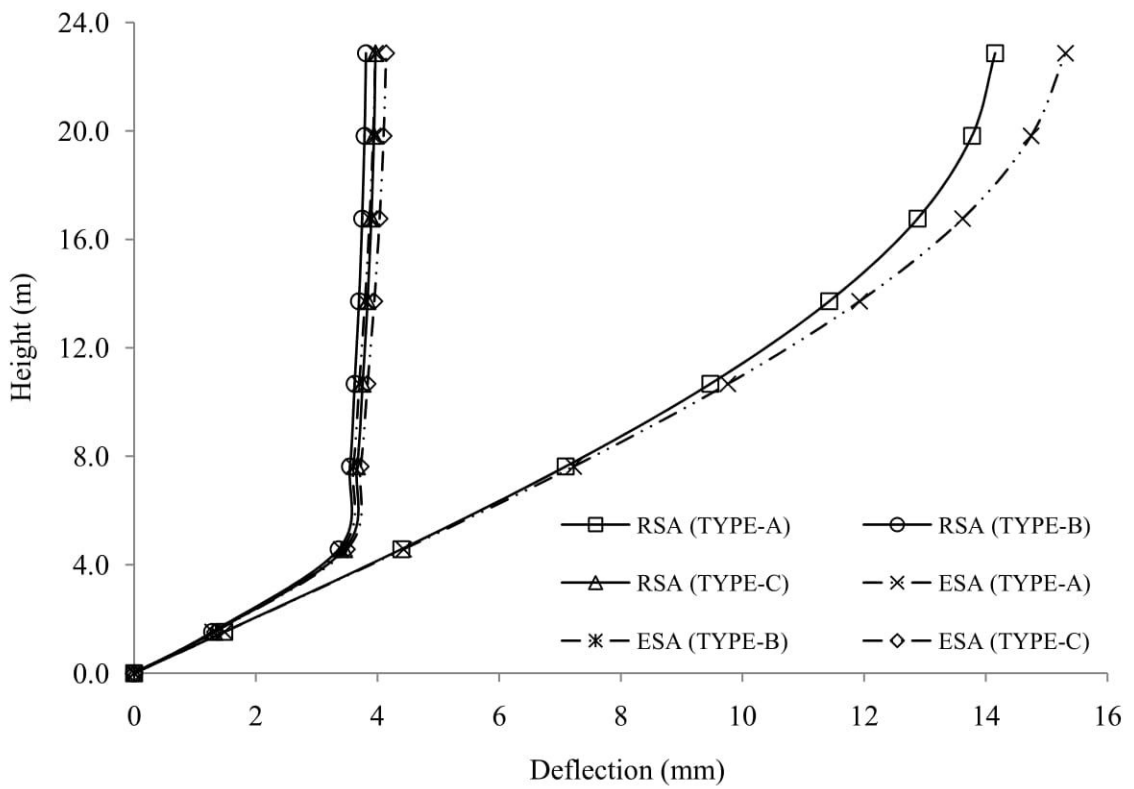


4 Bay 4 Storied Frame (Aspect Ratio 1:2)



(a)

4 Bay 7 Storied Frame (Aspect Ratio 1:2)



(b)

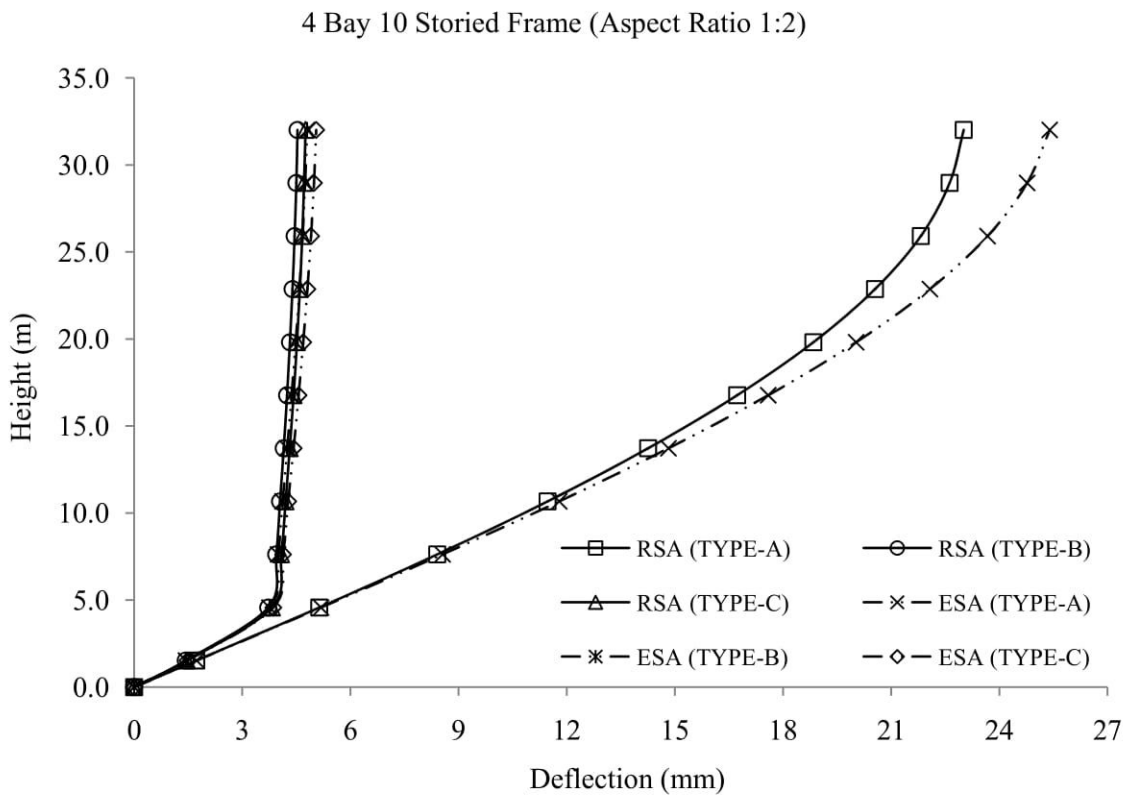
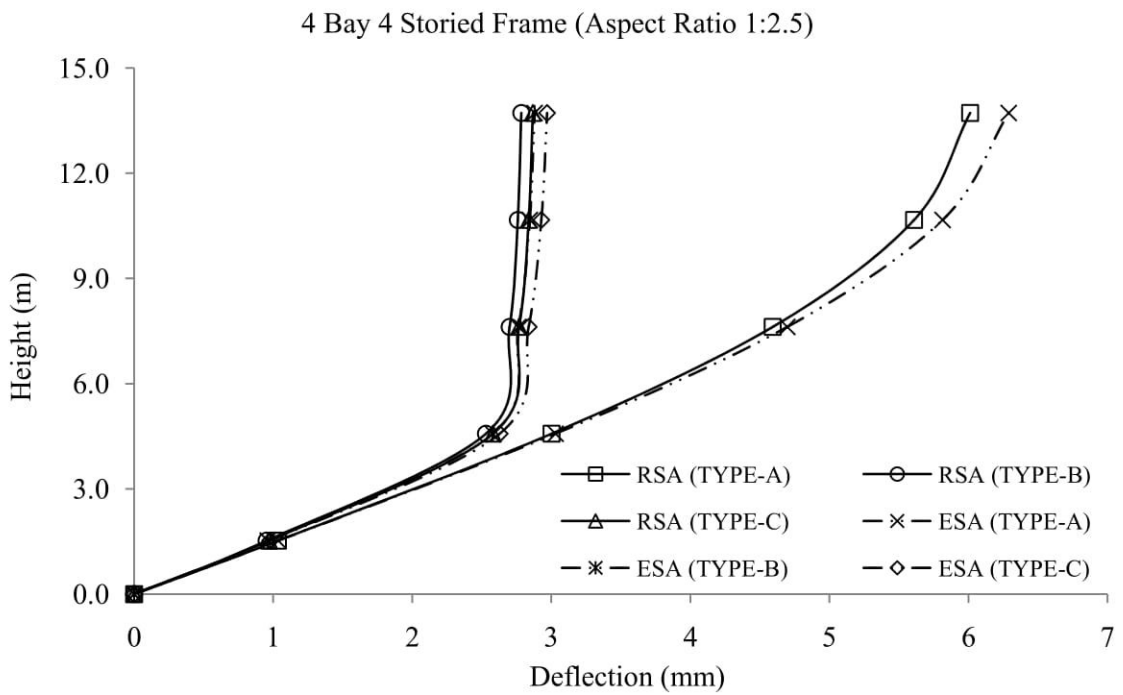


Figure B4.5: Story wise deflection of (a) 4 storied (b) 7 storied and (c) 10 storied building frames for hinged support with aspect ratio of 1:2



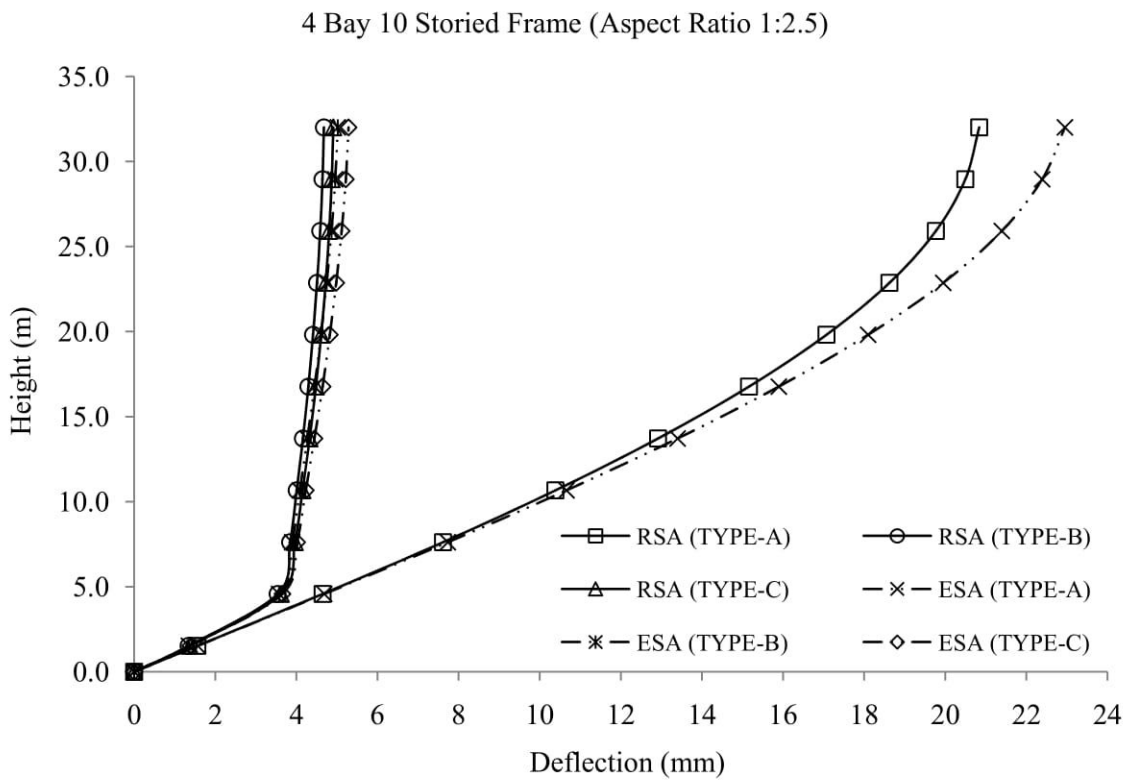
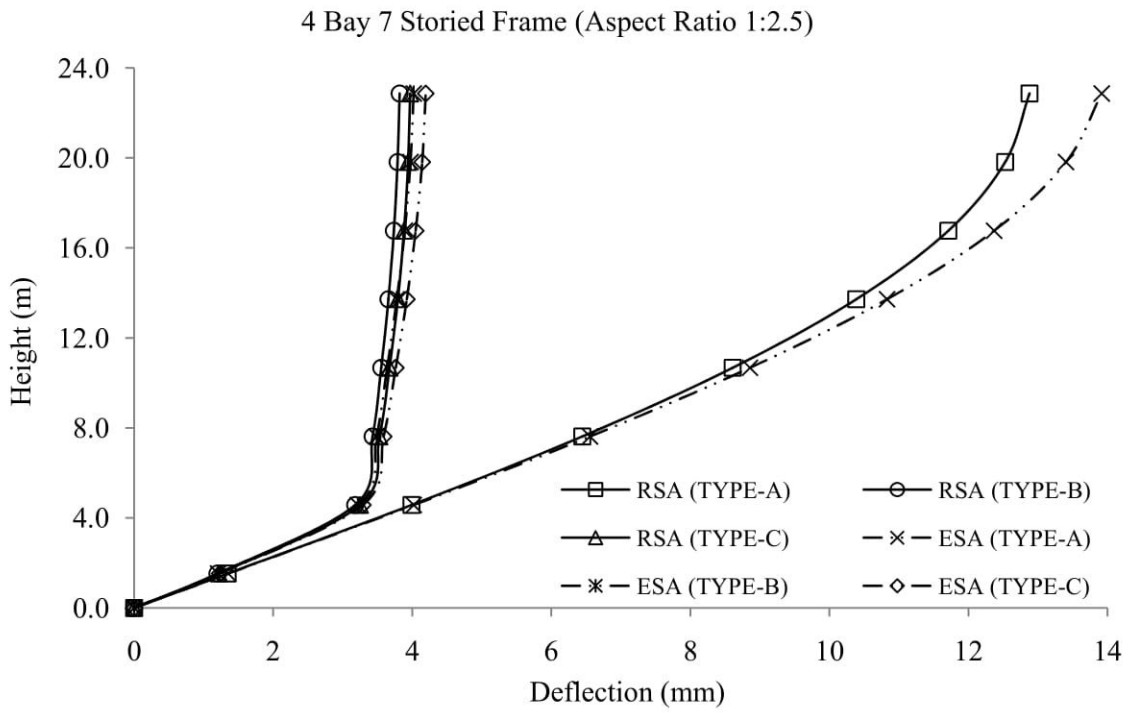
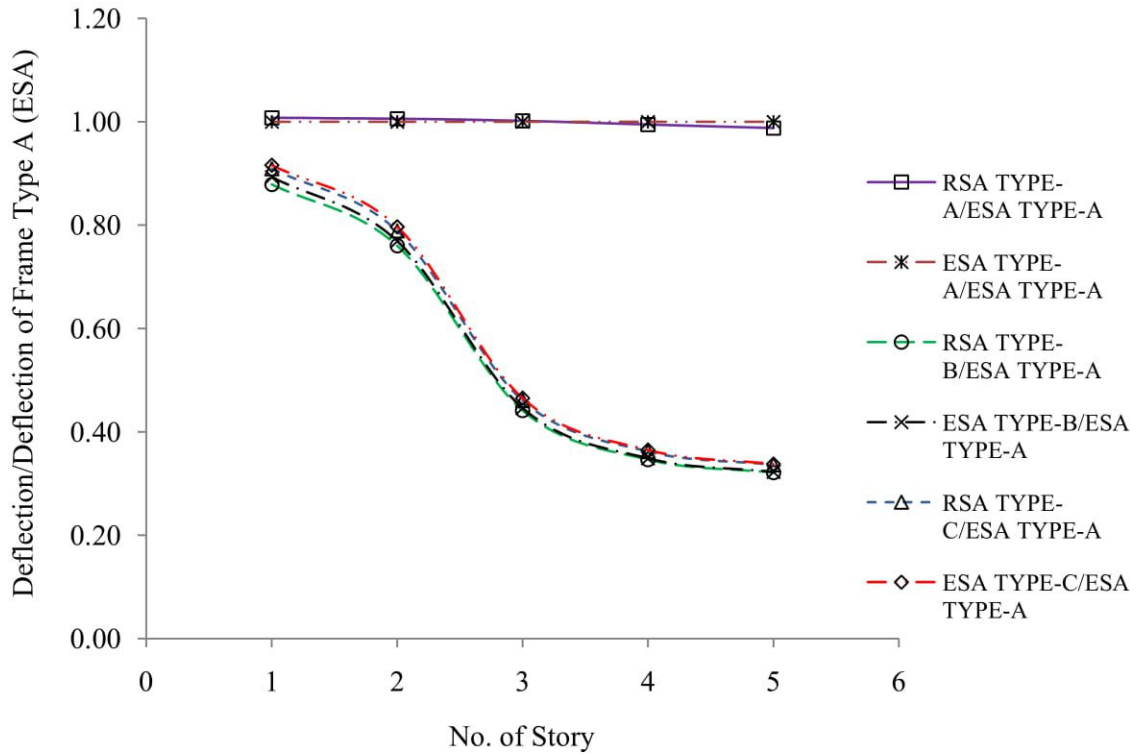


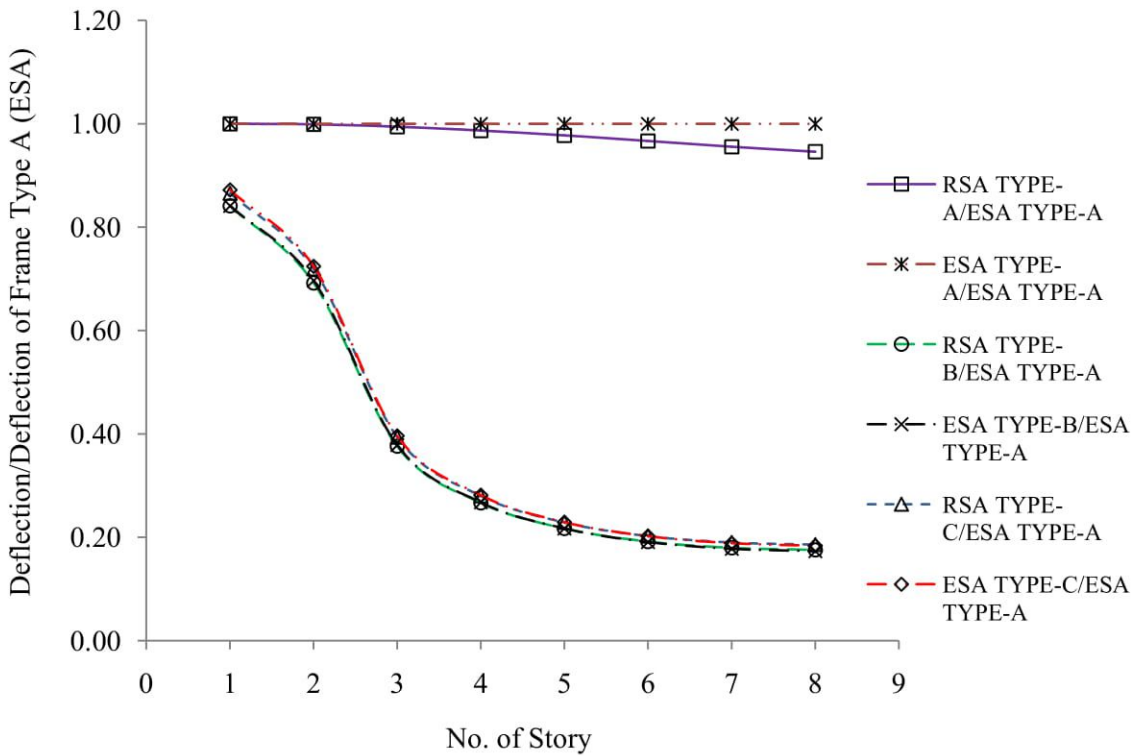
Figure B4.6: Story wise deflection of (a) 4 storied (b) 7 storied and (c) 10 storied building frames for hinged support with aspect ratio of 1:2.5

4 Bay 4 Storied Frame (Aspect ratio 1:1.5)

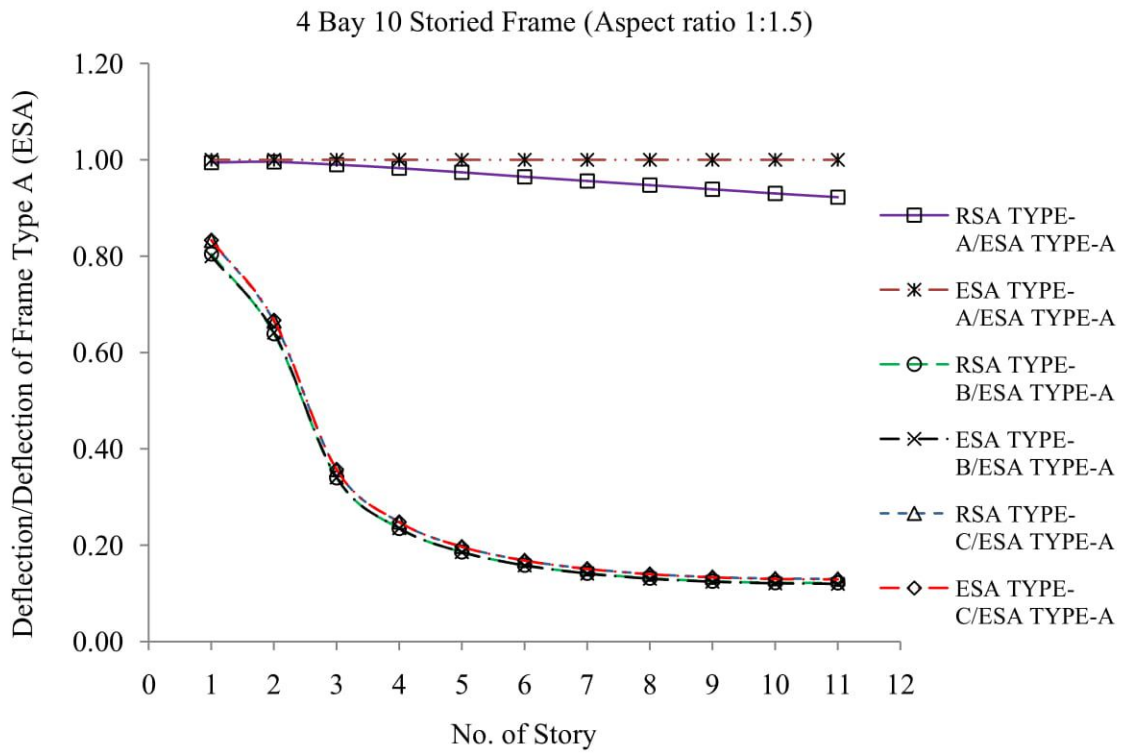


(a)

4 Bay 7 Storied Frame (Aspect ratio 1:1.5)

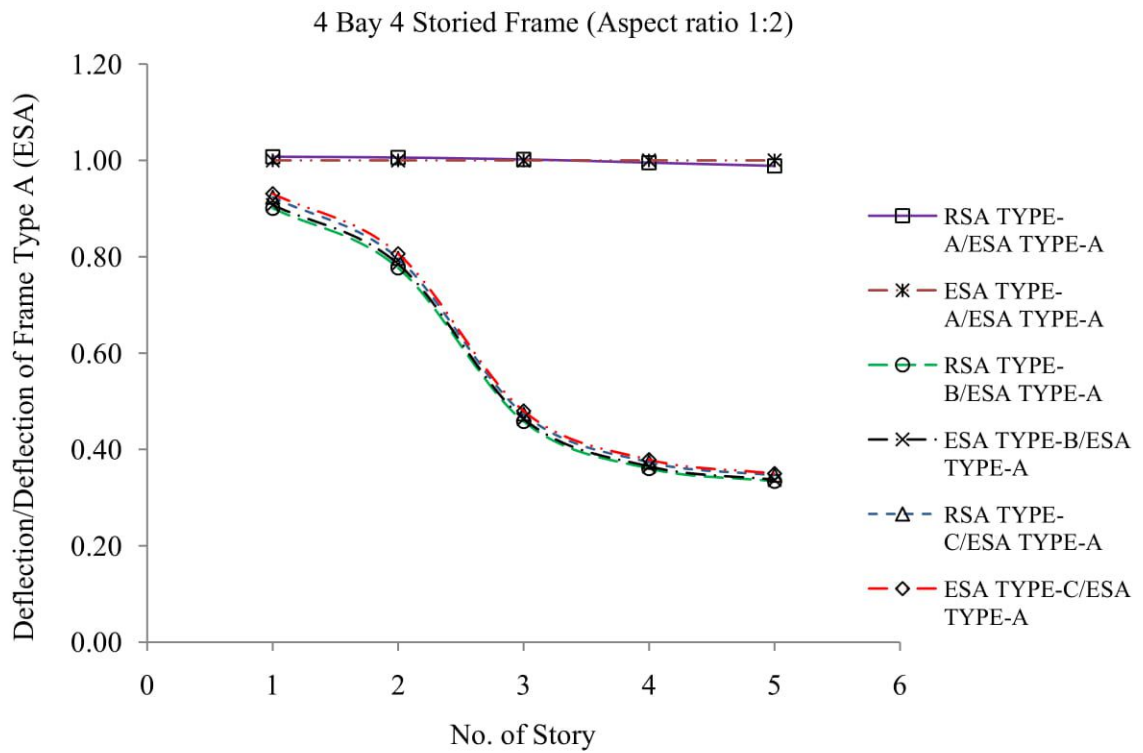


(b)



(c)

Figure B4.7: Story wise deflection pattern of (a) 4 storied (b) 7 storied and (c) 10 storied building for fixed support with respect to ESA deflection of bare frame with aspect ratio of 1:1.5



(a)

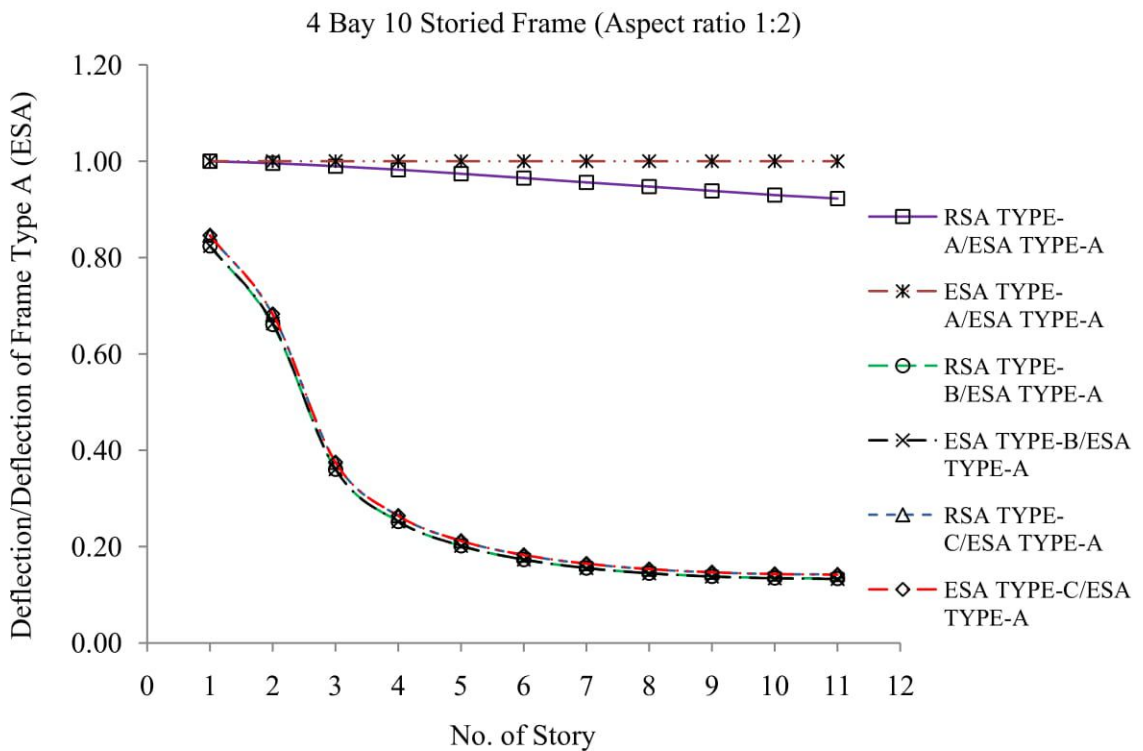
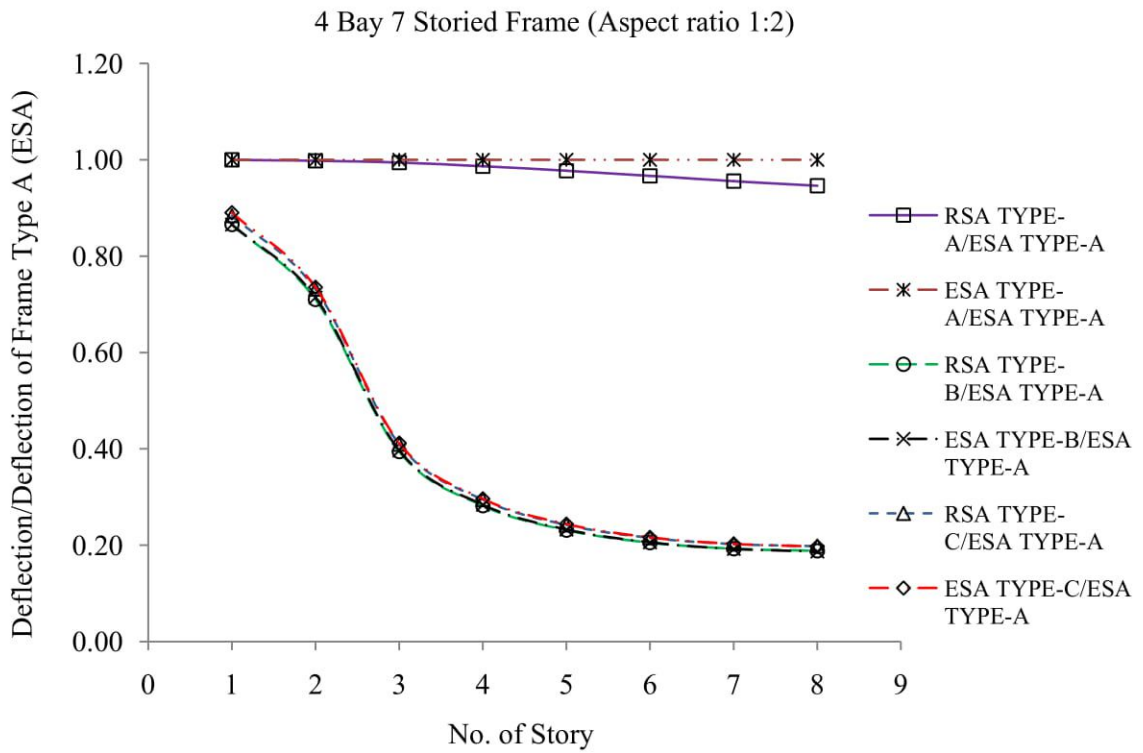
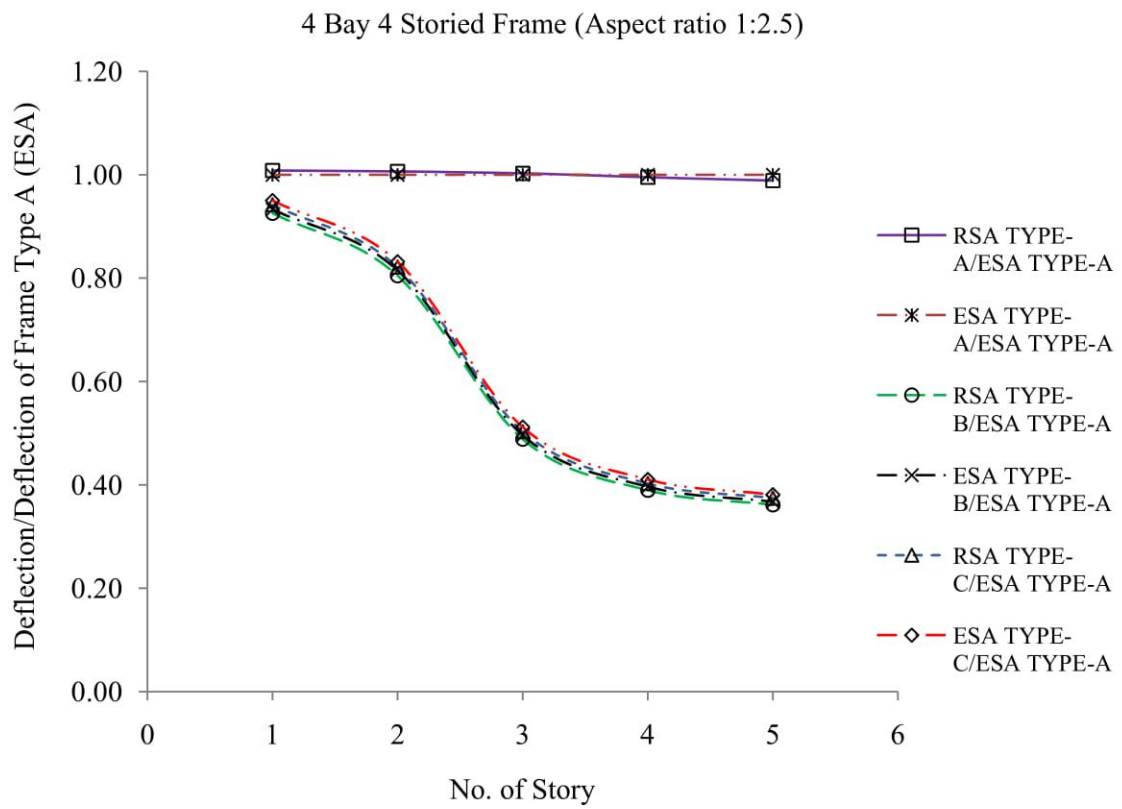
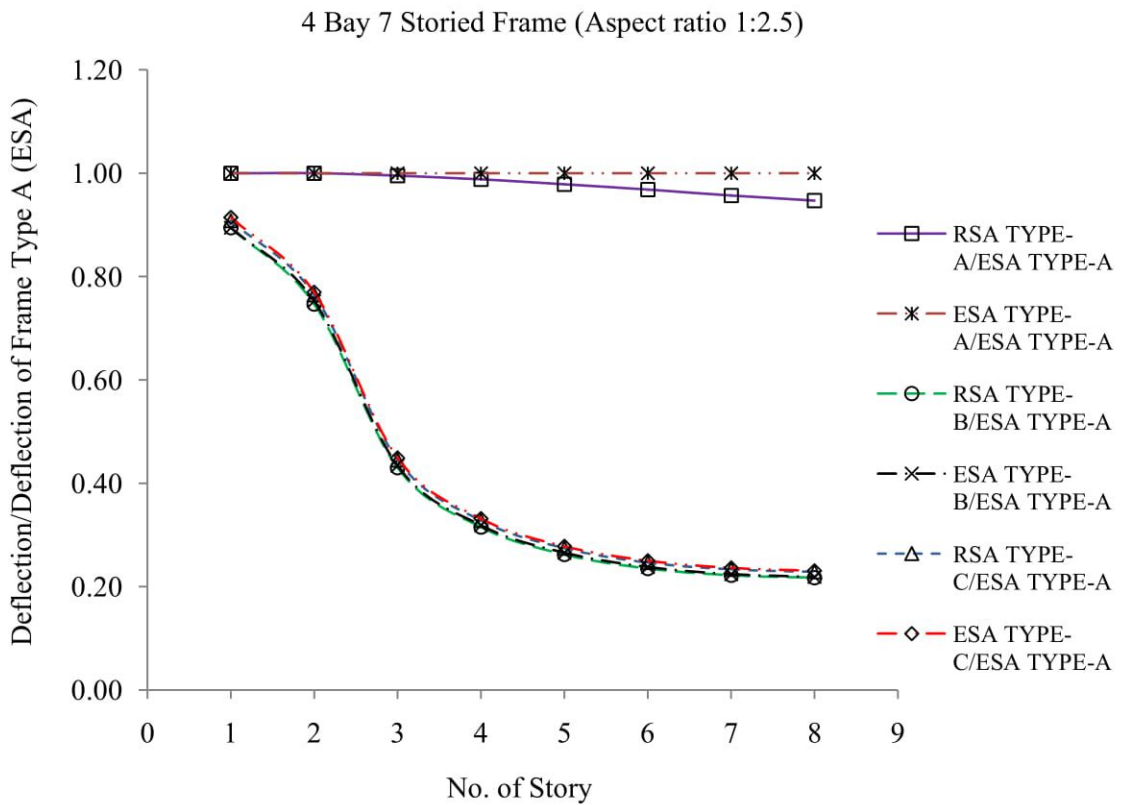


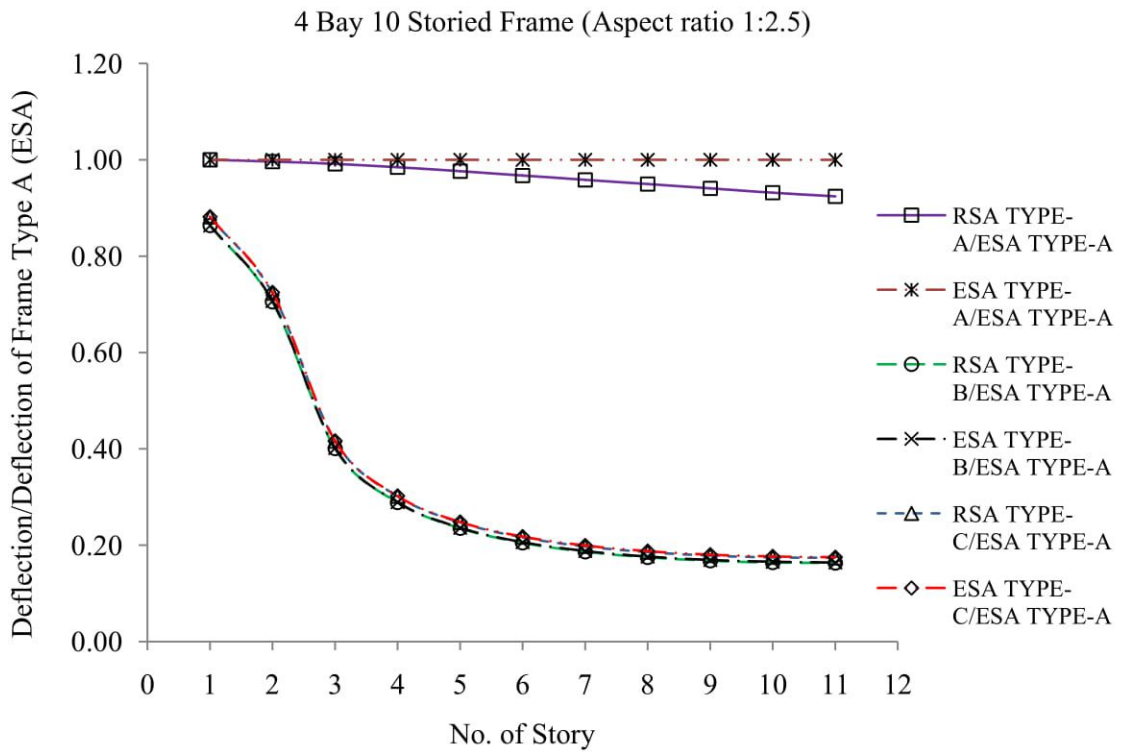
Figure B4.8: Story wise deflection pattern of (a) 4 storied (b) 7 storied and (c) 10 storied building for fixed support with respect to ESA deflection of bare frame with aspect ratio of 1:2



(a)

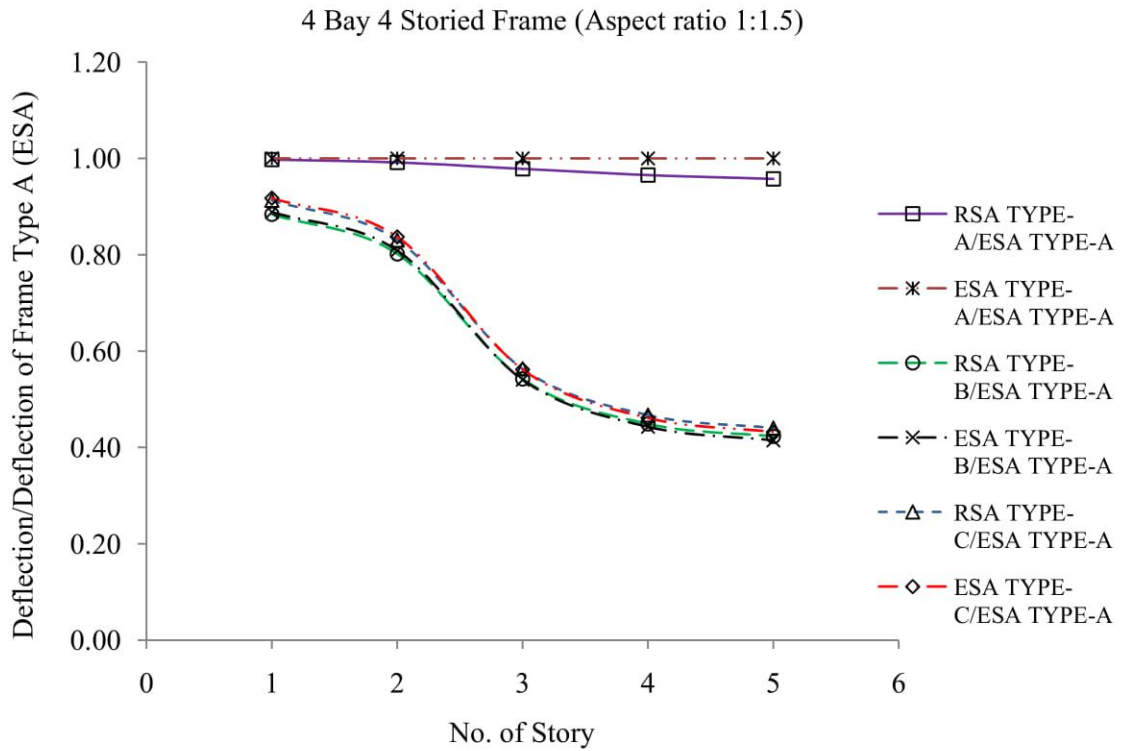


(b)



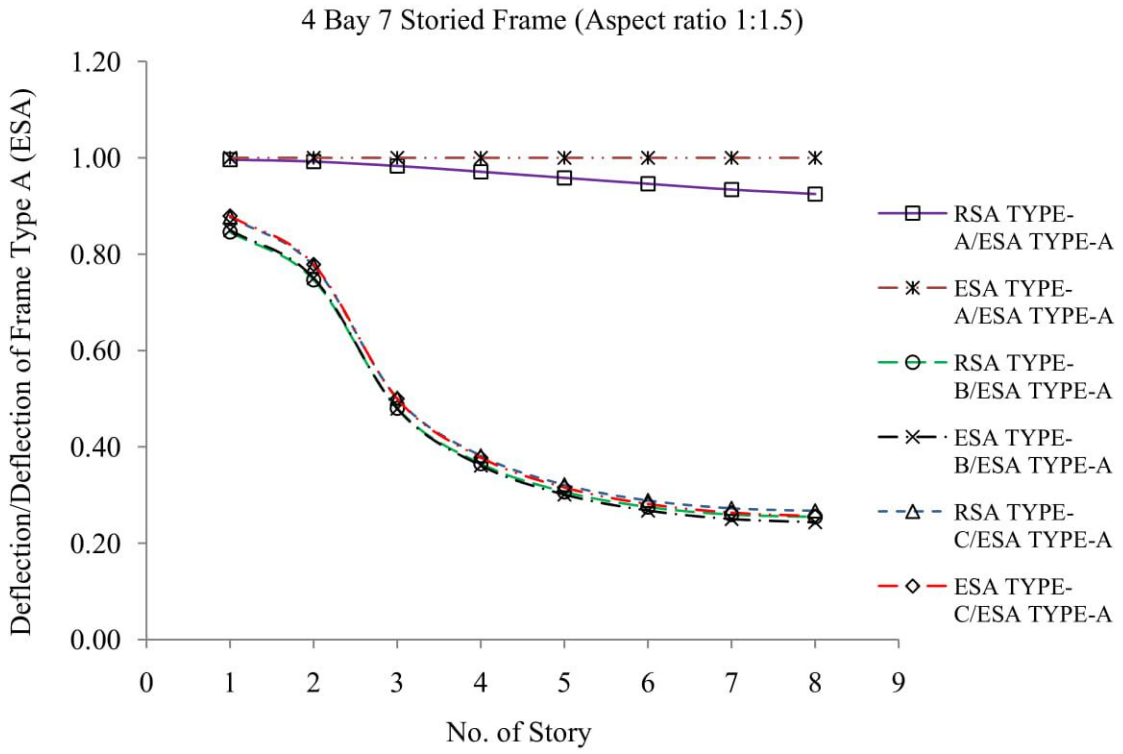
(c)

Figure B4.9: Story wise deflection pattern of (a) 4 storied (b) 7 storied and (c) 10 storied building for fixed support with respect to ESA deflection of bare frame with aspect ratio of 1:2.5

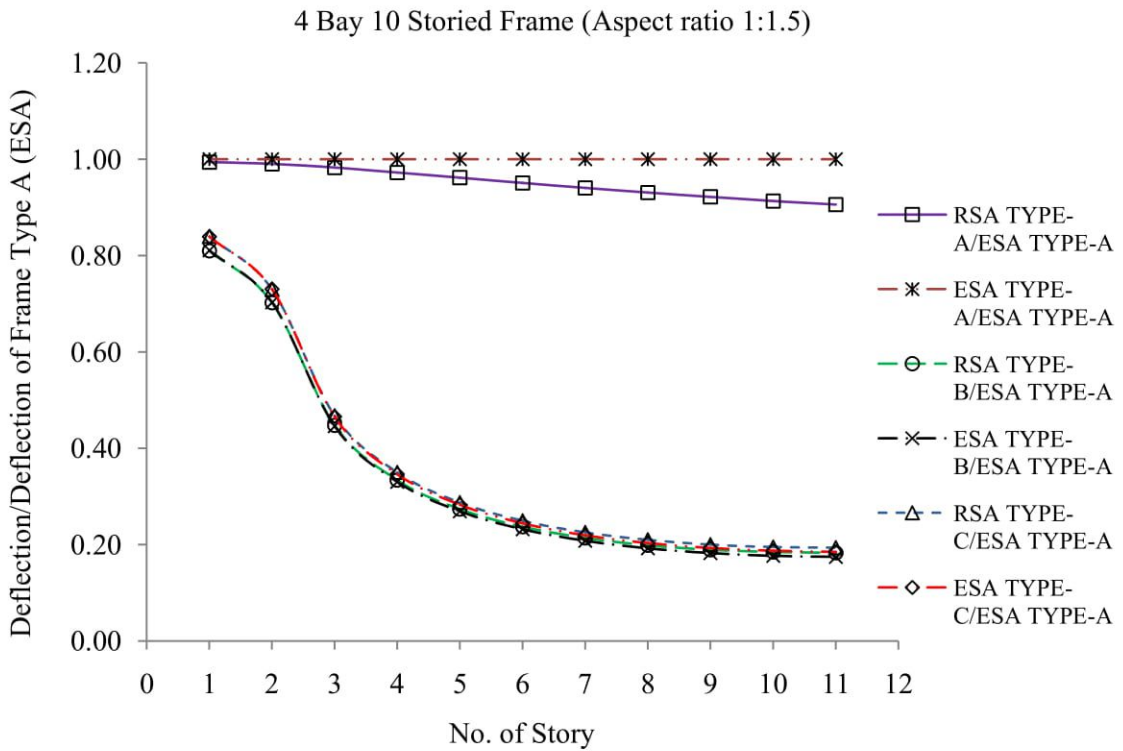


(a)



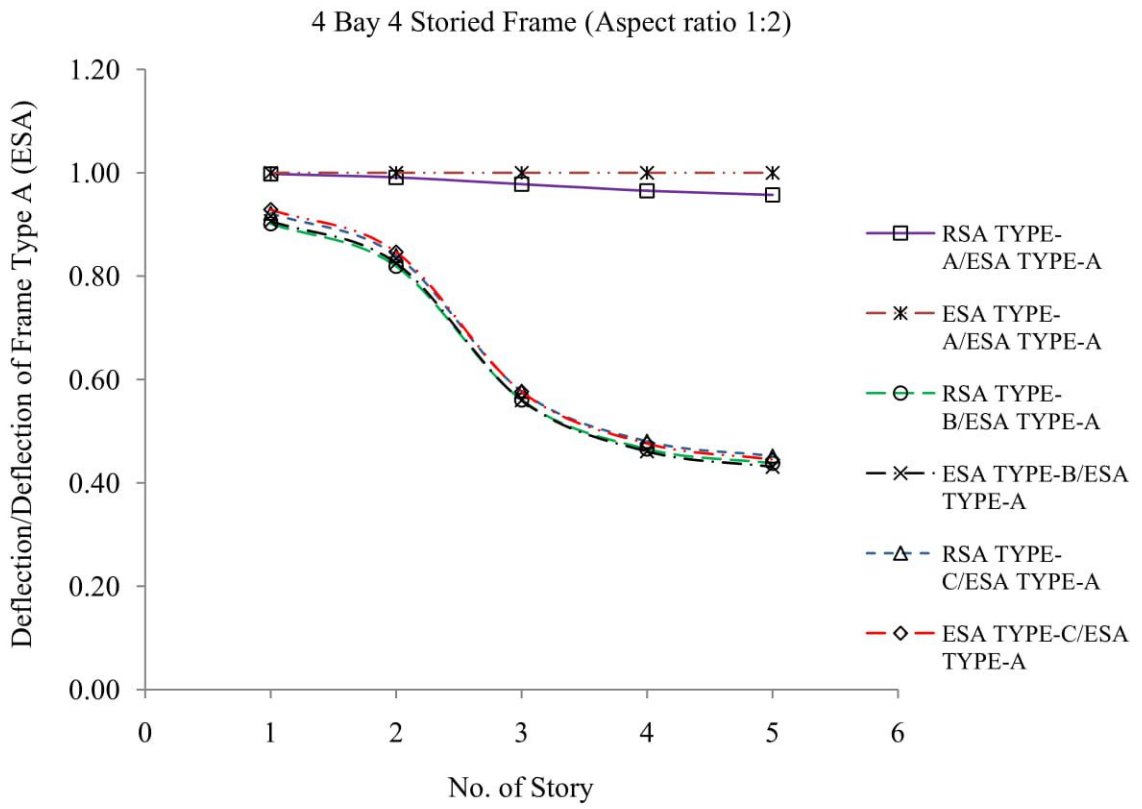


(b)

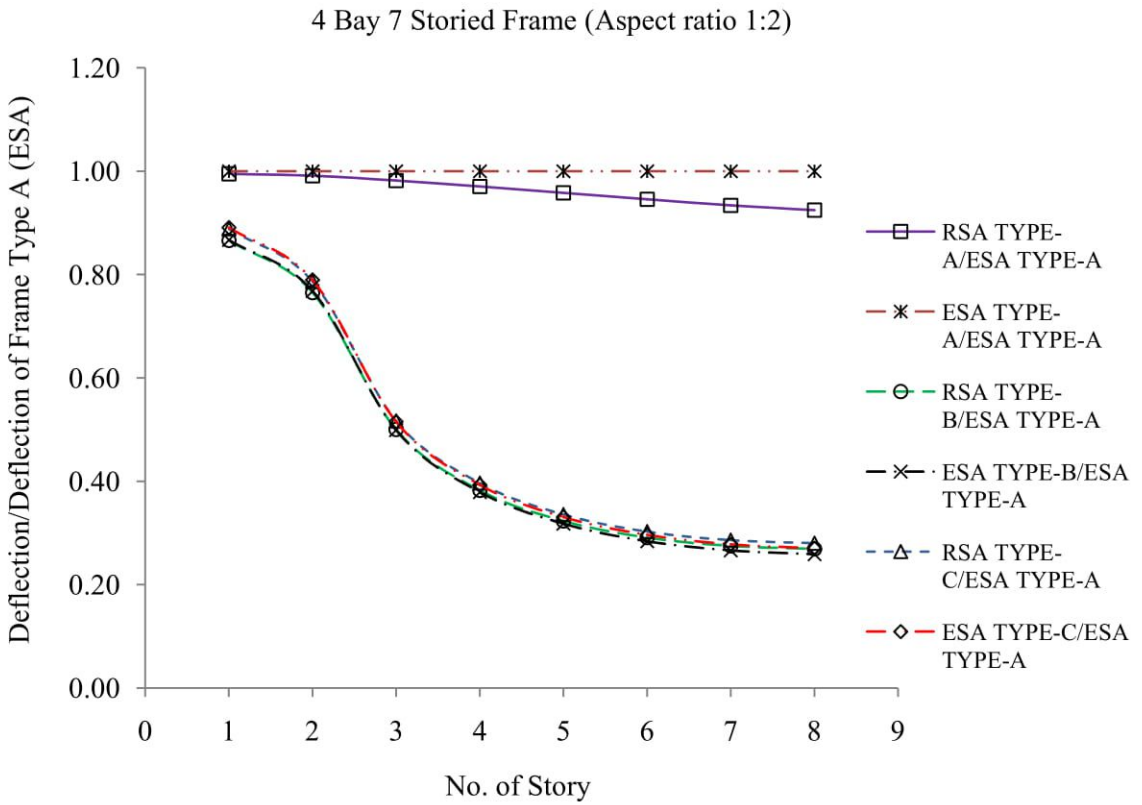


(c)

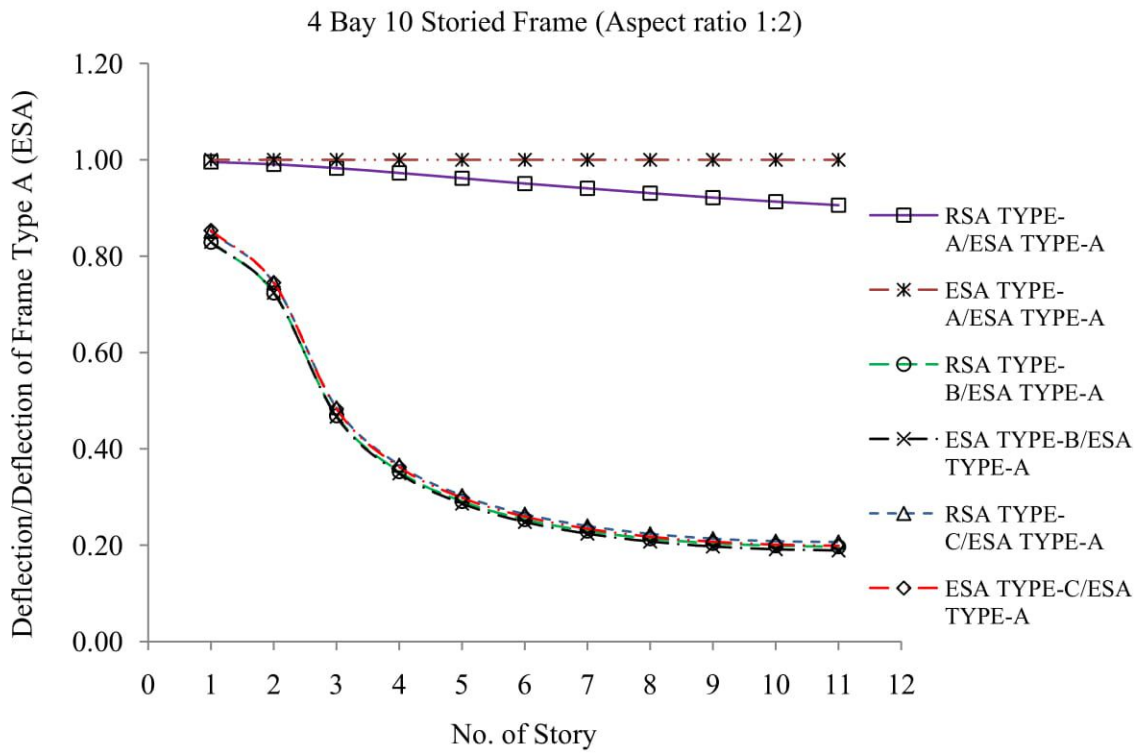
Figure B4.10: Story wise deflection pattern of (a) 4 storied (b) 7 storied and (c) 10 storied building for hinged support with respect to ESA deflection of bare frame with aspect ratio of 1:1.5



(a)

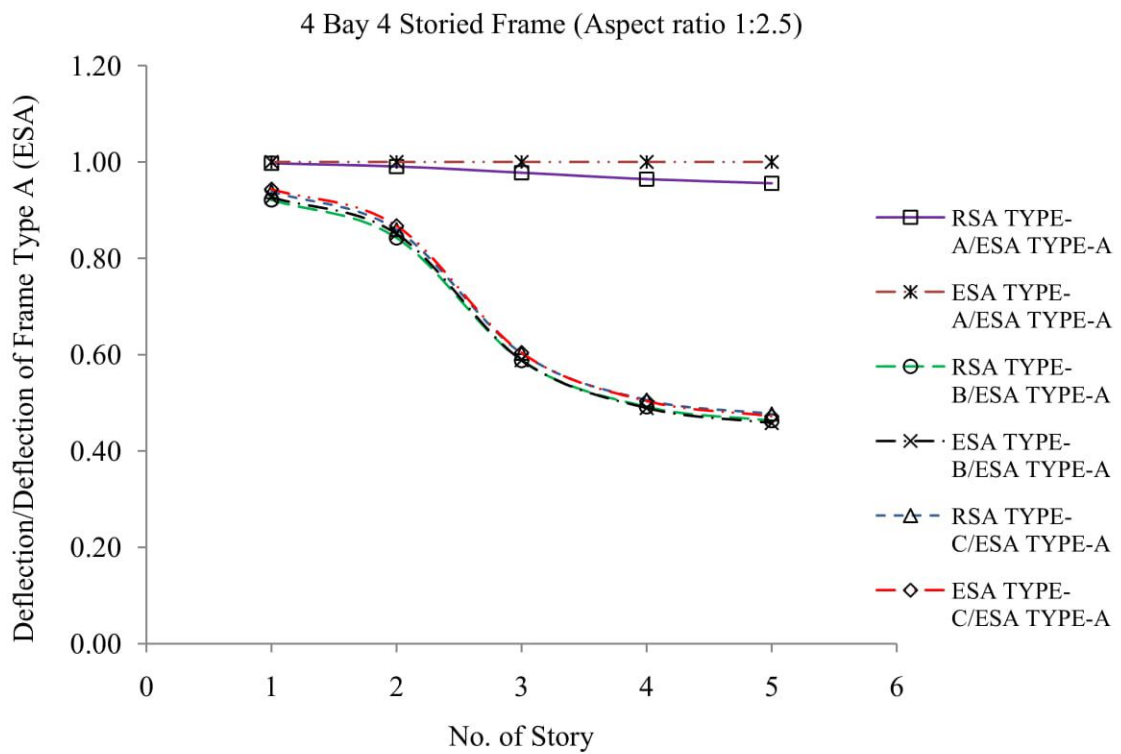


(b)

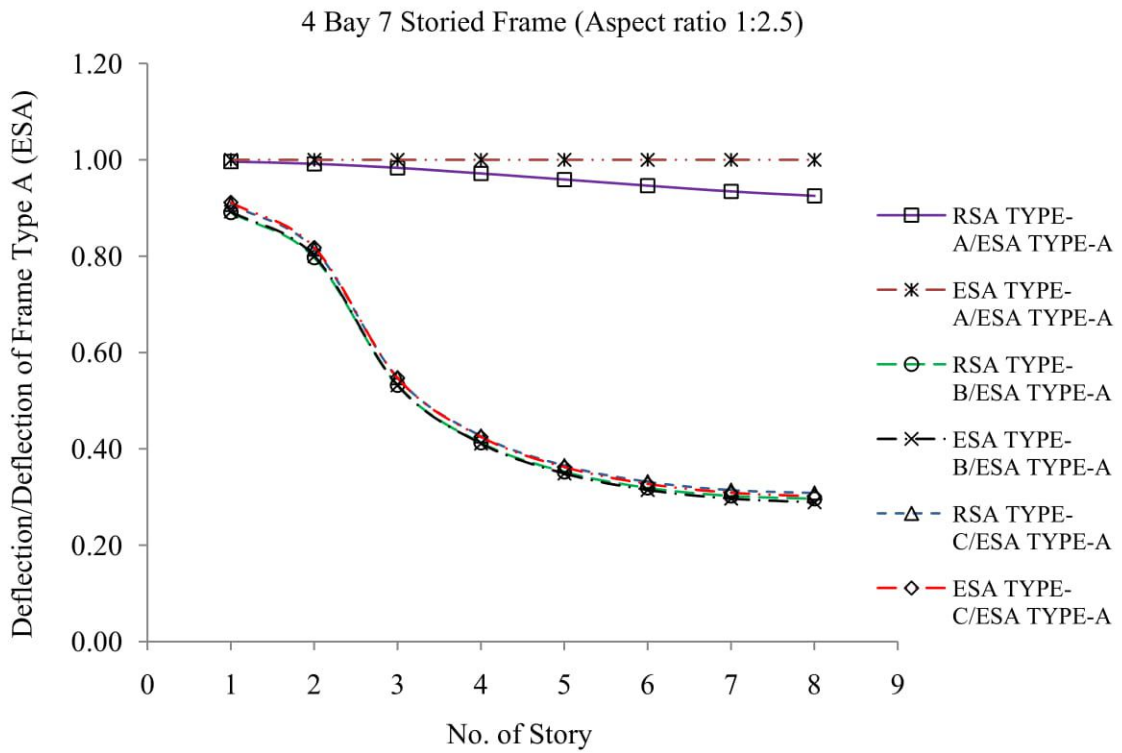


(c)

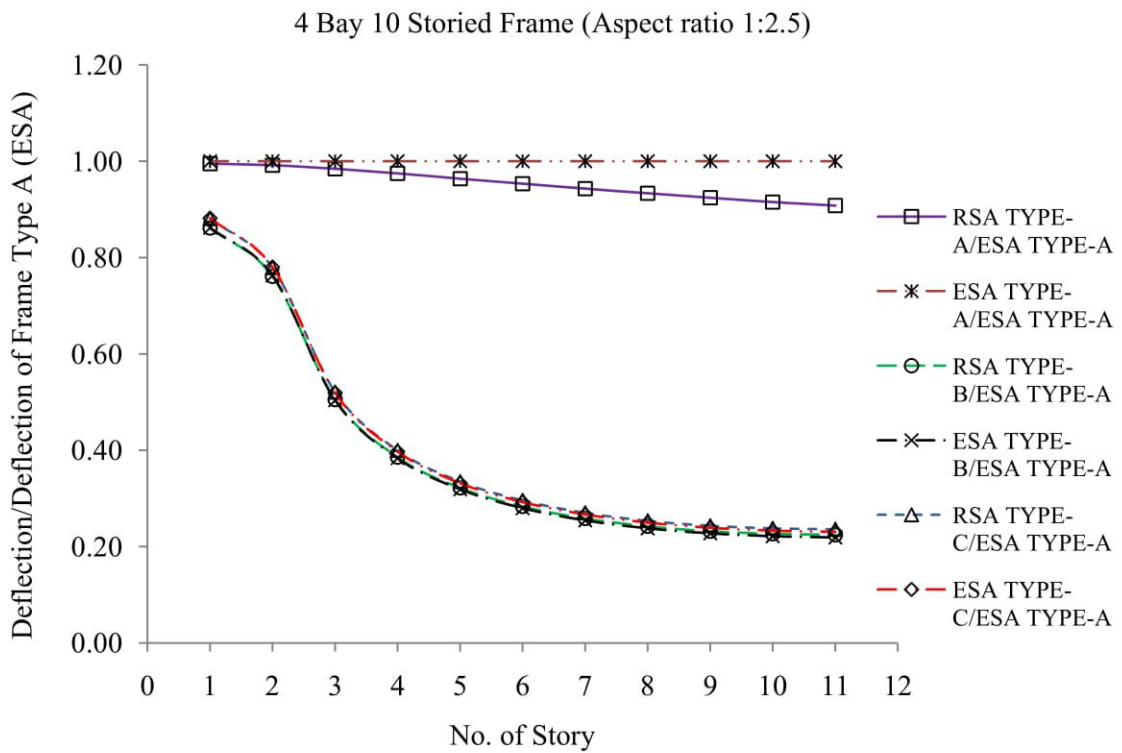
Figure B4.11: Story wise deflection pattern of (a) 4 storied (b) 7 storied and (c) 10 storied building for hinged support with respect to ESA deflection of bare frame with aspect ratio of 1:2



(a)



(b)



(c)

Figure B4.12: Story wise deflection pattern of (a) 4 storied (b) 7 storied and (c) 10 storied building for hinged support with respect to ESA deflection of bare frame with aspect ratio of 1:2.5